3rd Annual Jackson School Research Symposium

January 25th, 2014

Sponsored by ConocoPhillips

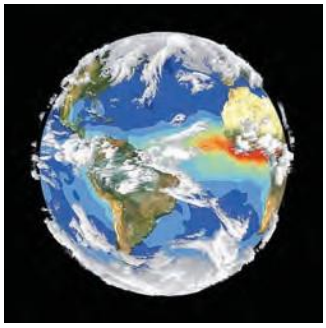

Climate, Carbon & Geobiology

Energy Geosciences

Marine Geosciences

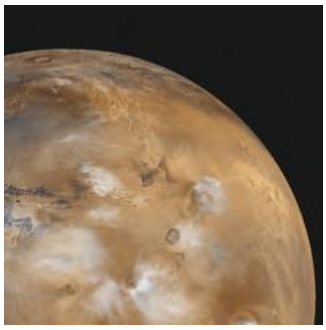

Planetary Geosciences

Solid Earth & Tectonic Processes

Surface & Hydrologic Processes

ConocoPhillips

GSEC
Graduate Student Executive Committee
Jackson School of Geosciences

THE UNIVERSITY OF TEXAS AT AUSTIN
JACKSON
SCHOOL OF GEOSCIENCES

Table of Contents

Welcome to the 3rd Annual Jackson School Research Symposium

It is with great pleasure we welcome you all to the 3rd Annual Jackson School Research Symposium at UT-Austin! This symposium would not have been possible without the hard work of student volunteers, the support of faculty/research scientists, and generous support from ConocoPhillips. Thank you for taking part in supporting our students and growing research program within the Jackson School. Enjoy the posters!

Schedule of Presentations and Events

Breakfast, A.M. session poster set-up.....8:30 a.m.

Climate, Carbon & Geobiology (CCG) posters.....9:00-11:30 a.m.

Marine Geosciences (MG) posters.....9:00-11:30 a.m.

Surface & Hydrologic Processes (SHP) posters.....9:00-11:30 a.m.

Lunch, A.M. session poster take-down.....11:30 a.m.

P.M. session poster set-up.....12:30 p.m.

Solid Earth and Tectonic Processes (SETP)….....1:00-3:30 p.m.

Energy Geoscience (EG) posters.....1:00-3:30 p.m.

Planetary Science (PS) posters.....1:00-3:30 p.m.

Energy and Earth Resources (EER)…….….....1:00-3:30 p.m.

Happy hour/judging.....3:30 p.m.

Awards/closing.....4:00 p.m.

A.M. POSTER LAYOUT

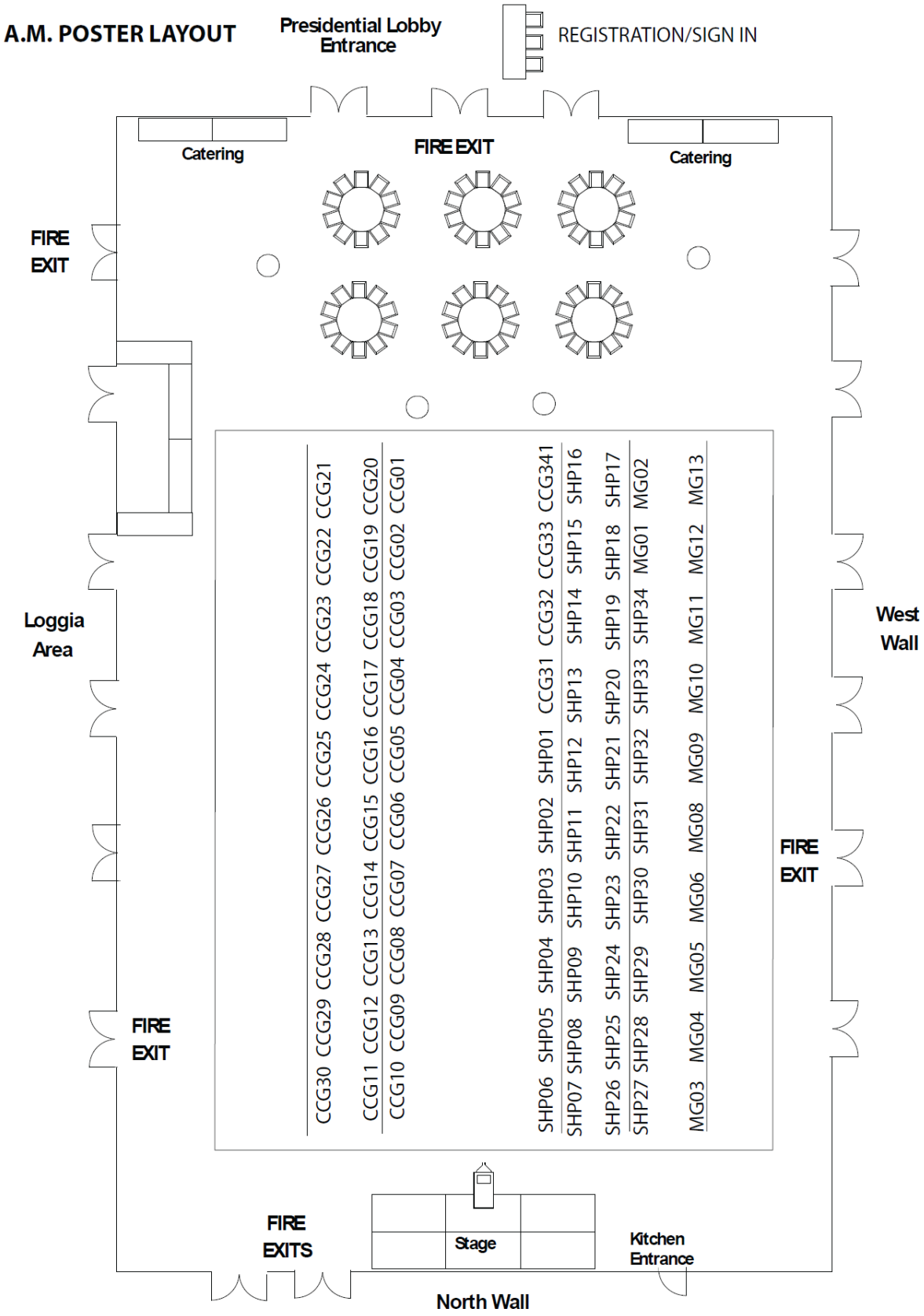

P.M. POSTER LAYOUT

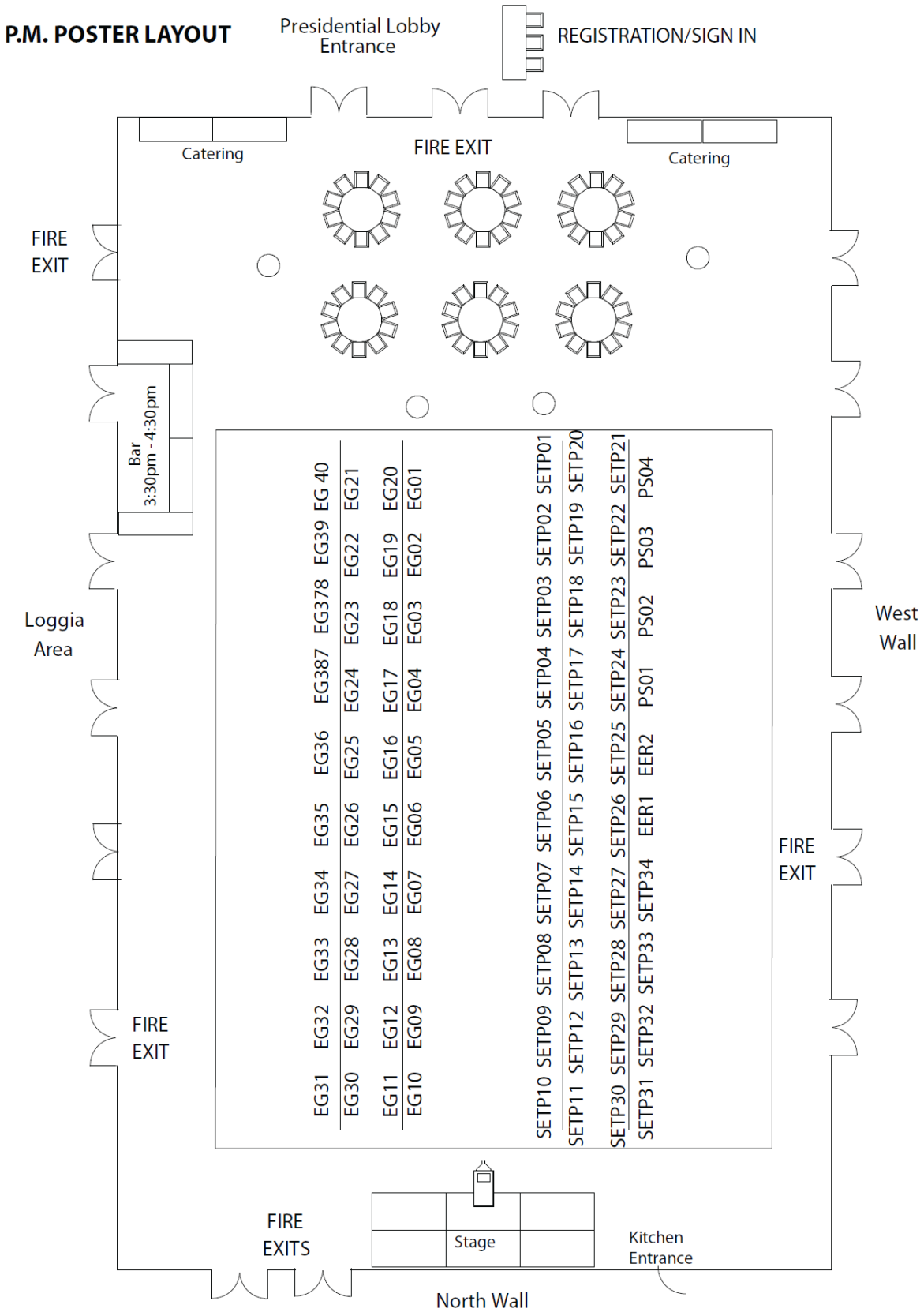

CCG-1

A stable isotopic investigation of resource partitioning among neosauropod dinosaurs of the Upper Jurassic Morrison Formation

Breeden, B. T.[1,2], Holtz, T. R.[2], Kaufman, A. J.[2], Carrano, M. T. [3]
bbreeden@utexas.edu
1. Jackson School of Geosciences, The University of Texas at Austin, Austin, TX
2. Department of Geology, University of Maryland, College Park, MD
3. Department of Paleobiology, Smithsonian Institution, Washington, DC

For more than a century, morphology has been used to attempt to understand the partitioning of food resources among the herbivorous dinosaurs of the Upper Jurassic Morrison Formation of western North America, particularly between members of the two major clades of Neosauropoda: Diplodocidae and Macronaria. While many studies exploring sauropod resource portioning have focused on morphological differences between the two groups, few have utilized geochemical evidence. Stable isotope geochemistry has become an increasingly common and reliable means of investigating paleoecological questions, and due to the resistance of enamel to diagenetic alteration, fossil teeth can provide paleoecological and behavioral data that would be otherwise unobtainable. $\delta^{13}C$ was measured in leaves of extant plants closely related to those present during the Late Jurassic, and it was observed that a significant variation of as much as ~3‰ in carbon isotope ratios occurs with height in trees. With this knowledge, it becomes possible to investigate the partitioning of resources via feeding height in herbivorous fossil animals, assuming that they fed largely on the same plants. In order to apply this to the question of resource partitioning in Morrison neosauropods, a small (n=9) assemblage of macronarian and diplodocid teeth was obtained from the Mygatt-Moore Quarry in western Colorado. Enamel powder was collected from each tooth and treated first with bleach to oxidize and remove any lingering organic matter and then with a calcium-acetate/acetic acid buffer to remove any non-structurally-bound carbonate in order to account for diagenetic alteration. $\delta^{13}C$ and $\delta^{18}O$ were then measured from the remaining carbonated hydroxyapatite ($Ca_{10}(PO_4)_6(OH_2,CO_3)$) of the enamel samples. Significant overlap in $\delta^{13}C$ and $\delta^{18}O$ values was observed between the two groups. $\delta^{13}C$ values averaged ~8.25‰ for both groups, which is consistant with at least one other preliminary study on carbon isotopes in sauropod teeth. These results support the hypothesis that diplodocids and macronarians did not partition resources strictly by height; however, the sample size was small for this study, and the issue warrants further attention.

Keywords: Palaeontology, paleoecology, Neosauropoda, stable isotope geochemistry, Late Jurassic

CCG-2

Connecting specimens and their derivative data in the Vertebrate Paleontology Lab's Navajo Nation collection

Brenskelle, L.[1]
lbrensk@utexas.edu
1. Jackson School of Geosciences, The University of Texas at Austin, Austin, TX

This study intends to create a database that incorporates all of the quintessential components of the specimens of the Navajo Nation Collection at the Vertebrate Paleontology Lab at The University of Texas at Austin and generate best practices for how to curate various formats of digital data. The Navajo Nation Collection contains fossils from the Lower Jurassic Kayenta Formation of Arizona and is an active research collection, producing computed tomography data, stable isotope analyses, and other forms of derivative specimen data. The database will mostly be for internal use by faculty, staff, and students, but the possibility of making this information available through an online interface also exists. Currently, most natural history collections do not curate digital data in association with the physical specimen. Because digital technology is continually evolving, advancing best practices for how to store this derivative data in association with the specimen is imperative, particularly within the field of paleontology where a number of different analytical techniques are applied to individual specimens to study the fossil's age and morphology.

Keywords: Vertebrate Paleontology Lab, database, data management, collections management

CCG-3

Integrating nitrogen dynamics into the Noah-MP land surface model for environmental prediction

Cai, X.T.[1,2], Yang, Z.-L.[1,2], Fisher, J.B.[3], Barlage, M.[4], Chen, F.[4]
Xitian.Cai@utexas.edu
1. Jackson School of Geosciences, The University of Texas at Austin, Austin, TX
2. Center for Integrated Earth System Science, The University of Texas at Austin, Austin, TX
3. Jet Propulsion Laboratory, California Institute of Technology, Pasadena, CA
4. National Center for Atmospheric Research, Boulder, CO

Climate and ecological models consider nitrogen an important factor in limiting plant carbon uptake, while operational environmental models view nitrogen as the leading nutrient for causing eutrophication in water bodies. The community Noah land surface model (LSM) with multi-parameterization options (hereafter Noah-MP, Niu et al., 2011; Yang et al., 2011) is a unique LSM in that it is the next generation LSM for the Weather Research and Forecasting (WRF) meteorological model and for the operational weather/climate models in the National Centers for Environmental Prediction (NOAA/NCEP). While Noah-MP does not currently contain a dynamic nitrogen cycle, this can readily be updated with the interactive vegetation canopy option, which predicts the leaf area index as a function of light, temperature, and soil moisture. Here, Noah-MP is coupled with a cutting-edge plant nitrogen model—the Fixation & Uptake of Nitrogen (FUN) model (Fisher et al., 2010)—and the soil nitrogen model from the Soil and Water Assessment Tool (SWAT), the combination of which has the strength in simulating the impacts of agricultural management (e.g. fertilizer use) on nitrogen leaching and transport to water bodies. The nitrogen dynamics has been coupled into Noah-MP with further testing underway. Preliminary results show that the coupled model is capable of simulating the nitrogen limitation on plant carbon uptake. Future work will use the coupled model to assess how nitrogen export responds to changes in climate and land use.

Keywords: Nitrogen, carbon, Noah-MP, land surface model, eutrophication

CCG-4

The Influence of the Permian Syndepositional Fracture Network on the Modern Geomorphology at Slaughter Canyon, New Mexico, U.S.A.

Camacho, Jason N.
jnc1@utexas.edu
1. Jackson School of Geosciences, The University of Texas at Austin, Austin, TX

The Guadalupe Mountains are a widely recognized field laboratory for carbonate geology. They are also analogous to the prolific West Texas Field. Preferential regional-scale trellis style weathering patterns driven by syndepositional deformation exist throughout the southeastern front of the Guadalupe Mountains. This study examines the relationship between the anomalous outcrop scale high-relief elongate fin structures in the mouth of Slaughter Canyon and preferential erosion related to the differential incidence of syndepositional fractures. This relationship was investigated by integrating traditional field controlled fracture mapping with a remote survey done via digital outcrop model to quantify the frequency and incidence of the fracture network at the mouth of Slaughter Canyon, NM. After field and remote surveys were conducted, built-for-purpose fracture diagnostic software using a normalized correlation count was implemented in the analysis. Results show that there is an inverse relationship between high density zones of deformation and the fin structures. Furthermore a statistically significant correlation exists for the combined field-remote data set at fracture length scales of ~20m and ~40m which occur at distances from the margin of 300-400m and 500m respectively.

Keywords: energy, oil and gas, carbonates, sedimentology, remote sensing, LiDAR, Guadalupe Mountains, Slaughter Canyon, New Mexico, syndepositional fractures, digital outcrop model

CCG-5

Comparison of Spring and Cave Drip Water in Westcave Preserve, Central Texas May Reveal Epikarst CO_2 Degassing

Carlson, P.E.[1], Banner, J.L.[1], Casteel, R.C.[1], Breecker, D.O.[1]
petercarlson@utexas.edu
1. Jackson School of Geosciences, The University of Texas at Austin, Austin, TX

The cave at Westcave Preserve, in central Texas, is a unique location to study karst processes due to its low, nearly atmospheric cave-air CO_2 levels and seasonally variable temperature. The source of water that drips into the cave, however, has not been constrained, limiting interpretation of climate proxies in the cave. It is possible that a nearby spring and the cave drip-waters share a common source. Alternatively, the drip-waters could represent local precipitation that has infiltrated the host rock immediately above the cave. If they do share a common source, analysis of dissolved inorganic carbon (DIC) concentration , $\delta^{13}C_{DIC}$, and cation concentrations of the two waters could provide insight into epikarst processes such as CO_2 degassing and prior calcite precipitation (PCP) that are otherwise difficult to constrain.

Westcave Preserve includes outcrops of the Hensell Sand, the Cow Creek Limestone, and the Hammett Shale, with a small cave at the contact between the Cow Creek and Hammett formations. The overlying Hensell Sand contains water that emerges at the surface as a spring near the cave. Water also drips directly into the cave, forming speleothems. Previous research has established that although $\delta^{18}O$ values of rainfall in the area vary seasonally, between -10.5 and 1.1‰ with a weighted mean of -6.5‰ (VSMOW), the drip-water varies only between -4.7 and -4.3‰ with a weighted mean of -4.5‰ (Feng et al., in press). This suggests a well-mixed reservoir above the cave.

The soils above the cave have high CO_2 of up to 17,500 ppmv, but because the cave is shallow with multiple large openings, cave CO_2 levels are near-atmospheric (Casteel and Banner, 2011). This creates a steep CO_2 gradient between the soil and the cave air.

The drip water and spring water have similar Na^+, K^+, Mg^{2+}, Cl^-, SO_4^{2-}, and NO_3^{2-} concentrations, but the spring water has significantly higher Ca^{2+} and HCO_3^- concentrations. This suggests the waters share a source, but that the drip waters have had more PCP occur than the spring water. Assuming all differences in Ca^{2+} are due to PCP, additional DIC must be lost from the drip waters, likely through degassing as the water percolates down the CO_2 gradient towards the cave ceiling. If the spring represents the source of the drip water, and PCP accounts for all loss in Ca^{2+} concentration, the calculated $\delta^{13}C$ value of degassed CO_2 is -45 to -50‰ VPDB.

Keywords: Speleothems, Paleoclimate, Aqueous Geochemistry, Stable Isotopes

CCG-6

Constraints on transient fast flow at South Pole in the last glacial cycle

Cavitte, M.G.P.[1], Blankenship, D.D. [1], Johnson, J.V.[2], Young, D.A.[1], Carter, S.P.[3], Gutowski, G.R.[1], Siegert, M.J.[4], Jackson, C.S.[1]
mcavitte@ig.utexas.edu
1. UTIG, The University of Texas at Austin, Austin, TX
2. College of Arts and Sciences, University of Montana, Missoula, MT, United States
3. Institute of Geophysics and Planetary Physics, Scripps Institution of Oceanography, La Jolla, CA, United States.
4. School of Geographical Sciences, Bristol University, Bristol, United Kingdom

Many parts of the East Antarctic Ice Sheet remain to be explored: in particular the South Pole region, where the lack of satellite data has limited our understanding of a key part of the East Antarctic interior. South Pole has been assumed to be a very stable part of the ice sheet, which drove the siting of the IceCube neutrino detection experiment. However, airborne radar data collected by UTIG between South Pole and the Trans-Antarctic Mountains has revealed a history of fast flow transients as evidenced from the disturbed radar layer record (Bingham et al, 2007). We further constrain the spatial and temporal extent of these perturbations in the ice sheet flow through the tracing and analysis of a set of extensive radar layers. This radio-stratigraphy has been age correlated with the IceCube dust age-depth record and the SPRESSO core timescale; vertical variations in age-depth across the South Pole region indicate enhanced flow at the height of the last glacial maximum, between 50 ka and 10 ka. Dating uncertainties are constrained for each radar layer as a function of the resolution of the radar system and the SNR of the layer record (Cavitte et al., in review).
The South Pole radio-stratigraphy shows distinct ice stream margins with an asymmetry suggestive of a complex temporal evolution of the margins. Paleo accumulation rates reconstructed from the radar layers via 1D strain modeling show anomalous linear accumulation features, suggestive of localized enhanced melt rates, consistent with the presence of subglacial lakes in the area (Peters et al, 2008). The dynamic relationship between accumulation rates and melt rates due to ice streaming is used to reconstruct potential ice streaming velocities in the past.

We numerically investigate a variety of ice stream geometries as well as the spatial migration of their margins through time, using a transverse 2D flow model, in which we compare and contrast discrete vs. continuous margin evolution, and hypothesize the distribution of basal melt corresponding to these scenarios.

Presence of fast flow reaching deep into the interior of the Antarctic Ice Sheet has crucial ramifications for ice sheet stability with implications for rapid sea level rise; our study will also support the "SPICECORE" intermediate ice coring in the South Pole area where the complex flow history will need to be understood in order to obtain a reliable age-depth reconstruction.

Keywords: remote sensing, ice stream dynamics, Antarctica, modeling.

CCG-7

Convective invigoration and lifecycle enhancement by Aerosols-Cloud Field Couple over the Tropical Region using the A-Train and ISCCP Satellites Datasets

Chakraborty, S.[1], Fu, R.[1], Massie, S.[2]
sudipm@utexas.edu
1. Jackson School of Geosciences, The University of Texas at Austin, Austin, TX
2. National center for atmospheric research, Boulder, CO

The influence of aerosols on cloud and precipitation on climate scales has been suggested by some numerical simulations and observational studies. However, counter examples also exist and whether the claimed influence is significant in general on climate scale remains unclear, in part due lack of information related to cloud life cycle. To address this limitation, we use along-track NASAA-Train satellites data, modern era retrospective – analysis for research and applications, and International Satellite Cloud Climatology Project (ISCCP) deep convection tracking data to evaluate interaction between aerosol and mesoscale convective systems as a function of convective life cycle. We have estimated the influence of aerosol on cloud microphysics over the regions of South Asia (0˚-40˚N, 70˚-100˚E), the Congo (10˚N-10˚S; 10˚W-40˚E), and the Amazon (5˚N-15˚S; 40˚W-80˚W) during June 2006 to May2008, when all these datasets were available Our results suggest a statistical significant correlation between an increase of cloud ice-to-liquid ratio associated with an increase of aerosols optical depth (AOD) over these three tropical continents during the two years analysis period ($p<5\%$), especially during the growing and mature phases of the convective life cycle. During the growing phase of the convective systems, the vertical wind shear appears to have strongest influence on the cloud ice-to-liquid ratio than AOD, whereas during the mature phase, AOD appears to have comparable influence to the vertical wind shear. Numerical of the convective core and radius of the convective systems have less influential compared to the vertical wind shear and AOD. The ice water content of the convective anvils, measured by AURA Microwave Limb Sounder, are also positively correlated with the AOD, as well as with the related humidity at 850 hPa, during the growing and mature phases of the convective systems. Whereas during the decay phase of the convective system, the anvil ice water is negatively correlated with the ambient AOD. We also explore the relationship between the convective lifecycle, ambient AOD, vertical wind shear and relative humidity, as well as size of the convective systems. Ambient AOD does not appear to be correlated with the convective duration at any stage of their lifecycle. Convective life time appear to be dominated by the convective dynamic structure, such as the radius, the number of convective cores, convective fraction of the convective systems, and the ambient relative humidity and vertical wind shear. Our work demonstrates that a clear dependence of the convection-aerosol relationship on the convective life cycle, and the potential of more clear diagnosis of the aerosols influence on convective system, relative to other ambient and convective dynamic conditions.

Keywords: Aerosol, Deep Convection

CCG-8

Investigation into the carbonate clumped isotope geothermometer through multi-variable controlled laboratory grown calcite

Charlton, T.[1], Banner, J.[1], Breecker, D.[1]
timcharlto@yahoo.com
1. Jackson School of Geosciences, The University of Texas at Austin, Austin, TX

A new geothermometer with application to carbonate minerals is known as the 'clumped isotope' method. Clumped isotope refers to substitution in the carbonate mineral lattice of multiple isotopologues of the minor isotopes of carbon and oxygen. This provides a potential climate proxy when applied to cave calcite deposits (speleothems). Speleothems are uniquely situated to potentially provide a robust climate proxy for the Quaternary due to their broad geologic distribution and their ability to preserve high-resolution geochemical variations. By investigating the statistical overabundance of ^{13}C-^{18}O bonds (Δ_{17}) compared to a random distribution in the sample, clumped isotope analysis is possible without inference of the formation water chemistry. This bypasses the major hurdle encountered when using traditional carbon and oxygen isotopes ($\delta^{13}C$ and $\delta^{18}O$) for paleoclimatic reconstructions. For the majority of biogenic and abiogenic calcite examined using the clumped method, there is a linear relationship between Δ_{17} and T. Speleothem calcite does not plot on the calibration line. There are several potential mechanisms responsible for this disequilibrium. Degassing effects, impact physics or biochemical fractionation could be in effect in cave environments. Due to the complex geochemistry, geobiology and hydrology leading to calcite deposition, no single in-situ study is able to quantify the potential variables and there has not been a laboratory experiment operating under realistic pCO_2 that could analyze the likely potential variables.

By creating a laboratory device in which degassing rate and impact physics can be controlled in cave-analogous conditions, the control on speleothem disequilibrium relative to other calcite formation environments can be assessed. Once quantitatively recognized, calibration equations may be generated that will provide climate researchers with a means to increase the accuracy of terrestrial climatic reconstructions.

Keywords: clumped isotopes, isotopologue, speleothem, climate

CCG-9

Relative contributions of postcranial and purported ecological characters in phylogenetic analyses of Crocodylomorpha

English, L.[1]
englishl@utexas.edu
1. Jackson School of Geosciences, The University of Texas at Austin, Austin, TX

Crocodylomorphs were an originally highly diverse group of archosaurs that have been known to demonstrate clear but conflicting signals in phylogenetic analyses. Most morphological characters used in these analyses are cranial and many of them are considered to be primarily influenced by ecological niche (e.g., longirostrine skull) or to almost exclusively reflect phylogenetic history (i.e., skull bone configurations and basicranium), which have been suggested to be the source of these conflicting signals. A preliminary reverse successive weighting analysis of a small dataset by Wu and Sues (1996) spanning all of Crocodyliformes suggests that postcranial characters and putative eco-morphological characters provide the dominant "phylogenetic" signal, and characters thought to be independent of ecology provide inconsistent signals. To test whether this pattern was simply a phenomenon of this particular dataset or if it holds true for larger more inclusive datasets, another reverse successive weighting analysis and a data partitioning analysis was performed on the dataset compiled by Wilberg (2012). The results of this second analysis suggests that neither characters traditionally regarded as ecological nor phylogenetic had as much of an impact on tree topology as other characters which are thought to be influenced by both or have never been evaluated. However, these analyses did support the finding that the few postcranial characters coded had a disproportionately large influence on tree topology.

Keywords: Crocodylomorpha, Thalattosuchia, *Gavialis*, reverse successive weighting, paleontology, systematics, characters

CCG-10

Subglacial sedimentary basin characterization of Wilkes Land, East Antarctica via applied aerogeophysical inverse methods

Frederick, B.C.[1], Gooch, B.T.[1], Richter, T.G.[1], Young, D.A.[1], Blankenship, D.D.[1], Aitken, A.R.A.[2], Siegert, M.J.[3]
Bruce@ig.utexas.edu
1. Institute for Geophysics, Jackson School of Geosciences, University of Texas, Austin, Texas, UNITED STATES;
2. School of Earth and Environment, The University of Western Australia, Perth, Western Australia;
3. School of GeoSciences, The University of Edinburgh, Edinburgh, UK;

Topography, sediment distribution and heat flux are all key boundary conditions governing the stability of the East Antarctic ice sheet (EAIS). Recent scientific scrutiny has been focused on several large, deep, interior EAIS basins including the submarine basal topography characterizing the Aurora Subglacial Basin (ASB). Numerical ice sheet models require accurate deformable sediment distribution and lithologic character constraints to estimate overall flow velocities and potential instability. To date, such estimates across the ASB have been derived from low-resolution satellite data or historic aerogeophysical surveys conducted prior to the advent of GPS. These rough basal condition estimates have led to poorly-constrained ice sheet stability models for this remote 200,000 sq km expanse of the ASB. Here we present a significantly improved quantitative model characterizing the subglacial lithology and sediment in the ASB region. The product of comprehensive ICECAP (2008-2013) aerogeophysical data processing, this sedimentary basin model details the expanse and thickness of probable Wilkes Land subglacial sedimentary deposits and density contrast boundaries indicative of distinct subglacial lithologic units. As part of the process, BEDMAP2 subglacial topographic results were improved through the additional incorporation of ice-penetrating radar data collected during ICECAP field seasons 2010-2013. Detailed potential field data pre-processing was completed as well as a comprehensive evaluation of crustal density contrasts based on the gravity power spectrum, a subsequent high pass data filter was also applied to remove longer crustal wavelengths from the gravity dataset prior to inversion. Gridded BEDMAP2+ ice and bed radar surfaces were then utilized to establish bounding density models for the 3D gravity inversion process to yield probable sedimentary basin anomalies. Gravity inversion results were iteratively evaluated against radar along-track RMS deviation and gravity and magnetic depth to basement results. This geophysical data processing methodology provides a substantial improvement over prior Wilkes Land sedimentary basin estimates yielding a higher resolution model based upon iteration of several aerogeophysical datasets concurrently. This more detailed subglacial sedimentary basin model for Wilkes Land, East Antarctica will not only contribute to vast improvements on EAIS ice sheet model constraints, but will also provide significant quantifiable controls for subglacial hydrologic and geothermal flux estimates that are also sizable contributors to the cold-based, deep interior basal ice dynamics dominant in the Wilkes Land region.

Keywords: Basin analysis, Antarctic geology, Subglacial sedimentary basin modeling, Cryosphere modeling, Antarctic glacier processes, Antarctic potential fields,

CCG-11

Bayesian Uncertainty of Thwaites Glacier Catchment Radar Stratigraphy

G. Gutowski[1], C.S. Jackson[1], D.D. Blankenship[1], D. A. Young[1]

Information about the history and dynamics of ice sheets is contained in basin-scale radar sounding surveys. Englacial, isochronous radar horizons traced throughout the sampled domain of these basins can give a three-dimensional picture of past ice flow by revealing significant details of deformation within the ice column. We focus our efforts in the Thwaites Glacier catchment, West Antarctica, which previous studies have shown to be a bellwether in future WAIS deglaciation scenarios.

Here we present a Bayesian determination of the age-depth profile at the Byrd ice core, Antarctica, based on robust uncertainty estimates in ice core ages and radar sounding depths. A simple ice flow model is used to determine the age-depth relationship in ice near the core and a Markov Chain Monte Carlo technique is used to sample a posterior distribution of age as a function of depth to within uncertainty.

We propagate the age-depth information, including uncertainty, for several prominent radar reflectors from the Byrd ice-coring site in the Interior Ross Embayment across the ice divide and throughout the Thwaites Glacier catchment using airborne ice-penetrating radar data collected and processed by the University of Texas Institute for Geophysics.

Keywords: Antarctica, radar, uncertainty, ice, Bayesian

CCG-12

Investigating the Influence of the 2011 Texas Drought on Vegetation Cover Characteristics

Halubok, M.[1], Shi, M.[2], Yang, Z-L.[1]
m.halubok@gmail.com
1. Jackson School of Geosciences, The University of Texas at Austin, Austin, TX
2. California Institute of Technology Jet Propulsion Laboratory, Pasadena, CA

Severe droughts are nothing new to Texas. Climate proxies such as tree rings clearly indicate that this region is prone to cycles of droughts which lead to significant vegetation and wildlife losses while making survival difficult for human inhabitants as well. As the state's most extreme single-year drought in history, the 2011 drought caused loss of approximately 300 million trees, as much as 6 percent of all trees in the state (Texas Forest Service Press Release 09/25/2012).

The primary purpose of this study is to identify the influence of high air temperatures and extremely low amounts of precipitation during the 2011 drought on vegetation cover properties with special attention to tree mortality. In order to address this question, the Community Land Model's Dynamic Global Vegetation Model version 4 (CLM4-DGVM) was used. Using mechanistic parameterizations of large-scale vegetation processes, this model simulates the distribution and structure of natural vegetation dynamically. The preliminary results of model simulations show that during the drought year of 2011 tree cover almost disappeared in West Texas and decreased significantly in East Texas in comparison with the 2004 climate regime. Moreover, vegetation cover maps which are result of substituting either high temperatures or low precipitation of 2011 into the 2004 climate scenario indicate that 1) high air temperatures alone do not cause considerable changes in vegetation cover in the model, 2) region with maximal tree loss tends to be placed in the south-east of Texas under the "dry" regime, 3) combination of high temperatures and low precipitation observed in the drought year of 2011 is responsible for expanding the area of tree loss.

Keywords: Community Land Model's Dynamic Global Vegetation Model, vegetation cover, tree mortality, drought.

CCG-13

Controls on modern speleothem calcite growth in a central Texas cave and implications for paleoclimate reconstruction

Hatch, R.[1], Banner, J.[1], Wong, C.[2]
rlhatch@utexas.edu
1. Jackson School of Geosciences, The University of Texas at Austin, Austin, TX
2. Univ. of California at Davis , Department of Geology, Davis, CA 95616

A 12-year monitoring study in a central Texas cave provides insight into the seasonal controls on modern calcite growth. Speleothems, or cave calcite deposits, are commonly used as climate proxies due to their ability to record paleoenvironmental change. Speleothem trace element ratios, such as Mg/Ca, Sr/Ca and Ba/Ca, have been used to reconstruct relative rainfall variations. To interpret past rainfall variations from speleothem trace element ratios, the processes controlling the incorporation of drip-water trace elements into speleothem calcite must be known. Growth rate, saturation state, and temperature are all factors that have the potential to influence trace element partitioning coefficients. This study compares the variables controlling calcite growth with the factors controlling dripwater and modern calcite trace element ratios in order to better interpret speleothem records. While the factors controlling growth rate are well established theoretically, observing the system empirically enables the assessment of the relative dominance of each factor on calcite growth rates. Cave-air temperature and CO_2 concentrations, relative humidity and drip rate were measured each month at multiple drip sites in Natural Bridge Caverns, central Texas beginning in 2001. Artificial substrates (glass-plates) were placed at five of these sites and collected monthly to determine growth rate. While previous studies have determined changes in substrate calcite growth rate are driven by drip rate and density-driven ventilation of cave-air CO_2, the research here focuses on how variations in dripwater trace element ratios are related to variations in calcite growth. Dripwaters at two sites in Natural Bridge (NBBC and NBWS) were analyzed for Mg/Ca, Sr/Ca and Ba/Ca ratios to determine the relationship between trace elements in drip water and the parameters affecting calcite growth rate. At site NBBC, trace element ratios are negatively correlated with CO_2 concentrations (r^2=0.55, $p<0.01$) reflecting changes due to seasonal ventilation in cave-air CO_2 concentrations driven by differences between surface- and cave-air temperatures. At NBWS, trace element ratios are most strongly correlated with drip rate (r^2=0.31, $p<0.05$), but do not show seasonal variation. Trace element concentrations were also measured on calcite grown on glass plates at NBWS, using both solution-mode and laser-ablation ICP-MS. The ratios were not found to correlate to either drip rate or CO_2 for the time period analyzed. The trace-element distribution coefficient, a measure of the degree to which trace elements are incorporated into calcite, is relatively constant throughout the time period analyzed. Determining the trace element partitioning coefficient is important for determining the extent to which speleothem calcite tracks changes in dripwater chemistry. The relationships observed in this study are important in understanding speleothem trace element changes where variations in both CO_2 and rainfall have the potential to influence the dripwater chemistry.

Keywords: Speleothem, calcite, trace elements, paleoclimate

CCG-14

Regional assessment of geochemical response in cave drip waters to recent drought, central Texas, USA

Hulewicz, M.[1], Banner, J.L.[1]
hulewicz@utexas.edu
1. Jackson School of Geosciences, The University of Texas at Austin, Austin, TX

In 2011, Texas suffered from one of the worst dry periods recorded in the state's climatic history and drought conditions have persisted ever since. Identifying a geochemical signal of drought in cave drip water is important so that signals can be reconstructed in speleothems as paleoclimate records. Knowledge of drought periodicity in the past will help our understanding of drought recurrence in the future. Better constraints on the variation of geochemical parameters in response to regional drought may also lead to an improved understanding of changes in flow paths within the vadose zone as a function of rainfall. A range of geochemical proxies for relative rainfall variation can be applied to drip waters from caves in central Texas, including $\delta^{18}O$ values, which may tell us about relative rainfall amounts. If prolonged drought conditions of 2011-2013 are reflected in the drip water $\delta^{18}O$ values, a threshold for duration and severity of drought may be constrained. As proxies, $^{87}Sr/^{86}Sr$ values and trace element ratios (Mg/Ca and Sr/Ca) can provide insight into water-rock interaction pathways and changes in residence time of water in the vadose zone. Longer residence times are associated with drier climatic periods. A regional assessment of geochemical response to drought may provide more detailed information on processes controlling water chemistry and the regional vs. local scale of those processes. We will determine the extent to which drip sites from three spatially distributed caves are fed by either conduit flow or matrix flow based on drip rate and its covariation with changes in effective precipitation. Based on these results, we will analyze drip waters collected monthly as part of a long-term monitoring project from 2010 to 2013 for $\delta^{18}O$, $^{87}Sr/^{86}Sr$ values, and trace elements. Results may have implications for the understanding of water-rock interaction and residence time of water in karst systems during severe drought, as well as the interpretation of geochemical variations in speleothems as paleoclimate records.

Keywords: Cave drip water, Stable isotopes, Trace elements, Drought,

CCG-15

Positive Response of Indian Summer Rainfall to Arabian Dust

Jin, Q[1], Wei, J[1], Yang, Z.-L.[1]
Jinqj10@utexas.edu
1. Jackson School of Geosciences, The University of Texas at Austin, Austin, TX

Aerosols scatter and absorb solar radiation, thereby reducing its flux reaching the Earth's surface. These processes not only affect temperature and pressure in the low troposphere, but also alter local and regional atmospheric circulations and precipitation. Such aerosol effects depend on the spatial distribution of aerosols and their interactions with meteorological factors. Here, we study the impact of Arabian dust aerosols on the Indian summer monsoon (ISM) rainfall, employing 13-year datasets of satellite observations and meteorological reanalyses. Satellite-retrieved aerosol optical depth (AOD) shows the Arabian Sea (AS) experiences the highest aerosol loadings in the ISM season in each year. Correlation analyses and back-trajectory simulations indicate that high AOD over the AS is mainly due to the dust aerosols transported from the Arabian Peninsula (AP) by strong summer northwesterly winds (namely "Shamal"). Using AOD and surface-based rainfall observations datasets, we find for the first time that these aerosols over the AS and the southern AP are significantly correlated (R=0.5) with rainfall over central and eastern India during the ISM season. This correlation is attributed to aerosol-induced enhancement of the meridional thermal contrast, which in turn strengthens the ISM circulation and moisture transport from the AS to the Indian subcontinent. We further show that the interaction timescale between aerosols and the ISM rainfall is within one to two weeks. Our findings highlight the radiative effect of Arabian dust on the ISM large-scale circulation and rainfall on weekly timescales, and motivate more studies focusing on the contribution of Arabian dust aerosols to the observed ISM rainfall trend on longer (e.g. interannual and decadal) timescales.

Keywords: dust aerosols, sea surface temperature, Indian monsoon, and rainfall

CCG-16

Examination of Gentoo Penguin (*Pygoscelis papua*) Feather Microstructure

Kulp, F.[1], Clarke, J.[1], and Shawkey, M.[2]
fkulp@utexas.edu
1. Jackson School of Geosciences, The University of Texas at Austin, Austin, TX
2. Biology Department and Integrated BioScience Program, University of Akron, Akron, OH

Penguins are unique birds when it comes to their feathers and color production. In addition to abnormally large melanosomes (pigment-containing organelles) and a novel yellow pigment in the feathers of some species, penguins produce blue structural color via different internal feather microstructures than any other blue-colored bird. These structures comprise ß-keratin nanofiber bundles that coherently scatter light and thus reflect blue wavelengths. However, the nanofibers have only been found in the blue feathers of one penguin species, the Little Penguin (*Eudyptula minor*), although they have been reported to be in other penguin species. I assessed the presence of nanofibers in the black and white feathers of the Gentoo Penguin (*Pygoscelis papua*) in order to assess the distribution of the nanofibers in penguins. I also examined the color properties of these penguin feathers. Feather barbs from the white and black feathers were embedded and sectioned in resin and observed using scanning electron microscopy and transmission electron microscopy. The reflectance spectra of whole feathers were obtained using an Avantes AvaSpec-2048 spectrophotometer. Specular (mirror-like) reflectance spectra were obtained at 30° and 80° to horizontal. Diffuse reflectance spectra were also obtained using an integrating sphere so that glossiness could be calculated. Keratin nanofibers were found in black feathers and not in white feathers. More analyses will be performed to further examine Gentoo penguin feather microstructure.

Keywords: Penguin, feathers, microstructure, structural color

CCG-17

The use of multiple radiative transfer models for snow in radiance assimilation

Kwon, Y.[1], Zhang, Y. [1], Yang, Z. -L.[1], Toure, A. M.[2,3], Hoar, T. J. [4], Rodell, M.[2], Picard, G.[5]
yhkwon@utexas.edu
1. Jackson School of Geosciences, The University of Texas at Austin, Austin, TX
2. Hydrological Sciences laboratory, Code 617, NASA GSFC, Greenbelt, MD
3. Universities Space Research Association (USRA), Columbia, MD
4. The National Center for Atmospheric Research, Boulder, Colorado
5. UJF – Grenoble 1/CNRS, UMR5183, Laboratoire de Glaciologie et Géophysique de l'Environnement (LGGE), Grenoble, France

Land data assimilation has been an important tool to obtain the distribution of snow depth and snow water equivalent (SWE), which are critical for climate and water resource applications. In radiance assimilation (RA), passive microwave brightness temperature (T_B) observations are assimilated into a land surface model (LSM) that incorporates a microwave radiative transfer model (RTM) as an observational operator. RA has been successfully used by previous studies to update SWE simulations at point, local, and basin scales. However, obtaining SWE at continental scales demands a substantial amount of further research. In this study, we hypothesize that errors related to RTM uncertainties at a continental scale can be reduced by using multiple snowpack RTMs (i.e., multi-RTM ensemble RA) that are based on different theories. We use the Community Land Model version 4 (CLM4) and two snowpack RTMs, the Microwave Emission Model for Layered Snowpacks (MEMLS) and the Dense Media Radiative Transfer–Multi Layers model (DMRT-ML). We assimilate the Advanced Microwave Scanning Radiometer-Earth Observing System (AMSR-E) T_B observations into the coupled CLM4/DMRT–ML and CLM4/MEMLS using the Data Assimilation Research Testbed (DART) developed by the National Center for Atmospheric Research (NCAR). We address the impacts of snowpack stratigraphy, vegetation canopy structure, and different parameterizations of snowpack physics on radiance assimilation and SWE retrieval. The RA results are compared with the Canadian Meteorological Centre (CMC) snow observations.

Keywords: Snow water equivalent, Radiance assimilation, Passive microwave brightness temperature, Land surface model, Radiative transfer model

CCG-18

Redescription of platypus (Ornithorhynchus anatinus) teeth and epithelial plates: morphological, evolutionary, and systematic implications

Latimer, Ashley[1]
Latimer.ae@utexas.edu
1. Jackson School of Geosciences, The University of Texas at Austin, Austin, TX

Deciduous teeth and thickened epithelial plates of the extant platypus *Ornithorhynchus anatinus* are sparsely figured in literature due to specimen rarity in collections. New CT, SEM, and thick section images of these teeth and plates contribute to the understanding of mammal evolution, unique species morphology, and change the way the teeth have been used in phylogenetic analysis. The evolutionary history of mammals, including extinct taxa, is mainly reconstructed using teeth and employs terminology based on non-monotreme mammals. While adult monotremes are edentulous, juvenile platypuses have teeth useful to compare with extinct monotremes, but terminology can be a barrier to efficient comparison to non monotreme mammals. Transverse lophs on monotreme teeth contain complexity not reflected in cusps alone, unlike therian mammals. This difference reinforces the need for caution when applying dental terminology produced for other mammals. New imagery highlights potentially phylogenetically informative morphology, including the pulp cavity and roots. The teeth of the juveniles are also variable, and analysis of new imagery identifies characters stable enough for comparison.

While the roots of the juvenile teeth degenerate, the epithelium below the teeth thickens into epithelial plates. New images of the epithelial plates offer insight into a series of tubes centered under the juvenile teeth. The tubes are a continuous conduit to the plate surface, potentially enervated, suggesting an extended sensory system in the extant platypus seen nowhere else among mammals.

Keywords: *Ornithorhynchus anatinus*, platypus, monotremes, teeth, dental terminology, character choice, epithelium, paleontology

CCG-19

Effect of Hydrodynamic Dispersion on CO2 Convective Dissolution

Yu Liang1, 2, Marc Hesse 1, David Dicarlo2

liangyu@utexas.edu
1. Department of Geological Sciences, The University of Texas at Austin, 1 University Station C9000, Austin, TX 78712, USA
2. Department of Petroleum and Geosystems Engineering, The University of Texas at Austin, 1 University Station C0300, Austin, TX 78712, USA

Carbon capture and storage in deep geological formations has the potential to reduce anthropogenic carbon dioxide (CO2) emissions from industrial point sources. The technology is only viable, if the long-term security of the geological CO2 storage can be demonstrated. Dissolution of CO2 into the brine, resulting in stable stratification, has been identified as the key to long-term storage security. Here we present new analogue laboratory experiments to characterize convective dissolution and to study the effect of hydrodynamic dispersion on the CO2 convective dissolution. Understanding the effect of hydrodynamic dispersion is essential to evaluate whether convective dissolution occurs, as well as to predict how fast it occurs in the field. The effect can also be applied to estimate the security of geological CO2 storage fields. In particular we want to optimize related simulation work by including the dispersion effect for the first time.

The large experimental assembly will allow us to quantify in detail for the first time the relationship between convective dissolution rate and the controlling factors of the system, including permeability and driven force, which could be essential to trapping process at Bravo Dome. Convective dissolution rate is represented by the Sherwood number and controlling factors are presented by the Rayleigh number. By conducting experiments in the system carefully we find previous definition of Rayleigh number is not enough to describe the convective motion, and we advocate a new Rayleigh number including dispersion effect. Then we conduct related experiments and optimize simulation to understand this hydrodynamic dispersion effect, which also plays an important role in the geological CO2 dissolution at Bravo dome. Also we plan to complement the homogeneous experiments with a detailed study of the scaling law of the convective flux in heterogeneous, layered media with dispersion effect; in particular, low permeability layers are ubiquitous in geological storage formations and have been observed at Bravo Dome. We plan to measure the reduction in the convective flux due to these barriers compared to that in homogeneous media, to determine if convective dissolution is an important trapping process at Bravo Dome.

Keywords: CO2 Sequestration, CO2 Dissolution Trapping, Dispersion, Bravo Dome

CCG-20

Evaluation and Post-Processing on the Climate Forecast System Version 2 (CFSv2) as Meteorological Forcing to a Test-Bed Seasonal Streamflow Forecasting System

Lin, P.[1], Yang, Z.-L.[1]
prlin@utexas.edu
1. Jackson School of Geosciences, The University of Texas at Austin, Austin, TX

Streamflow forecast with seasonal lead times (i.e. 3-9 months) is important for reservoir operations, water management, and flood/drought warning; the predictive skill of which is essential in ensuring appropriate decision-making. In an experimental streamflow forecast system which attempts to integrate atmospheric forcing from the second version of Climate Forecast System (CFSv2), the state-of-the-art land surface model Noah-MP (Noah-MP LSM), and the hydrologic river routing model RAPID, the uncertainties in prediction can be traced back to three sources: 1) atmospheric forcing biases and downscaling errors; 2) uncertainties in runoff parameterization in the LSM; and 3) inappropriate representation of horizontal river transport in the routing scheme.

In this study, the error source from atmospheric forcing is examined closely by firstly evaluating 25-year historical CFSv2 forecasts (hindcasts) with NLDAS-2 forcing (reference data) over Texas. Precipitation field, the most important driver for land surface hydrological processes, is then post-processed using an empirical quantile-mapping (QM) and spatial interpolation technique to reduce model biases and match the spatial scales of CFSv2 (~100-km) with that of the hydrologic models (generally ~12.5-km). A set of real-time runoff forecast (up to June 2014) is derived by feeding Noah-MP with bias-corrected/spatially-downscaled CFSv2, and compared with original CFSv2 runoff forecast. It is shown that meteorological variables other than precipitation (e.g. solar radiation, wind, humidity, surface air temperature, surface air pressure) are predicted reasonably well by CFSv2 hindcasts. Post-processing on precipitation field such as bias-correction and downscaling before driving Noah-MP LSM is more effective than directly processing runoff forecasts in CFSv2, which is important in terms of improving hydrologic predictive skills in the proposed seasonal streamflow forecast system.

Keywords: Seasonal streamflow forecast, CFSv2, precipitation bias-correction/downscaling, Noah-MP, RAPID

CCG-21

Eocene *Gyrolithes*-*Thalassinoides* ichnocoenoses from Alabama and Peru: implications for marine vertebrate taphonomy

Lively, Joshua Ryan[1]
joshuarlively@utexas.edu
1. Jackson School of Geosciences, The University of Texas at Austin, Austin, TX

Ichnocoenoses dominated by *Gyrolithes* and *Thalassinoides* were observed at two middle Eocene (Bartonian) localities, one in the coastal plain of Alabama and the other in the Pisco Basin of Peru. These localities are significant because they both preserve archaeocete cetaceans and other important marine vertebrates. *Gyrolithes* is a vertical, helically-coiled burrow found in marginal marine settings. This burrow is commonly attributed to crustaceans, and often grades into other burrows linked to crustacean trace-makers, particularly *Thalassinoides* and *Ophiomorpha*. At both localities described in this study, *Gyrolithes* and *Thalassinoides* are the only trace fossils present in the units they are observed.

At a locality in the upper Lisbon Formation of Alabama, *Gyrolithes* and *Thalassinoides* exhibit bioglyphs parallel to the axis of the burrows, suggesting the trace-maker burrowed into a chalky firmground. This may be indicative of erosion of surface softground substrates during rapid regression, exposing underlying firmground substrates to bioturbation by *Gyrolithes*-producing organisms. A specimen of the protocetid cetacean *Georgiacetus* was collected from shoreface sands within a transgressive sequence at this locality. In the Paracas Formation of Peru, *Thalassinoides* are preserved as convex hyporelief on the base of a sandstone event bed overlying laminated siltstones and claystones. *Gyrolithes* descend from this network of *Thalassinoides* into the mudstone. The Peruvian traces likely represent "doomed pioneers" that at least temporarily colonized a muddy softground below wave base following a high-energy event. Facies similar to the *Gyrolithes*-bearing mudstone within the Eocene of the Pisco Basin preserve protocetids, basilosaurids, and a giant basal penguin, the latter of which exhibits soft tissue preservation. The sedimentology and ichnology of these localities suggest preservation in a shelf setting frequently affected by high-energy events.

The ichnocoenosis of *Gyrolithes* and *Thalassinoides*, in concert with sedimentologic observations, provides insights into the taphonomy of these marine vertebrates. This repeated trace fossil association in different sedimentary sequences may imply common environmental conditions during the middle Eocene at these localities.

Keywords: Eocene; ichnology; *Gyrolithes*; *Thalassinoides*; Alabama; Peru

CCG-22

Identifying spatial heterogeneity in the elemental concentration of Early Jurassic dinosaur bones: implications for the direct radiometric dating of fossil bone

Marsh, A. D.[1]
admarsh@utexas.edu
1. Jackson School of Geosciences, The University of Texas at Austin, Austin, TX

In life, bone is a complex structure composed mostly of organic and inorganic phases. Bone cells lay down the organic collagen framework around which carbonated hydroxylapatite ($Ca_{10}(PO_4,CO_3)_6OH_2$) is mineralized. Bone has a porous macroscopic and microscopic texture owing to the number of osteocyte lacunae, blood vessel canals, cancellous openings, and spaces between hydroxylapatite crystallites. This enormous internal surface area and available volume makes bone quite reactive and soluble during fossilization, which generally takes the form of recrystallization of the bioapatite and permineralization in the pore spaces. Fossil bone also is known to be an excellent reservoir for non-biologic metals and trace elements, which can be concentrated in bone in quantities orders of magnitude greater than those of adjacent sediments.

Here, I report concentrations of major and trace elements in two fossil dinosaur bones from the Early Jurassic Kayenta Formation of northeastern Arizona measured using electron-dispersive spectroscopy, laser ablation and solution mode ICP-MS, and high-resolution multicollector LA-ICP-MS. The P in the hydroxylapatite decreases moving away from the surface of the bone, suggesting that more recrystallization occurred closer to the outer regions of bone. Other elements commonly found in fossil bones such as Sr, Ba, Y, Mn, and Fe are also found in these dinosaur bones. Sr reflects the concentration of P, because it substitutes for Ca in the bioapatite crystal lattice. Mn and Fe concentrations are opposite to one another, where Fe is especially concentrated in regions of lamellar bone growth that include red iron oxide mineralization. Ba is found primarily as authigenic barite that grew in the larger open spaces in the medullary cavity in the middle of the bone. U concentrations in these two bones can be as high as 14,000 ppm and the Pb concentrations are highly variable within them.

Ever-advancing technologies in geochemistry are allowing researchers to explore fossil bone in ways that have previously been impossible. Recent efforts to obtain U-Pb dates directly from fossil bone lent support to the hypothesis that some groups of non-avian dinosaurs survived the Cretaceous-Paleogene mass extinction. I utilized those same methods on Early Jurassic dinosaur bones, but recovered much younger dates that were not corroborated by the overwhelming lithostratigraphic and biostratigraphic evidence that suggest an Early Jurassic age. Results from my investigations suggest that such methods can be significantly biased by open-system behavior in the reactive fossil bone.

Keywords: Fossilization, bone, hydroxylapatite, Kayenta Formation, Jurassic, ICP-MS

CCG-23

Cranial Anatomy of *Notochelys platynota*

Muller, S.[1], Bell C.[1], Burroughs, R.[1]
ssmuller@utexas.edu
1. Jackson School of Geosciences, The University of Texas at Austin, Austin, TX

Notochelys platynota is an endangered turtle native to various parts of southeast Asia. *Notochelys platynota* traditionally was classified as a batagurid turtle, a poorly understood group of mostly Asian freshwater turtles. There is little published information about the biology, natural history, and morphology of *Notochelys platynota*. Brief physical descriptions are available in various books but it remains one of the most enigmatic batagurids. IUCN classifies the species as "data deficient" (IUCN, 2013). Previous authors provided brief comments on the morphology of *Notochelys platynota* but produced conflicting results (Hirayam, 1985; Joyce and Bell, 2004). We provide a detailed description of the cranial anatomy of *Notochelys platynota* in order to advance knowledge of the species and to help shed light on evolutionary relationships among batagurids. We used CT scans of the skull to document and illustrate anatomical details.

Keywords: Testudines, Bataguridae, *Notochelys platynota*, cranial anatomy

CCG, EG, SHP-24

Arsenic-redox controls Cyanobacteria and Chloroflexus abundance and carbon cycling in microbial mats at El Tatio Geyser Field, Chile

Myers, K.[1], Omelon, C.[1], Bennett, P.[1]
myers.kd@utexas.edu
1. Jackson School of Geosciences, The University of Texas at Austin, Austin, TX

Cyanobacteria and chloroflexus are important primary producers that form the basis of most hot spring microbial mat communities in waters between 30-74°C. Primary producers shape microbial mat communities by fixing the dissolved inorganic carbon (DIC) pool to organic carbon and providing nutrients for diverse microorganisms that perform a broad range of biogeochemical transformations. This study compares the microbial community structure and net primary production of cyanobacteria-based and chloroflexus-based microbial mats collected at El Tatio Geyser Field, a high elevation geyser complex in the Andes Mountains in Region II, Chile. In addition to extreme conditions imparted by high elevation and its location in the Atacama Desert, El Tatio has a suite of extreme geochemical stressors for life, including high arsenic as As(III) and As(V) (0.4-0.6 mM). El Tatio also has unusually low concentrations of DIC in some streams (0.1-0.3 mM), low enough to severely limit primary production in microbial mats. In contrast to other geothermal sites around the world where the abundance of cyanobacteria and chloroflexus is controlled primarily by temperature, observations of unusual patterns in their abundance at El Tatio suggest alternate controls, such as [DIC], [As(III)], and [As(V)]. For instance, we observe less biomass in low-DIC streams compared to nearby high DIC streams, and less biomass in high [As(III)], chloroflexus-dominated regions of low-DIC streams, compared to high [As(V)] locations that are dominated by cyanobacteria.

To investigate these patterns, a field assay was conducted to compare carbon assimilation at a cyanobacteria-dominated site and chloroflexus-dominated site in a low-DIC stream at El Tatio. Water temperature at the chloroflexus-dominated site was 60°C, arsenic-redox is dominated by high As(III), and the stream in this area contains sparse, red-colored mat material. In contrast, the downstream site is 40°C, dominated by high As(V), and composed of high-biomass green-pigmented microbial mat. The sequence abundance of the 60°C, high As(III) site is dominated by Phylum Chloroflexi (38%), and chemoautotrophy accounted for net DIC assimilation. The 40°C location, however, was dominated by Phylum Cyanobacteria (46%) with photosynthesis accounting for much higher net DIC assimilation, as well as much higher overall respiration, corresponding to a more active and productive microbial community. We observed no cyanobacteria at 60°C in this stream, even though it is well within their habitable temperature range and they are commonly observed at 60°C in other geothermal systems. Temperature is typically the only control on cyanobacterial diversity and abundance in geothermal systems, however at El Tatio cyanobacteria abundance has a strong negative association with [As(III)] (r^2=0.68, $p<0.05$). When only low-DIC sites are considered, cyanobacteria have a positive association with [As(V)] (r^2=0.85, $p<0.05$). Chloroflexus abundance is not significantly related to any environmental variables (r^2=0.09-0.22, $p>0.05$), but is significantly negatively associated with the abundance of cyanobacteria (r^2=0.59, $p<0.05$), suggesting competition between these two groups for limited DIC.

Keywords: El Tatio, geothermal, arsenic, carbon, geochemistry, microbial ecology, cyanobacteria, chloroflexus, primary production

CCG-25

Identification of a Congo Basin Walker Circulation and its Interaction with the West African Monsoon

Neupane, N.[1], Cook, K. H.[1], and Crétat, J.[1]
nareshneupane@utexas.edu
1. Jackson School of Geosciences, The University of Texas at Austin, Austin, TX

The Gulf of Guinea in the equatorial Atlantic is characterized by the presence of strong subsidence at certain times of the year. This subsidence, which suppresses convection over the region, appears in June and is well established from July–September. Since much of the West African monsoon flow originates over the Gulf of Guinea, this subsidence is important for determining the moisture sources for the West African monsoon. Using reanalyses products here we contribute to a physical understanding of what causes this seasonal subsidence, and how it relates to precipitation distributions across West Africa.

We identify a seasonal Walker circulation with upward branch over the Congo basin and downward branch over the eastern Gulf of Guinea in the ERA Interim, ERA40, NCEP2, and MERRA reanalyses. The subsiding branch diverges at 2°W near the surface, with winds to the east flowing toward the Congo basin to complete the overturning circulation. The Walker circulation is driven and maintained by surface temperature differences between the eastern Gulf of Guinea and the Congo basin. The Congo basin surface temperature remains almost uniform throughout the year, for example, the average monthly surface temperature over the Congo basin varies between 296K and 298K. But Gulf of Guinea sea surface temperatures have pronounced seasonality characterized by rapid cooling from May-August, in association with the formation of the Atlantic cold tongue. These sea surface temperature changes increase the ocean/land temperature contrast and drive the Congo basin Walker circulation.

We hypothesize that when the Walker circulation is anomalously strong, the Gulf of Guinea subsidence, the monsoon flow, and moisture transport across West Africa are also strong. This hypothesis is supported by the ERAI reanalysis. Composites of years with strong and weak Walker circulation show increased and decreased monsoon flows and the northward moisture transport associated with the flows, respectively.

Keywords: West African Monsoon, Congo Basin, Gulf of Guinea, Walker circulation

CCG-26

Investigating evaporation and soil water movement by measuring the stable isotope composition of water in Vertisols

Okafor, B.J.[1], Breecker, D.O.[1], Driese, S.G.[2], Nordt, L.C.[2], and Warden, J.[1]
Bokafor1208@gmail.com
1. Jackson School of Geosciences, University of Texas at Austin, Austin, TX, USA
2. Department of Geology, Baylor University, Waco, TX, USA

Water movement in soils plays an important role in plant growth, the transport of dissolved species, formation of pedogenic minerals and the recharge of groundwater reservoirs. In this study we trace water using stable oxygen and hydrogen isotope ratios in clay-rich soils (Vertisols) to evaluate water movement and evaporation. Common on floodplains, Vertisols are frequently cultivated and are good modern analogs for many of the paleosols typically used to reconstruct past climates. We hypothesize that: 1) evaporation occurs deeper in Vertisols than other soils (typically 20-30 cm) due to the tendency of Vertisols to crack when dry and 2) that soil water at the depth of soil carbonate formation (140 cm in the soil studied) has oxygen isotope compositions similar to mean annual precipitation, as typically assumed when interpreting $\delta^{18}O$ values of paleoVertisol carbonates. From September 2012 to July 2013, we collected samples by auger from the top 140cm of a Trinity River floodplain Vertisol on Richland Creek Wildlife Management Area, near Fairfield, Texas. Water was extracted from soil samples via vacuum distillation for isotopic analysis and gravimetric water content was measured for each soil sample. Measured $\delta^{18}O$ and δD values of soil water range from -2‰ to -8‰ and -20‰ to -50‰ respectively. All of the water samples measured thus far plot (δD versus $\delta^{18}O$) within the field defining a local meteoric water line (LMWL) for nearby Waco, TX. The $\delta^{18}O$ deviations (‰) of soil water samples from the Waco LMWL indicate that samples collected above/below 50cm tend to lie on the right/left of the LMWL. Evaporation of water from the soil above 50 cm is consistent with this observation but is not required by the data. Isotopic compositions and water contents are more variable near the surface (above ~50cm) than they are below ~50cm, which might be due to evaporation and/or change in the isotopic composition of incoming precipitation. The $\delta^{18}O$ values of soil water are lower during the winter and higher during the summer. Below ~100cm, soil water $\delta^{18}O$ values converge to -7 ± 1 ‰ (1σ, n=25), which is significantly different (t-test, $p < 0.0001$) from the mean $\delta^{18}O$ value of Waco precipitation (-4 ± 2 ‰, 1σ, n=96). These more negative $\delta^{18}O$ values at depth could be a result of preferential infiltration and percolation below the root zone of winter rain and/or large rain events. The larger-than-typical variability of 140 cm $\delta^{18}O$ values during July (-5‰ to -8‰) when soil cracks were observed could be a result of crack facilitated preferential downward flow of shallower, higher $\delta^{18}O$ water and/or evaporation from the deep soil. The effect of preferential percolation could be magnified compared to other soils due to the variable shrink-swell controlled permeability of these soils. If the range of measured isotope compositions does record preferential percolation, then Vertisols may provide records of the range in isotope composition of meteoric precipitation.

Keywords: Vertisols, Stable Isotopes, Water movement, Evaporation, Pedogenic Carbonate

CCG-27

Mapping soil erodibility using geomorphology, meteorology and remote sensing

Sagar Parajuli [1], Zong-Liang Yang [1] and Gary Kocurek [1]
psagar@utexas.edu
1. Jackson School of Geosciences, The University of Texas at Austin, Austin, TX

Dust is known to affect the earth radiation budget, biogeochemical cycle, precipitation, human health and visibility. Dust emission modeling remains challenging because dust emission is affected both by geomorphic processes and atmospheric phenomena. Existing dust models overestimate dust emission and rely on tuning and static erodibility factor so as to make simulated results comparable to remote sensing and ground-based observations. In most of current models, dust emission is expressed in terms of threshold friction speed which ultimately depends mainly upon percentage clay content and soil moisture. Unfortunately, due to the unavailability of accurate and high resolution input data of percentage clay content and soil moisture, estimated threshold friction speed doesn't represent the variability in field condition.

In this work, we aim to improve dust emission characterization in climate models by developing a high resolution geomorphic map of the Middle East and North Africa (MENA), which is responsible for more than 50% of global dust emission. We develop such geomorphic map by visually examining the high resolution satellite images obtained from Google Earth Pro and ESRI base map. Albeit subjective, our mapping technique is more reliable compared to automatic image classification technique since knowledge of geological/geographical setting is important for understanding the fine sediment availability. We hypothesize that the erodibility is unique for different geomorphic types and can be quantified by the correlation between observed wind speed and satellite retrieved aerosol optical depth (AOD). We classify the study area into several key geomorphic categories keeping in mind their fine sediment availability. Then, we quantify their erodibility using the correlation between observed wind speed and satellite retrieved aerosol optical depth (AOD). The resulting dynamic geomorphic erodibility map can be integrated in climate models to represent the spatio-temporal dynamics of dust sources. The reference dust scheme used in this study is the Dust Entrainment and Deposition (DEAD) model which is also a component of the community land model (CLM). Integration of the proposed erodibility map in climate models will improve quantification of vertical dust mass flux which will ultimately help us to better understand the effect of mineral dust on climate processes.

Keywords: Dust, Geomorphology, Aerosol Optical Depth (AOD), Wind Speed, Soil Erodibility

CCG-28

Patterns of morphological evolution during a locomotor transition: Lessons from the evolution of wing-propelled diving in penguins

Proffitt, JV[1]; Middleton, KM[2]; Clarke, JA[1]
jvproffitt@utexas.edu
1. Jackson School of Geosciences, The University of Texas at Austin, Austin, TX
2. University of Missouri, School of Medicine

Evolutionary transitions in locomotion provide excellent opportunities for exploring patterns of whole-organism morphological change associated with shifts in ecology. More specifically, these scenarios can act as investigatory frameworks for examining differential rates of evolution in separate anatomical elements, informing our understanding of the relationship between adaptation, anatomical form, and biological function. The evolution of wing-propelled diving in penguins represents a model system in which to pursue these questions due to their distinctive modes of locomotion relative to immediate outgroups, robust fossil record, and well-constrained phylogeny. New morphological characters developed through study of fossils, extant skeletons, and dissection were combined with previously developed character matrices to form the most complete dataset of penguin osteological characters to date. Patterns of character change in the forelimb and hind limb of penguins were assessed in Parsimony and Bayesian frameworks to infer relative rates of evolutionary change in each anatomical element across penguin phylogeny. We find that the forelimb and hind limb show similar rates of character change early on in penguin evolution, emphasizing the importance of examining whole-organism patterns of change rather than approaches only based on single character complexes or key innovations. These data, when combined with further anatomical and functional data obtained from extant penguins, will provide greater insight into the evolution of ecological and morphological diversification within birds, additionally serving as a basis for further study of major macroevolutionary events in other taxa.

Keywords: Birds, Evolution, Locomotion, Phylogenetics

CCG-29

Effects of urbanization on the surface energy and water balance: A case study using a hypothetical mega-city in the central United States

Alex Resovsky
aresovsky@utexas.edu
1. Jackson School of Geosciences, The University of Texas at Austin, Austin, TX
2. Land, Environment and Atmospheric Dynamics
3. Faculty advisor: Dr. Zong-Liang Yang

This study intends to use a land surface model (LSM) to assess the effects of urbanization on the surface energy and water balance. An offline model run is conducted to examine ground sensible heat flux and surface air temperature variations across a proposed "hyperurban" landscape using model default atmospheric forcing. Initial results may be used to investigate parameterizations of surface energy balance processes over urbanized regions by the Community Land Model version 4, in order to evaluate potential applications of LSMs in understanding changes in regional microclimate due to land use and land cover change.

Keywords: Climate, microclimate, LSMs, CLM4, urbanization, surface energy and water balance, precipitation patterns.

CCG-30

Terrestrial Origin of Monotremata

Wallace, R.[1], Rowe, T.[1]
rvsimon@utexas.edu
1. Jackson School of Geosciences, The University of Texas at Austin, Austin, TX

The evolutionary history of Monotremata is hotly debated due to a limited diversity of extant taxa and a fragmentary fossil record that stretches back to the Early Cretaceous. The phylogenetic position of extinct taxa in the crown or on the stem has implications for the ancestral monotreme condition. Many early mammals from the Mesozoic are hypothesized to be fossorial or arborial, while the ancestral monotreme has recently been hypothesized to be semi-aquatic; a primitive condition that would be unique to the monotremes. For the first time, we used high resolution x-ray computed tomography (CT) scans of the skull of the poorly studied long-beaked echidna, *Zaglossus*, to observe cranial anatomy in detail and compare *Zaglossus* to other extinct and extant mammalian taxa. New monotreme characters were added to a morphological character matrix of mammals and run in a parsimony analysis. Characters were distributed via accelerated transformation and delayed transformation and plotted on a most-parsimonious tree. The ancestral monotreme likely had an acute sense of smell, with the platypus derived among other monotremes in having reduced olfactory bulbs and ethmoturninals. A complex turbinal system in the echidnas compared to the reduced turbinals in the platypus suggests a terrestrial habit for the ancestral monotreme.

Keywords: Monotremata, Tachylgossidae, Ornithorhynchidae, evolution, turbinals, computed tomography

CCG-31

50 Million Years of Severe Osteopathology in Rhinocerotidae

Stilson, K.[1], Hopkins, S.[2], Davis, E.[2]
stilson@utexas.edu
1. Jackson School of Geosciences, The University of Texas at Austin, Austin, TX
2. The University of Oregon Department of Geosciences, Eugene, OR
3. The University of Oregon Honors College, Eugene, OR
4. The University of Oregon Museum of Natural and Cultural History, Eugene, OR

Skeletal pathologies in the fossil record are commonly considered indicators of an individual animal's life history and development, and not reflections of processes related to all or part of a lineage's history. Individual elements of many extinct and extant rhinocerotids display arthritis-like osteopathologies. The proportion of severe osteopathology increases over the last 50 million years from about 30% of all elements in a taxon from the Eocene showing some form of osteopathology to 100% of all elements in modern taxa. The Rhinocerotidae preserved in the fossil record do not represent a direct lineage, but a group of closely related organisms that present a study system for pathological evolution and development. Osteopathology is examined here in six extinct taxa spanning 50 Ma (*Hyrachyus eximus, Trigonias osborni*, *Menoceras arikarense*, *Diceratherium niobrarebse*, *Aphelops mutilus*, and *Teleoceras hicksi*) as well as the five living species of rhinoceroses. Seven pathological indicators (overgrowth, lipping, remodeling, erosions, worn articular surface, and variable foramen shape and size) were scored for each element on a scale of 1-4 and mapped on a phylogenetic tree using Mesquite to establish ancestral and lineage expression of osteopathology (i.e., that present in the common ancestor and also that present as successive points along the tree). We estimated mass from femur length and compared resulting values with the literature. We measured cursoriality using the established proxies of metatarsal length over femur length (MT/F), and total hind-leg length (femur + tibia + metatarsal). Estimated mass increases from 50 Ma to the present and correlates with the increased expression of osteopathology while cursoriality, the other trait examined as a possible contributing factor, did not. This degree of osteopatholgical expression may be an example of evolutionary compromise.

Keywords: paleopathology, rhniocerotidae, perissodactyla, paleontology, geobiology, skeletal morphology, osteopathology, Cenozoic.

CCG-32

A GIS-based modeling approach to estimate nitrogen loading and load reduction in lakes/reservoirs with application to the San Antonio and Guadalupe basins

Ahmad A. Tavakoly[1], Zong-Liang Yang[2], David R Maidment[1],
tavakoly@utexas.edu
1. Civil, Environmental and Architecture, The University of Texas at Austin, Austin, TX
2. Jackson School of Geosciences, The University of Texas at Austin, Austin, TX
3. Civil, Environmental and Architecture, The University of Texas at Austin, Austin, TX

The movement of nitrogen (N) from the landscape to the coastal waters is a complex process, which involves natural and anthropogenic input of N to the landscape, N leaching to the rivers, and N transport, attenuation, and transformation along the river channels. Various water quality models exist, ranging from sophisticated deterministic methods to simple export coefficient approaches. While deterministic models allow in-depth understanding of spatial and temporal variations of sources and sinks, insufficient water quality data and uncertainties in measurement prevent the implementation of these models. This study develops and applies a simple export coefficient approach, which integrates a GIS-based N dataset (Texas Anthropogenic Nitrogen Dataset) and a GIS-based river routing model to simulate steady-state riverine N transport and chemical reactions in large river networks. We are conducting a 2-year case study (2008–09) along all rivers in the San Antonio and Guadalupe basins and investigating total nitrogen changes in urban and rural regions during wet and dry years.

Keywords: Steady-state modeling, Texas Anthropogenic Nitrogen Dataset, river routing model, GIS

CCG-33

The value of GRACE TWS data in improving CLM4 snow simulation

Yongfei Zhang[1], Hua Su[1], Zong-Liang Yang[1], Tim Hoar[2], Jeffrey Anderson[2]
1. The University of Texas at Austin, Jackson School of Geosciences, Austin, Texas
2. The National Center for Atmospheric Research, Boulder, Colorado

The Gravity Recovery and Climate Experiment (GRACE) terrestrial water storage anomaly data are assimilated into the Community Land Model version 4 (CLM4) via the Data Assimilation Research Testbed (DART) to improve the snowpack estimate. The Moderate Resolution Imaging Spectrumradiometer (MODIS) snow cover data are assimilated jointly. A freely available ensemble of reanalysis data created by DART and the Community Atmospheric Model (CAM4.0) is used as the meteorological forcing for each CLM ensemble member. This induces spread in the CLM ensemble during a spin-up phase and helps maintain spread during the assimilation. The spatial map of the error of the GRACE data provided along with the data is used in this work.

Comparisons are made to the open loop run, and the model run that assimilates the MODIS snow cover data only. Snow cover data assimilation has limitations when snow cover reaches unity, while the GRACE data assimilation can adjust model snowpack as long as the snow mass changes. Improvements over the model run that assimilates MODIS only are noteworthy in the high latitudes where the MODIS snow cover data can hardly influence the model. The effectiveness of the assimilation is further assessed by evaluating the daily model forecast against the Canadian Meteorological Center (CMC) snow depth data in the regions with dense observation sites.

Keywords: Data assimilation, Snow water equivalent, GRACE observations

CCG-34

The Influence of Climate Variations over Tibetan Plateau on the Interannual and Long-term Variation of the Upper Troposphere and Lower Stratosphere Water Vapor

Kai Zhang[1], Rong Fu[1]
kzkaizhang@gmail.com
1. Jackson School of Geosciences, The University of Texas at Austin, Austin, TX

ERA-Interim reanalysis and the Whole Atmosphere Community Climate Model version 4 (WACCM4) historical datasets are used to identify the influence of climate variation over the Tibetan Plateau (TP) on the interannual and long-term variation of water vapor in the upper troposphere and lower stratosphere (UTLS). During boreal summer, increasing surface temperature leads to higher specific humidity over the TP near-surface and then enhanced transport to the global UTLS through quasi-isentropic layers. The interannual variability of specific humidity at the 340K isentrope (near surface over the TP) can explain more than 30% of the variability over the extratropical UTLS especially in the Northern Hemisphere. In the tropical UTLS, water vapor is approximately saturated and thus its variability is mainly modulated by temperature. A large percent of the increasing specific humidity trend at 380K can be well reconstructed using 340K specific humidity over the TP, indicating the strong positive effect of the increasing temperature over the TP on the long-term trend of water vapor in the UTLS.

Keywords: stratospheric water vapor, Tibetan Plateau (TP), surface temperature

EG-1

Depth-Registration of 9-Component 3-Dimensional Seismic Data in Stephens County, Oklahoma

Al-Waily, M.[1] and Hardage, B. A.[1]
alwaily.mustafa@utexas.edu
1. Jackson School of Geosciences, The University of Texas at Austin, Austin, TX

Multicomponent seismic techniques improve imaging by providing additional information about subsurface characteristics. It delivers different images of the same subsurface using multiple waveforms. Compressional and shear waves perceive lithology and fluid variations differently, providing independent measurements (Vp/Vs, Poisson's ratio, etc.) of reservoir rock and fluid properties. Joint interpretation of multiple component images requires the events to be aligned in depth. The process of identifying and registering (matching) events from similar reflectors is called depth-registration.

This study will focus on depth-registration of a 9-component 3-dimensional seismic dataset targeting the Sycamore formation in Stephens County, Oklahoma. The survey area is 16 square miles located in Sho-Vel-Tum oilfield. Processed compressional, radial-shear, and transverse-shear wave data are used in a post-stack analysis. Image registration will be achieved by simultaneous horizon and fault picking on vertical seismic profiles of P-P, Sv-Sv, and Sh-Sh images. Moreover, seismic attributes and well data will further optimize image registration.

The data are located in a complexly folded and faulted area in the northwest part of the Ardmore basin, between the eastern Arbuckle Mountains and the western Wichita Mountains. Large hydrocarbon volumes are produced from stratigraphic traps, fault closures, anticlines, and combination traps. Sho-Vel-Tum field was ranked 31st in terms of proved oil reserves, and 93rd in proved gas reserves, in the United States by a 2009 survey.

Preliminary interpretations show two different fault patterns can be recognized from the seismic data, a series of high intensity NW-SE trending reverse faults, and less intense NE-SW faults. A limitation to the analysis is the lack of any type of sonic logs within the area of interest, which led to the use of pseudo-logs when creating well ties.

I will present several methods to interpret and verify the accuracy of event-registration, including structural and well log interpretation, and geologic analysis of the study area. Other seismic attributes like Vp/Vs ratio, Poisson's ratio, reflection amplitude extraction, combined with production and well data, may provide further information about hydrocarbon distribution and reservoir compartmentalization. However, the focus of this work will be on event-registration and multicomponent seismic attribute analysis.

Keywords: multicomponent seismology, event-registration, seismic attributes, sho-vel-tum, 3D seismic, 9-component

EG-2

Fracture Growth Processes in Tight Sandstone Reservoirs Inferred by Textural Investigations of Crack-seal Fracture Cements

Alzayer, Y.[1], Eichhubl, P.[1] Laubach, S.[1]
zayer@utexas.edu
1. Bureau of Economic Geology, Jackson School of Geosciences, The University of Texas at Austin, Austin, TX

Opening-mode fractures are widespread structures in sedimentary rocks even in slightly deformed and flat-lying sequences. It is generally assumed that fractures widen in aperture while they propagate in length or height. However, it is also conceivable that a phase of proportional aperture to length or height growth is followed by a phase of aperture growth without further growth in length or height. This mechanism of aperture growth can occur when the fracture propagation is prevented by material strength heterogeneities or if the material elastic properties change over time.

Fractures in sandstone are often partially or completely cemented in deep reservoirs (>1 km depth). These fractures form by repeated opening increments, with each increment recorded by crack-seal quartz cement that bridges the fractures. To test for concurrent length versus aperture growth of these fractures, we reconstructed the crack-seal opening history for multiple cement bridges sampled at different distances from the tip of three opening-mode fractures in Travis Peak Sandstone of the SFOT-1 well, East Texas. Crack-seal cement textures were imaged using a scanning electron microscope with a cathodoluminescence detector, and the number and thickness of crack-seal cement increments determined. Results were compared to analytical solutions for fracture aperture as a function of position relative to the fracture tip in an elastic medium. We find that crack-seal increments decrease both in number and thickness toward the fracture tips, consistent with the elastic model and with proportional aperture to length/height growth. Such trends are observed for both length and height dimensions. Opening increments in two bridges suggest that an initial phase of proportional aperture and length or height growth was followed by a period of aperture growth without concurrent lengthening.

Keywords: Natural fractures, fractured reservoirs, fracture growth, crack-seal cement, quartz bridges.

EG-3

The effect of spacing, aperture, and infill on the seismic detectability of fracture networks: a numerical wave propagation study

Becker, L.[1]
lebecker12@yahoo.com
1. Jackson School of Geosciences, The University of Texas at Austin, Austin, TX

The location, geometry, and fill attributes of subsurface fracture networks can be characterized by seismic surveying through the study of seismic energy attenuation, wavefield scattering, and directional phase velocities. This method of understanding in-situ reservoir features is an indirect approach, however, and requires an in-depth understanding of the seismic response to each property and how the signatures of these properties combine to form seismic observations. To understand any characteristic of a fracture network, a model must be implemented to accurately represent the subsurface and predict the outcome of changes in individual fracture attributes. The work presented here uses finite-element wave propagation modeling techniques to study how the seismic response changes due to variations in fracture spacing, aperture, and infill. Previous studies using effective-medium and finite-difference modeling techniques have correlated some of these properties to patterns in energy attenuation and scattering in transversely isotropic media. For more complex systems, such as heterogeneous fracture clustering or fracture networks with realistically small apertures, these older modeling techniques fall short. Both are greatly limited in their ability to discern fracture parameters due to their oversimplified representation of realistic fractured media. To advance this study, I implement finite element wave propagation techniques that offer more freedom to modeling parameters. Finite element modeling techniques allow the contouring of discontinuous fracture interfaces and, therefore, can more accurately represent the reflections and diffractions from these surfaces. Through the application of this better suited method of modeling, I am able to more accurately identify the presence of and characterize complex fracture networks.

Keywords: finite element modeling, fracture modeling, numerical wave propagation, seismic attenuation, wavefield scattering

EG-4

Late Miocene to Recent Evolution of Growth Faults in Greater Breton Sound, Louisiana, USA

Brown, David M.[1], Mohrig, D.[1]
davidmbrown@utexas.edu
1. Jackson School of Geosciences, TheUniversity of Texas at Austin, Austin, TX

Using industry-grade 3D reflection seismic data covering 1400 km2 of greater Breton Sound in southern Louisiana, USA, and coupling it with paleontological and well log data, we are able to characterize the latest Miocene-to-Recent behavior of 6 synsedimentary normal faults down to the 10-meter scale, in both the strike and dip direction. These faults range from 11 to 5.7 km in length and have fault-plane dips between 83 and 88 degrees.

Ideal normal-fault models place the maximum displacement (dmax) at the center of the strike-length (L) of the fault, with zero displacement at the fault tips. By mapping greater than 8 displaced horizons across each growth fault, we find that the position of dmax occurs within 16-35% of L from a fault tip. Concordantly, vertical displacement across the faults is not symmetrically distributed along the length of a fault. Instead, these displacements are noticeably skewed toward one fault tip or the other. Fault length is found to increase with both fault displacement and overall burial depth. The highest observed, long-term rate of fault-tip propagation is 0.52 mm/yr. This rate corresponds to 2.6 m of tip propagation per 1 m of vertical fault displacement. The lowest observed rate of fault-tip propagation is very close to 0 mm/yr. Geologic rates for maximum vertical displacement on the faults ranged from 3 – 8 % of the regional burial or subsidence rate of 0.23 mm/yr. These displacement rates have remained roughly constant over the past 7 million years.

Keywords: Growth Faults, 3D Seismic Data

EG, SETP-5

Interactions between chemical alteration, brittle deformation, and hydrothermal fluid flow in the Boyer Ranch Formation, Dixie Valley, NV

Callahan, O.[1], and Eichhubl, P.[1]
ocallahan@utexas.edu
1. Jackson School of Geosciences, The University of Texas at Austin, Austin, TX

Faults and fractures are the dominant fluid flow pathways in most of the power producing geothermal fields around the world, particularly in structurally controlled Basin and Range style systems. The location and longevity of fracture controlled hydrothermal flow can be viewed as a result of competing mechanical and chemical processes – mechanical fracture opening versus fracture cementation. However, the role of each process may be more nuanced, with faults and fractures acting both as conduit and barrier, and alteration potentially influencing the mechanical and hydrologic properties of the bulk reservoir. The goal of this study is to characterize the chemical and mechanical response of rocks to hydrothermal fluids, and to describe the impact that these changes may ultimately have on hydrologic behavior (i.e. focusing or dispersion of flow) in hydrothermal systems.

The Dixie Valley geothermal field, located in northern Nevada, is the largest and hottest non-magmatic geothermal system in the Basin and Range. The field generates 62 MWe from 248°C hydrothermal fluids extracted from major basin-bounding faults and associated fractures at reservoir depths between 2 and 3 km. The most productive fractures in the reservoir are associated with Cretaceous granite in the footwall of the seismically active Dixie Valley fault, and in a sequence of allochthonous Jurassic marine sedimentary and mafic plutonic to volcanic rocks (the Boyer Ranch Formation and Humboldt Igneous Complex) in the hanging wall.

Two surface exposures of the Boyer Ranch Formation, a naturally fractured quartz arenite, have undergone different degrees of alteration – from burial diagenetic to acid-sulfate alteration and silicification. Despite locally intense alteration, relict and open fractures are still preserved in both outcrops. Field and microscale structural observations using petrographic and SEM-CL techniques are combined with compositional analyses (SEM-EDS, XRD) to correlate the intensity and extent of alteration and deformation. Variability in the $\delta^{18}O$ and $\delta^{13}C$ composition of vein and bulk rock, and analysis of fluid inclusions in vein material, help constrain the magnitude and temperature of past hydrothermal fluid flow through the altered and fractured rock. Our initial observations suggest that the relative influence of chemical versus mechanical processes on the focusing of hydrothermal flow may vary at different time and length scales in this tectonically active and chemically reactive environment.

Keywords: Dixie Valley, geothermal, hydrothermal, alteration, deformation, fracture, fluid inclusion

EG-6

Least-squares migration with shaping regularization for simultaneous-source seismic data

Chen, Y.[1], Fomel, S.[1]
ykchen@utexas.edu
1. Jackson School of Geosciences, The University of Texas at Austin, Austin, TX

The interference caused in the simultaneous-source acquisition will cause artifacts in the image. We propose to directly migrate the blended data without deblending. We treat the imaging for blended seismic data as an inversion problem, and use shaping regularization to iteratively solve it. In the shaping regularized iterative framework, the forward and backward operators are chosen as a pair of modeling and migration operators, the shaping operator can be chosen as any structure enhancing denoising filter, which can be used to attenuate artifacts. Two synthetic examples both demonstrate an excellent performance of the proposed approach.
Keywords: simultaneous source, shaping regularization, least-squares migration

EG-7

Effects of diagenesis and structural position on size and spatial distributions of fractures in tight-gas sandstones: Frontier Fm and Flathead Fm, Wyoming

Copley, L.[1]
lcopley@utexas.edu
1. Jackson School of Geosciences, The University of Texas at Austin, Austin, TX

The presence and distribution of fractures is key to understanding fluid flow potential in rocks. However, it is extremely difficult to sample subsurface fractures because vertical wells generally are not oriented at high angles to fracture orientation. Therefore, much study has been devoted to the characterization of fracture patterns in outcrop and in core taken at high angle to fracture strike (horizontal core).

In this study, I will be looking at (1) effects of diagenesis (cement precipitation) due to burial history on fracture patterns and growth processes, and (2) how these patterns and growth processes are affected by position on folds (i.e., strain variation). For part 1, I will examine fractured sandstone using core and outcrop to test a model proposed by Hooker et al. (2012; 2013) postulating that amount of quartz precipitation during fracture opening affects size- and spatial-distribution patterns of fractures. Specifically, under high temperatures if abundant quartz accumulates many initially-formed fractures readily seal allowing for some partly-cemented fractures to grow and for some new fracture to form, creating a power law distribution; whereas under cooler temperatures little quartz accumulates and initially-formed fractures grow preferentially, creating a characteristic distribution. For part 2, I will examine another fractured sandstone using outcrop to test the theory that strain variation will affect the size- and spatial- distribution patterns of fractures. I will sample this sandstone at intervals along a fold to determine whether different fracture patterns emerge on the hinge vs. the limbs.

To test these theories, I will use several methods that have been developed to analyze quartz-filled fractures in sandstones. Macrofracture quantification will be done with a handlens on the core and outcrop. Thin sections will be made from all samples and will be examined using polarized light microscopy, SEM-CL imaging, and petrographic point counting. Scanlines will be constructed on both the large scale (outcrop and core) and small scale (thin sections) to quantify aperture and spacing of fractures over several orders of magnitude, and this data will then be analyzed using the distribution analysis software *CorrCount*. For part 1, I will compare similar fracture sets between rocks of the same formation that experienced different burial histories, and therefore different amounts of quartz precipitation. For part 2, I will compare fracture sets in the same rock with the same burial histories but which have undergone different fold-related strain.

Keywords: Fractures, structural diagenesis, sandstone

EG-8

Rock-type Discrimination of Composition and Fabric in the Haynesville

Coyle, S.[1], Spikes, K.[1]
sarahcoylel@utexas.edu
1. Jackson School of Geosciences, The University of Texas at Austin, Austin, TX

The best recovery of hydrocarbons from unconventional reservoirs occurs in zones optimal for horizontal drilling and hydraulic fracturing. Characterization of the relationship between important rock properties, such as mineralogy and rock fabric, with elastic properties of the Haynesville will improve our ability to identify these optimal locations. This study investigates effectiveness of rock typing as a technique for improving rock physics modeling of elastic properties of the Haynesville Shale in Panola County, Texas. Rock typing is the division of the Haynesville into regions with varying mineralogy and rock fabric into distinct intervals to be modeled separately. In this work, the Haynesville is modeled using the differential effective medium (DEM) model which allows for parameterization of pore and grain aspect ratio, mineral composition, and load bearing matrix. A similar procedure is also used to model the whole Haynesville unit as a single interval with the DEM. The effectiveness of the rock-type models versus the full-interval model is evaluated in terms of their abilities to replicate sonic logs. By comparing both models, we found that rock type models allowed for better discrimination of small changes in composition throughout the Haynesville. In both model types, reproducing both sonic log p-wave and s-wave velocities requires correlation of grain and pore shape distribution inputs to model lines. In either model type, low Vp/Vs can be attributed to the mineralogy of the Haynesville.

Keywords: Rock Physics, Effective Medium, Gas Shale, Haynesville, Rock-Typing

EG-9

Core-scale heterogeneity and dual-permeability pore structure in the Barnett Shale

Cronin, M.[1], Bhandari, A.[2], Flemings, P.[2], Polito, P.[2], Bryant, S.[3]
mcronin@utexas.edu
1. Jackson School of Geosciences, The University of Texas at Austin, Austin, TX
2. Bureau of Economic Geology, The University of Texas at Austin, Austin, TX
3. Department of Petroleum & Geosystems Engineering, The University of Texas at Austin, Austin, TX

Core permeability experiments are routinely conducted to help characterize reservoir-scale matrix permeability in shales. However, shale matrix is heterogeneous at multiple length scales; from the wellbore-scale (~$1x10^{1}$ m) all the way down to the micro-scale (< $1x10^{-6}$ m). Therefore, understanding permeability heterogeneity in cores is crucial. We conducted pulse-transient decay (PTD) permeability tests on layer-parallel cores samples of Barnett Shale and observed two timescales of dissipation: 1) rapid (~10's of minutes) equalization in pressure between the upstream and downstream pressure sensors; and 2) a slow (~10's of hours) decrease in pressure of both upstream and downstream sensors towards a final equilibrium value. We constructed a dual-permeability model composed of layers of high permeability and low permeability material of constant thickness to simulate the observed dual-timescale behavior. Thin (~8 mm) thick low permeability (~1.4 nD) layers interbedded with high permeability layers (~240 nD) and ~6mm layer spacing reproduce the observed pressure behavior. X-ray micro-computed tomography and thin section analysis independently confirm this layered architecture and document mm-scale layer parallel bedding corresponding to variations in matrix fabric. The sample matrix is siliceous mudstone with abundant agglutinated foraminifera. Low permeability layers are likely associated with higher clay and organic matter content. The layered model successfully simulates the observed Barnett matrix permeability anisotropy ratio: (k_H = 93nD) (k_V = 2.3nD). Experiment and theory support a dual permeability structure at the core scale in the Barnett Shale. A better understanding of permeability heterogeneity can be used to understand gas flow at the reservoir scale.

Keywords: Shale, dual porosity, core analysis, permeability, unconventional, transient

EG-10

Comparison of seismic diffraction imaging techniques: plane wave destruction versus apex destruction

Decker, L.[1], Klokov, A.[1], Fomel, S.[1].
decker.luke@utexas.edu
1. Bureau of Economic Geology, The University of Texas at Austin, Austin, TX

Seismic diffraction imaging provides a method for identifying subsurface scattering features with improved resolution relative to conventional seismic reflection imaging. Successfully separating signals corresponding to diffraction events from reflection events is an essential component of diffraction imaging. Different techniques for separation exist, including plane wave destruction (PWD) and apex destruction in the migrated dip-angle domain (AD). We analyze separating diffractions from reflection events using a simple toy model and a field data set from the Piceance Basin, and evaluate the ability of each method to resolve scattering features. Results indicate that the PWD method leads to an image that preserves more diffraction energy and has fewer migration artifacts, but might be unable to eliminate reflection events whose slope is not continuously variable.

Seismic waves can either be reflected or diffracted. Diffractions can be used to determine details about the small scale features that produce them, such as karsts, voids, pinchouts, faults, and. Diffraction imaging may even lead to image resolution smaller than the seismic wavelength. Scattered waves are recorded as significantly lower- energy signal than reflected waves, requiring that diffractions be separated from reflections. Several means for separating diffractions from seismic data have been developed, including plane wave destruction and apex destruction.

Reflections are planar when viewed in common offset sections of unmigrated data. This property may be used to extract them by plane wave destruction. PWD functions by calculating local slopes using a filter that attempts to predict traces from their neighbors. This filter determines the dominant local slope by following pat terns of linear seismic energy. A residual containing all energy not conforming to local slope patterns is calculated and iteratively minimized. All data following dominant local slopes is removed, leaving only the residual. The residual contains seismic diffraction data and other non-linearly conforming noise present in the data.

Apex destruction amounts to Fresnel zone elimination. When migrated data are viewed in the dip-angle domain, seismic reflection events appear as upward pointing hyperbolic shapes with minima, or stationary points, at the dip value of their reflector. The effective portion of reflection events, stationary points, can be removed from migrated data using this relationship: dip information is calculated on a migrated data volume, and for each depth dip- angles within a certain angle of the dominant local slope are muted. Diffraction events appear flat when properly migrated and viewed from a dip-angle gather above the scattering center. When stacking to create a seismic image, apex-less reflection hyperbolas cancel each other out and disappear. Flat diffractions do not, and they remain in the image.

This study compares the separation of diffractions on unmigrated data using a plane wave destruction filter and on migrated data in the dip angle domain through apex destruction using test data sets.

Keywords: Diffraction, Imaging, Fracture Characterization, Fault Detection, Kirchhoff-Angle Migration

EG-11

Compositional classification of mudrock grain assemblages: A test case in the Eagle Ford Formation, South Texas

Ergene, S. M.[1], Milliken, K.L.[1]
smergene@utexas.edu
1. Jackson School of Geosciences, The University of Texas at Austin, Austin, TX

Grain assemblages in organic-rich mudrocks of the Eagle Ford Formation of South Texas are assessed to determine the relative contributions of intra- and extrabasinal sediment sources. Integrated light microscopy, BSE imaging, and X-ray mapping reveal a mixed grain assemblage of calcareous allochems, biosiliceous grains (radiolaria), quartz, feldspar, lithics, and clay minerals. Dominant fossils are pelagic and benthic foraminifers and thin-walled and prismatic mollusks; echinoderms, calcispheres, and oysters are present. Early-formed authigenic minerals including calcite, kaolinite, dolomite, albite, pyrite, quartz, and Ca-phosphate, some reworked, add to the overall lithologic heterogeneity, but are not used for our classification. The detrital grain assemblage of the Eagle Ford is a subequal mix of grains of intrabasinal and extrabasinal origins, presenting a formidable challenge to the task of applying lithologic classification to this unit, as neither conventional limestone nor sandstone classifications can be readily applied.

Point counting of X-ray maps is used to provide observations at a scale appropriate to classifying the mudrocks based on the composition of the grain assemblage. Each sample is plotted on a triangle, whose vertices correspond to terrigenous and volcanic grains (extrabasinal components), calcareous allochems, and biosiliceous grains. As a result of comparison of samples coming from different maturity levels in Upper and Lower Eagle Ford in terms of grains and authigenic components, differences and similarities are determined. While there is not a pronounced change in timing and variety of authigenic minerals, their amount and distribution differ in Lower and Upper Eagle Ford. Linking the grain assemblage to the authigenic assemblage at in samples of contrasting maturity levels in Upper and Lower Eagle Ford will be used to test the practical value of this classification in the next phase of our study. The relationship between the amount of extrabasinal grains and diagenesis is going to be assessed to see whether there is a systematic change or not. We hope the classification is useful for predicting diagenesis.

Keywords: Eagle Ford, diagenesis, mudrocks, classification, authigenic

EG-12

Numerical and Experimental Analysis of Texturally Equilibrated Salt-Brine Systems

Soheil Ghanbarzadeh[1], Marc A. Hesse[2], Maša Prodanović[1], James E. Gardner[2]
gh.soheil@utexas.edu
1. Department of Petroleum and Geosystems Engineering, The University of Texas at Austin, Austin, TX
2. Department of Geological Sciences, The University of Texas at Austin, Austin, TX

Salt deposits in sedimentary basins have long been considered to be a seal against fluid penetration. However, experimental, theoretical and field evidence suggests brine (and oil) can wet salt crystal surfaces at higher pressures and temperatures, which can form a percolating network. This network may act as flow conduits even at low porosities. The aim of this work is to investigate the effects of dihedral angle and porosity on the formation of percolating paths in different salt network lattices. Previous studies considered only simple homogeneous and isotropic crystal networks but this work extends the analysis to realistic salt textures by presenting a novel numerical method to describe the texturally equilibrated pore shapes in polycrystalline rock salt and brine systems.

First, a theoretical interfacial topology was formulated to minimize the interfacial surface between brine and salt. Textural equilibrium can be reached when a material has minimized the energy bound up in interfaces and within individual grains. The essential condition for texturally equilibrium under hydrostatic pressure and isotropic surface energy is that solid-liquid interfacial surface has constant mean curvature and satisfies dihedral angle boundary condition at triple-or-quadruple junctions. A level set method formulation has been developed in order to obtain fluid distribution between different crystal networks in textural equilibrium. Results show that the formation of connected fluid channels is guaranteed in dihedral angle less than 60 degree even in very small porosities (<0.5%). Fluid pockets in cases with dihedral angle more than 60 degree can create a percolating path at relatively high porosities (>3%). In porous media with anisotropic solids and dihedral angle less than 60 degree, fluid tends to be in planar features in direction of stretched crystals. For elongated solid structure with dihedral angle more than 60, pores initially connect in the direction of the shorter crystal axis and only at much higher porosities in the other directions. Consequently, even an infinitesimal elongation of the crystal shape can give rise to very strong anisotropy in permeability of the pore network. This work enabled us to investigate the opening of pore space and sealing capacity of rock salts. The obtained pore geometries determine a wide range of petrophysical properties such as permeability and capillary entry pressure.

Second, a series of experiments in different P-T conditions was carried out to investigate the actual shape of equilibrated channels in salt. The synthetic salt samples were scanned at the High Resolution X-ray CT Facility at DGS, UT Austin, with resolution in 1-3 micron range. The experimental results show both equilibrated (tubular pores) and non-equilibrated (planar features) in salt structure. Image processing was carried out by two open source software programs: ImageJ, which is a public domain Java image processing program, and 3DMA-Rock, which is a software package for quantitative analyzing of the pore space in three-dimensional X-ray computed microtomographic images of rock. We obtain medial axis and medial surface of the pore space, as well as find and characterize the corresponding pore-throat network.

Keywords: Rock Salt, Dihedral Angle, Textural Equilibrium, Level Set Method

EG-13

Quantitative Fracture Characterization Using Rock Physics and Multi-component AVO modeling

Gupta, M.[1], Spikes, K.[1], Far, E., M. [2], Sava[2], D., Hardage, B.[2]
menalgupta@utexas.edu
1. Jackson School of Geosciences, The University of Texas at Austin, Austin, TX
2. Bureau of Economic Geology, The University of Texas at Austin, Austin, TX

Understanding the effects of fracture-induced seismic anisotropy on seismic amplitudes is an important area of research in exploration seismology. This study focuses on how fractures affect the elastic properties of a rock and illustrates which seismic attributes may be helpful for quantitative interpretation of fracture properties. A rock physics model is constructed for Ordovician age carbonates called the Arbuckle Formation, encountered in wells drilled in Wellington Field, Kansas. Formation Micro-Imaging (FMI) data acquired in wells suggest, fractures with very high dip angles are present in the upper Arbuckle Unit. Consequently, the model assumes a single set of vertically aligned fractures superimposed on a porous isotropic carbonate background, which creates horizontal transverse isotropy (hti) type anisotropy. This model incorporates a priori information about matrix porosity distribution and pore shapes obtained from well logs and analysis done on drill cores. Model results provide robust estimations of fast and slow P and S-wave seismic velocities and Thomsen parameters. These estimates are used to model Amplitude Variation with Offset (AVO) behaviors of P-waves and fast and slow S-waves in directions parallel to and perpendicular to fractures. Realistic variations in crack density and crack aspect ratios assumed for superimposed fractures help to understand their effect on elastic properties and AVO attributes. Modeling results show that S-wave AVO gradients contain information about fracture direction and nature of fracture fill; whereas, S-wave AVO intercepts tell us information about the fracture density. Unlike S-waves, P-waves are less reliable for quantitative interpretation of fractures but do contain vital information about fluid fill in the matrix porosity. Results of this study underscore the importance of S-waves for characterizing fractures and provide the necessary background and motivation to study S-wave AVO in detail.

Keywords: Fracture characterization, seismic anisotropy, rock physics modeling, carbonates, P-wave AVO, S-wave AVO

EG-14

Distribution and Connectivity of Micropores in a Low-Resistivity Pay Carbonate Reservoir from Lower Cretaceous Lekhwair Formation, Abu Dhabi, United Arab Emirates

Hassan, A.[1], Kerans, C.[1], Loucks, R. G.[2], Steuber, T.[3]
ahahassan@utexas.edu
1. Jackson School of Geosciences, The University of Texas at Austin, Austin, TX
2. Bureau of Economic Geology, Jackson School of Geosciences, The University of Texas at Austin, Austin, Texas
3. The Petroleum Institute of Abu Dhabi, United Arab Emirates

Many carbonate reservoirs worldwide produce water-free hydrocarbons despite exhibiting low-resistivity and high-calculated-water saturations on the basis of wireline log analysis. This paradox between resistivity and productivity has been recognized for more than three decades in oolitic reservoirs from Upper Jurassic Smackover Formation. Previous studies postulated that resistivity in oolitic reservoirs is controlled by a connected network of micropores holding conductive and immobile brine. However, details regarding distribution and connectivity of micropores are not well-documented. A clear understanding of micropore network in oolites will help in the recognition of overlooked pay zones.
This study investigates distribution and connectivity of micropores in low-resistivity oolitic pay carbonates producing from Lower Cretaceous Lekhwair Formation in Abu Dhabi, United Arab Emirates. The reservoir has an average density and neutron porosity of 18%, average wireline resistivity of 1 Ωm, and water saturations up to 80%. Production, however, confirmed water-free hydrocarbons. We combined methods of mercury capillary pressure, fluorescence microscopy, and scanning electron microscopy to characterize the micropore network.

Capillary pressure data of skeletal-ooid grainstone revealed heterogeneous pore-throat sizes with a strong bimodal distribution; macropores (*i.e.*, pore-throat-radius >0.5 μm) and micropores (*i.e.,* pore-throat-radius <0.5 μm). Macropores are intergranular pore space between ooids and other allochems forming a highly permeable reservoir reaching up to 2200 md. Fluorescence microscopy showed predominant distribution of micropores in the outer portion of ooid cortices. This distribution along with common interpenetrating ooids resulted in a connected network of micropores, providing an explanation for the low-resistivity readings. Results of this study can be applied to similar oolitic low-resistivity pay units such as those of Lower Cretaceous Sligo, and Rodessa Formations.

Keywords: Electrical Resistivity, Permeability, Microporosity, Mesoporosity, Macroporosity, Carbonates, Thamama Group

EG-15

Chronostratigraphy at the Seismic Scale: Rethinking Vail et al.'s Basic Assumption

He, Y.[1], Zeng, H.[2], Kerans, C.[1]
yawenhe@utexas.edu
1. Jackson School of Geosciences, The University of Texas at Austin, Austin, TX
2. Bureau of Economic Geology, The University of Texas at Austin, Austin, TX

Vail and his co-workers invented seismic stratigraphy on the basis of a fundamental assumption (Mitchum et al.,1977; Vail et al., 1977a, b, c) that primary seismic reflectors follow chronostratigraphic surfaces (strata surfaces and unconformities) rather than time-transgressive lithostratigraphic surfaces. Conforming to this assumption, they used seismic sections to delineate regional-scale depositional sequences, as well as to construct regional chronostratigraphic correlation charts and integrate global curves of sea-level change up to the third order (1 to 10 m.y.). Since then, with the widespread use of seismic data, the assumption has been extended to prospect and reservoir scale.

In this study, we started from the duplication of the Tertiary example in South America (Vail et al., 1977c) to check the validity of the basic assumption, by subjecting it to various dominant frequencies. Results show that, the time-transgression phenomenon may occur in a broad range of frequencies, depending on the lateral lithofacies change. Afterward, for the sake of representing more general situations, a set of geostatistical models with increasing lateral lithofacies variation was constructed, extrapolating from randomly selected wireline logs in the Tertiary of South Texas. The corresponding synthetic seismic records manifested various tendencies of time transgression for seismic reflections.

This study proved the feasibility of a detailed study on chronostratigraphy at the seismic scale, using a geologically reasonable approach. Using the confidently mapped stratigraphic surfaces and pseudowells in the digital outcrop model (DOM) as the conditional data, a set of geostatistical model with increasing lithofacies variation could be constructed. And in the next step, we are aiming at locate the optimum seismic attributes, which positively/ negatively correlate to the time-transgression phenomenon, to assist the interpretation in higher-order seismic stratigraphy.

Keywords: chronostratigraphy, seismic interpretation, geostatistics

EG-16

Using Seismic Reflectivity of P and S Wave Modes and Inclusion Based Modeling to Evaluate Multiple Fracture Sets, Andrews, Tx

Ileri, S.[1]
saygin.ileri@utexas.edu
1. Jackson School of Geosciences, The University of Texas at Austin, Austin, TX

An 818 ft depth, low permeability and naturally fractured subsurface is analyzed in this study from Andrews, Texas. The model is assumed to be formed of two different lithologies which are siliciclastics and calcareous rocks. In this model, there are two vertical fracture sets which are orthogonal to each other and they are assumed to be filled with gas inclusions. In order to evaluate the fracture densities, orientations and potential gas reservoirs, I examined the P-P and P-SV reflectivities using amplitude versus angle with azimuth (AVAZ) analysis. Moreover, a penny-shaped crack model is employed in this research for better understanding of the subsurface in terms of gas potentials within the cracks systems. Employing two different models was helpful for a better comparison of the results. As expected, I could see the large decrease in both S-wave and P-wave velocities with the effect of the fractures systems and the gas saturation in the inclusions from the penny shaped crack modeling. Furthermore, despite the fact that we need to make many different models such as lithology, fluid substitution and porosities changes for a complete AVAZ study, I only utilized from the PP and P-SV reflectivity results here. From the reflectivity results, I would say that the reflectivity values are low with the changing incidence angles because of the low contrast between the layers. The azimuthal variety in the reflection coefficients provided the information about the fracture orientations.

Keywords: AVAZ, orthorhombic, fractures, reflectivity, cracks

EG-17

Quantitative microtextural study of the silt fraction in mudrocks

Lunsford, J.D.[1], Hayman, N.W.[2], Milliken, K.L.[1]
jlunsford@utexas.edu
1. Bureau of Economic Geology, The University of Texas at Austin, Austin, TX
2. University of Texas Institute of Geophysics, The University of Texas at Austin, Austin, TX

To understand the history and physical properties of mudrocks requires data from the silt (2-63 μm) grain-size fraction. The volumetic content of silt grains in mudrocks reaches 40% or more and may partly control porosity. Mudrock microtextural variations between basins with contrasting histories may help to differentiate the relative importance of transport, deposition, and diagenesis in mudrock evolution. We have manually digitized silt grains using scanning electron microscope (SEM) images with elemental X-ray maps, and quantified the mudrock microtexture using Jmicrovision© software. We applied this approach to samples from: the Cretaceous Pearsall Formation of the Maverick Basin, the Mississippian Barnett Shale of the Fort Worth Basin, and the Devonian Marcellus Formation of the Appalachian Basin. All three formations are known hydrocarbon source rocks from predominantly siliciclastic clastic systems that have been buried to depths that cover a range of diagenetic conditions. However, each sample set provides specific opportunities: (i) the Pearsall allows us to track changes from the up-dip to the down-dip section of the regional Gulf of Mexico strata, (ii) the Barnett allows us to contrast microtexture across differing porosities, and (iii) the Marcellus allows us to see how these mudrocks respond to substantial increases in temperatures. In the Pearsall and Barnett formations, the preferred orientation of slightly elongate fine silt grains creates an anisotropy that dominates the fabric. In this 2D slice there are fewer observed grain contacts and more clay-size matrix. In contrast, preliminary results from the Marcellus appear to show more contacts between coarser silt particles, with only interstitial clay-size matrix. These microtextural differences may contain important clues to mechanical versus chemical diagenetic histories of these units. A key result from the study is that the relative abundance of detrital carbonate and silicate, and the presence of authigenic minerals has little effect on grain-size distribution. The silt framework and primary grain size distribution are preserved despite the diagenetic histories experienced by the mudrocks within these basins.

Keywords: mudrocks, hydrocarbon, porosity, diagenesis, Marcellus

EG-18

Volumetric estimation of curvature using predictive painting

Karimi, P.[1], Fomel, S.[1]
parvaneh@utexas.edu
1. Jackson School of Geosciences, The University of Texas at Austin, Austin, TX

Curvature is an attribute which measures the deviation of a surface from a plane. The more a surface is structurally folded or faulted, the larger its curvature. The degree of folding or curvature at a given point in a geologic layer and the amount of stress at that point are related (Price and Cosgrove, 1990). Consequently, there will be a relationship between the degree of fracturing in a geologic layer and its curvature, if the strain is largely accommodated by fracturing, but this relationship is so complicated and depends on so many factors. Since Lisle (1995) has shown the correlation of curvature values to fractures measured on an outcrop, the relation between these two has been approved as a reliable geologic model, and horizon-based curvature attributes have been successfully used in the prediction of fractures and faults. Among all the introduced curvature attributes during the last few years, most positive and most negative curvatures would make recognition of lineaments easier and are easier related to geologic structures. Picking horizons in noisy data (horizon picking), and nonexistence of consistent horizon in the zone of interest in 3D seismic data volumes are the main roadblocks in horizon-based curvature attributes. Volumetric estimation of curvature introduced by Al-Dossary and Marfurt (2006) has been an extremely successful approach and such a relief to the need for interpreted horizons. We offer an alternative strategy for computing volumetric curvature which uses predictive painting algorithm introduced by Fomel (2010). Structural information of a seismic image ($I(x,y,z)$) is important and assigning a dominant local slope attribute to all elements in a volume of data is a way to characterize the structure of seismic data (Fomel, 2010). In the predictive painting algorithm, Sergey followed the method of plane-wave destruction (Claerbout, 1992) to measure local slopes of seismic events. Once we spread information from a reference trace to its neighbors by following the local slope of seismic events, horizons ($H(x,y,z)$) are picked and amount of shift for each trace with respect to the reference trace is crystal clear. Using predictive painting, automatic picking of horizons would use the advantages of both conceptual simplicity and computational efficiency. The next step is to apply a flattening method called warping on the isosurfaces ($H(x,y,z)$) of the predictive painting results. Those predicted horizons ($H(x,y,z)$) are then warped until they are flat. By unshifting each trace we will get the automatic flattened image ($I(x,y,h)$), we also apply the same amount of shift on the cube of $z(x,y,z)$. The result will be a cube of horizons ($z(x,y,h)$), meaning that we can assign a horizon to each point in the whole volume. After that we can fit a local quadratic surface to each horizon and compute different curvature attributes.

Keywords: Predictive-painting, plane-wave-destruction, curvature, horizon

EG-19

Eagle Ford Formation Pore Evolution - Results from Laboratory Heating Experiments (Anhydrous Gold-Tube Pyrolysis)

Ko, (Lucy) T.[1, 2], Zhang, T.[2], Loucks, R.G.[2], Ruppel, S.C.[2]
tingwei.ko@utexas.edu
1. Jackson School of Geosciences, The University of Texas at Austin, Austin, Texas
2. Bureau of Economic Geology, Jackson School of Geosciences, The University of Texas at Austin, University Station, Box X, Austin, Texas

Low maturity Boquillas B (Eagle Ford equivalent) outcrop samples (limestone-rich facies) were heated anhydrously under confined pressure to study the evolution of organic-matter (OM)-hosted pores and mineral pores in these samples with those from higher maturity subsurface Eagle Ford mudrocks.

The outcrop samples were cored to small diameter cylinders 6 mm in diameter and 2 to 3 centimeter in length and heated in sealed gold tubes for 72 hours at seven different temperatures ranging from 130 to 425°C. These temperatures correspond to different hydrocarbon generation stages, ranging from early bitumen generation to late dry gas generation. Oil and gas yields, Rock-Eval and Leco TOC analyses will be used to characterize the type of kerogen, organic matter conversion, and relative thermal maturation of the samples. In addition, one third of small-cylinder samples were prepared using Ar-ion milling to look at pore evolution under field-emission scanning electron microscopy (FE-SEM).

Calculated vitrinite reflectance (from T_{max}) suggested that the outcrop Boquillas samples have reached thermal maturation at about 0.65 to 0.7%R_o, implying that they have reached the stage of early-hydrocarbon generation. From SEM petrography, we observed several diagenetic features that formed prior to hydrocarbon migration. These features include carbonate cement, quartz cement, kaolinite cement, minor chlorite cement and minor dolomite replacement.

Organic matter (kerogen or bitumen or both) tends to be redistributed and concentrated around calcite grains or cement. Also, most organic matter is aligned with bedding. Three types of pores were observed in outcrop samples; OM-hosted pores, mineral pores, and interface pores (OM-pores formed in association with mineral grains). We interpreted the occurrence of OM-hosted and interface pores as the result of fluid-rock interactions (eg. wettability differences of different mineral grains, release of organic acid and carbon dioxide during thermal maturation).

With increasing heating temperature, both OM pores and pore connectivity increase; new types of OM-pores were formed as well. The character of OM changed through different heating stages. Several different pore types co-exist at oil cracking stage, in association with solid kerogen, liquid oil, liquid bitumen, and products from secondary cracking. Morphology of OM-hosted pores changed from no pores to few pores, to elongated slit pores, to crack-like pore, to small pores, to pores between OM-coated grains, and then finally to small equant pores. Euqant pores are similar to pores we observed in natural samples, which are most likely associated with methane generation (dry gas stage).

Keywords: Eagle Ford, pore evolution, organic matter, diagenesis

EG-20

Geologic Setting and Reservoir Characterization of Barnett Shale in Southeast Fort Worth Basin, Central Texas.

Liu, X.[1], Loucks, R.[2]
xufeng@utexas.edu
1. Jackson School of Geosciences, The University of Texas at Austin, Austin, TX
2. Jackson School of Geosciences, The University of Texas at Austin, Austin, TX

The Barnett Formation that was deposited in the deeper water foreland Fort Worth Basin (north-central-Texas) is a well-known and economic shale-gas system. The Barnett Shale is not only a primary source rock for Paleozoic reservoirs in Texas, it is also a widespread unconventional gas reservoir. It is the first shale-gas reservoir that hydraulically fracked horizontal wells for production. Within the Fort Worth Basin, the areas of Denton, Wise, and Tarrant Counties are the core area of Barnett Shale production. Abundant research has been conducted on this main producing area. Until now, Barnett Formation in southeast Fort Worth Basin is not as well studied. Based on this fact, this study focuses on the Barnett Shale in Hamilton County, which is located in southeast Fort Worth Basin. This area is considered to have lower resource potential because the shallower burial (low Ro) and thin thickness.

Two vertical, continuous cores from Hamilton County are being studied to understand the depositional setting, lithofacies, pore network, and reservoir quality. For this purpose the following tasks are being performed: (1) the cores have been described and lithofacies have been defined, (2) thin sections have been analyzed for texture, fabric, biota, and mineralogy, (3) Rock Eval has been run to identify organic material and quantity of TOC, (4) XRD and XRF data have been collects to define mineralogy and understand paleoenvironmental setting, and (5) SEM analysis of Ar-ion milled samples will be comleted to define pore types and pore network. The dominated organic matter type is a mixture of Type II and Type III kerogen with the mean TOC content approximately 4%. Rock Eval data shows most of the interval is within oil window with a calculated vitrinite reflectance approximately 0.9%. Six lithofacies were defined by the two cores: (peloidal packstone to mudstone; siliceous mudstone; laminated calcareous mudstone, skeletal packstone to grainstone; phosphatic grainstone; carbonate concretion). This research suggests that the Barnett Shale is a mudrock unit whose deposition characteristics were controlled by basinal geometry, hemipelagic suspension settling, slope-originated gravity-flow events, and bottom current reworking. Skeletal deposits and carbonate-silt starved ripple suggests gravity-flow deposits and bottom-current reworking during deposition. Also, a high content of Cu and Ni may be evidence of high influx of organic matter; redox-sensitive elements and degree of pyritization both indicate anoxic/euxinic condition during the deposition. Additional work is being completed on brittleness (relates to propensity to fracture). What is learned about the Barnett Shale in Hamilton County will be compared to the published research from the core producing Barnett Area (Newark East Field) in the northern Fort Worth Basin.

Keywords: Barnett, shale gas, sedimentology, geochemistry, pores

EG-21

Extent and effect of fault-controlled CO2 alteration on reservoir and seal rocks and implications for geomechanical failure at Crystal Geyser, Green River, Utah

Major, J. R.[1], Eichhubl, P.[1]
JMajor@mail.utexas.edu
1. Jackson School of Geosciences, The University of Texas at Austin, Austin, TX

A structural diagenesis approach involving the coupled chemical and mechanical properties of reservoir and seal rocks is necessary for assessing the short and long term security of sequestered CO_2. Current numerical models used to model subsurface CO_2 reservoirs do not account for such processes, and typically these use only linear-elastic geomechanical properties, ignoring failure parameters such as fracture toughness. In addition, numerical models normally lack constraints on long-term, geologic time scales. Well-characterized field studies of natural analogs are crucial for providing realistic input parameters and calibration for the numerous numerical models that have been developed for addressing CO_2-related problems across a range of spatial and temporal scales. Study of fossil and active CO_2 seeps found at Little Grand Wash and Salt Wash fault systems near Green River, Utah are invaluable to assess long-term storage and leakage behavior in natural systems. Observations from the site and geomechanical testing also indicate that fracture systems play a crucial role in leakage, and the extent of fracturing and CO_2-related alteration extends from tens to over one-hundred meters. Failure parameters of reservoir and seal rocks under variable environmental conditions, such as fracture toughness should also be quantified as they likely play a role in fracturing and leakage. Subcritical fracture growth may also be involved.

Transects across the Little Grand Wash fault show distinct mineralogical and isotopic trends related to alteration by CO_2-rich fluids. Calcite is the dominant precipitated mineral, both in reservoir (sandstone) and seal (siltstone & mudrock) lithologies. Precipitated calcite is isotopically distinct and observed in bulk rock isotopic trends. Fracture toughness testing using both the short rod and double torsion test methods indicates that CO_2-related alteration of rocks exposed at the field site has weakened one reservoir lithology by approximately 50%. However, subcritical index, another parameter obtained from fracture testing is not significantly affected by CO_2-related alteration in reservoir sandstone. A full suite of lithologies are being tested and compared with the double torsion test method under ambient air conditions. These same samples will also be tested in environmental conditions more like those encountered in a CO_2 sequestration scenario. These data can and should be integrated into more sophisticated numerical models in order to assess their impact on the overall risk analysis of CO_2 injection sites and provide more geologically realistic and accurate results. In addition, these data and observations may also be applied to conventional hydrocarbon production, specifically the use of CO_2 injection for enhanced recovery.

Keywords: CO2, structure, geomechanics

EG-22

Rotation analysis of shear wave polarizations in the presence of depth-variant azimuthal anisotropy: a synthetic case study

Maleski, J.[1], Tatham, R.[1]
jacquelinem@utexas.edu
1. Jackson School of Geosciences, The University of Texas at Austin, Austin, TX

Azimuthal anisotropy, commonly caused by aligned fractures, causes shear waves to split into a fast component, polarized parallel to fracture strike, and a slow component, polarized perpendicular to fracture strike. Determining the polarization of each split shear wave and the time lag between them provides valuable insight regarding fracture azimuth and intensity. However, analysis of shear wave polarizations in seismic data is hampered by reflection induced polarization distortion. The reflectivity behavior of shear waves becomes increasingly complicated as source-receiver offset increases beyond normal-incidence geometry. Traditional polarization analysis methods, which attempt to isolate each shear mode by rotating source-receiver components (XX, XY, YX, YY) through an angle that optimally diagonalizes the 2x2 S-wave data matrix, are limited to the normal-incidence range and can produce incorrect results if implemented over the full range of offsets available in seismic surveys. By normalizing amplitudes recorded at non-normal incidence to values recorded at normal incidence, offset-dependent shear wave polarization distortion can be corrected and a larger range of offsets become available to constrain shear wave polarizations. Additional complexities arise if fracture orientation changes with depth, as reflections from layers with different fracture orientations will retain significant crossterm energy after initial rotations are applied. To properly analyze depth-variant azimuthal anisotropy, layer stripping removes time lags associated with each interval of constant anisotropy and additional rotations are applied to subsequent offset-normalized reflections in an iterative fashion. Synthetic data is presented to demonstrate the efficacy of these methods.

Keywords: seismic anisotropy, shear wave splitting, fractures, rotation analysis, layer stripping

EG-23

Geometric and Lithic Variability within the Syndepositional Cave Graben Fault System, Guadalupe Mountains, New Mexico

Mathisen, M.[1], Zahm, C.[1], Kerans, C.[2]
marenmathisen@utexas.edu
1. Department of Geological Sciences, Jackson School of Geosciences, The University of Texas at Austin, Austin, TX
2. Bureau of Ecomonic Geology, Jackson School of Geosciences, The University of Texas at Austin, Austin, TX

Permian Capitan shelf margin exposures in Rattlesnake and Slaughter Canyons in the Guadalupe Mountains, New Mexico, reveal a complex syndepositional fault and fracture system which has developed as a result of gravitational loading and differential compaction on and in front of the early cemented Guadalupian 24 shelf margin reef. Extensive syndepositional deformation within the Permian Capitan depositional system is known to have influenced the stratigraphic architecture of the system, as well as diagenetic patterns and karst development, and may influence the reservoir properties of the shelf margin system.

A real-time kinematic GPS was used to map faults and fractures exposed on the canyon walls, while high-resolution digital imagery and airborne lidar provide a context for 2 and 3-D visualization and interpretation. Detailed mapping of the fault system reveals a complex deformational history and high degree of variability in fault geometry, including the presence of vertical and lateral fault relays, highly variable fault apertures, and variable fracture intensity and strain magnitudes with distance from the main faults and within different stratigraphic units. Fault breccias ranging from less than a centimeter to several meters in aperture contain entrained sediment and clasts of variable age and composition. Deformation zones extend up to tens of meters in width and stratal geometries near the faults are characterized by thickness changes and inclined bedding.

Integration of the fault geometry, stratal relationships and breccia fills has revealed an episodic growth of the Cave Graven Fault System, which can be compared to similar work in Slaughter, Rattlesnake, Walnut and Dark Canyons. This comparison highlights a variable fault cessation and reactivation sequence for each canyon over the G24 through G30 high frequency cycles (5-15 my).

Keywords: Permian, Capitan, syndepositional deformation, fault breccia

EG-24

Thermodynamic state of hydrate-bearing sediments on continental margins around the world

Meyer, D. W.[1] and Flemings, P. B.[1]
meyerdw3@utexas.edu
1. Jackson School of Geosciences, The University of Texas at Austin, Austin, TX

In situ salinities within hydrate-bearing sediments in the gas hydrate stability zone (GHSZ) were calculated from Archie-derived water saturations at ODP Site 1249A at Hydrate Ridge, NGHP Site 01-10A in the Krishna-Godavari Basin, Mallik Site 5L-38 in the Mackenzie River Delta, and IODP Site U1328A offshore Vancouver Island. At these sites, we identified regions where in situ salinities are higher than those of seawater (~550 mM Cl-) and reach maximum values of 2520, 2190, 1500, and 2160 mM Cl- at Sites 1249A, 01-10A, 5L-38, and U1328A, respectively. We determined the in situ hydrate saturation using Logging-While-Drilling data in an iterative application of Archie's Law. The in situ salinities were calculated through a volumetric relationship between water saturation and the core-derived salinities. The salinity required for three-phase equilibrium was determined using an equilibrium thermodynamic model for methane hydrate. Zones at which three-phase equilibrium existed were identified by comparing the in situ salinity and the three-phase salinity. At Sites 1249A, 01-10A, and 5L-38, calculated in situ salinities reach the three-phase equilibrium boundary, as defined by the in situ pressures and temperatures for each site, over large portions of the GHSZ, indicating that three-phase equilibrium exists within these regions. At Site U1328A, however, calculated in situ salinities are not elevated to the three-phase boundary, indicating that this system is not near three-phase equilibrium.

Keywords: Methane hydrate, hydrate stability, hydrate saturation, archie's law, free gas migration

EG-25

Fracture Formation, Folding and Strain Distribution in the Cardium Sandstone, Alberta Fold and Thrust Belt, Canada

Ozkul, C[1]., Eichhubl, P[1]., Ukar, E[1].
canalp.ozkul@utexas.edu
1. Jackson School of Geosciences, The University of Texas at Austin, Austin, TX

The folded and thrusted Mesozoic clastic sequence of the Canadian Rocky Mountain foothills forms important hydrocarbon reservoirs with a long history of natural gas and oil production. Successful exploration and development of these unconventional reservoirs require understanding of fracture intensity, fracture evolution, and timing of fracture formation relative to the evolution of the fold and thrust system. The formation of fractures and their timing relationship relative to folding and thrusting have remained unclear. Ambiguity of fracture development and evolution has a large impact on fracture prediction and production of hydrocarbons.

The Upper Cretaceous Cardium Sandstone of the Alberta Foothills provides a good opportunity to study the relation between folding and fracture formation combining field structural observations and kinematic modeling of fold-and-thrust- belt evolution. We explore the relationship between fracture strain and structural position by analyzing fracture intensity in the forelimb, crest, and backlimb of the Red Deer anticline. Fracture strain calculations obtained from macroscanline data are similar to microfracture data. In addition, strains calculations indicate there are no considerable variations in fracture strain, and no consistent association with particular structural positions. Future work will include (i) calculation of folding strain using kinematic models; and (ii) comparison between folding strain and measured fracture strain.

Keywords: Fracture Strain, Fold and Thrust Belt, Balanced Cross- Section, Unconventional Reservoir

EG-26

The behavior of dissolved organic carbon in carbon capture and sequestration sites

Patson, M.[1], Larson, T. [1], Breecker, D.[1], Hovorka, S.[2], Yang, C.[2]
michael.patson@utexas.edu
1. Jackson School of Geosciences, The University of Texas at Austin, Austin, TX
2. Bureau of Economic Geology, The University of Texas at Austin, Austin, TX

Carbon capture and sequestration (CCS) is a proposed solution to mitigate anthropogenic carbon dioxide emissions. A large coal-fired plant (1,000 MW) produces 10 million tonnes of CO_2 annually. To sequester CO_2 of this scale an estimated subsurface area of 100 $km^2$is required. Over this large area, the possibility exists that natural or well-related imperfections in the cap-rock (fracture zones or faults) will be encountered by injected CO_2 which may result in the leakage of CO_2 across the cap-rock. The benefits of CCS would be diminished and hazards associated with leaking CO_2 increased if leaks were undetected and unresolved. Therefore, monitoring CCS sites is essential. Due to the reactive nature of CO_2 and the complications of detecting leaked CO_2 at surface, other indicators of unintended CO_2 migration into shallow reservoirs, such as changes in dissolved organic carbon (DOC) may provide useful information

Leaked CO_2 from deep sequestration reservoir that has migrated vertically will interact and dissolve into groundwater causing an increase in pCO_2 and a decrease in pH. While increased solubility of DOC with increased CO_2 has been demonstrated in peatland, the process has not been studied extensively in the subsurface. Increased CO_2 concentrations in groundwater have been shown to enhance the solubility of heavy metals in the subsurface. Most dissolved metal is found as a metal-organic complex and therefore, any factor that alters metal solubility should also affect DOC solubility. The maximum adsorption for metal-organic complexes is typically around pH 5. While other factors may influence adsorption, the amount of sorbed DOC is predominantly determined by to pH. Consequently any changes to pH from injected CO_2 should effect DOC concentrations. This effect may be amplified by selective adsorption of the CO_2 gas onto the rock.

This study will address how changes in groundwater chemistry will affect the concentration of DOC. We will use water saturated flow through column experiments to evaluate the interaction between dissolved CO_2 and DOC in porous media. Columns will be packed with geologic material and water with various concentrations of dissolved CO_2 will be pumped through the apparatus. Breakthrough curves comparing DOC and CO_2 (aq) will be collected and analyzed by gas chromatography and isotope-ratio mass spectrometry. These measurements will provide the basis in determining the sensitivity of dissolved organic carbon as a tracer for CO_2 leakage and the usefulness as a measure of increased CO_2 in the subsurface.

Keywords: Carbon sequestration, dissolved gases, dissolved organic matter, tracer, monitoring

EG-27

Potential impacts to landscapes and hydrologic flows from above-ground activities in the Eagle Ford Shale Play

Pierre, Jon Paul[1,2]; Abolt, Charles J.[2,3]; and Young, Michael H.[2]
jppierre@utexas.edu
1. Energy and Earth Resources Program, Jackson School of Geosciences, University of Texas at Austin, Austin, TX
2. Bureau of Economic Geology, Jackson School of Geosciences University of Texas at Austin, Austin, TX
3. Department of Geological Sciences, Jackson School of Geosciences University of Texas at Austin, Austin, TX

Producing hydrocarbons from tight formation source rocks has become one of the most important changes in the North American petroleum industry in decades. The Eagle Ford (EF) Shale Play in southern Texas is currently one of the most important with respect to oil and gas production. In a 12 year period, the number of wells drilled into the EF has nearly doubled the number of wells drilled over a 90 year period in the Austin Chalk, the overlying formation in the same geographic area. This rapid increase in activity in South Texas is also accompanied by a rapid increase in construction of drilling pads, roads, pipelines, and other necessary infrastructure. Though substantial research is devoted to potential below-ground impacts from drilling and hydraulic fracturing, less research has focused on landscape impacts, like fragmentation, soil erosion, etc. In this study, we assess the spatial and geomorphic fragmentation effects of the recent shale boom in south Texas, where reduced rainfall rates could substantially lengthen landscape reclamation periods. The play sits within several ecological regions, including the Southern Texas Plains, the Central Texas Plains, and the Blackland Prairies. In this work, we have created a database (ArcGIS) that includes all wells drilled, pipelines, and many roadways across the play, and have placed these features onto base maps of land cover (NLCD), soil type, vegetation assemblages, and hydrologic units. We then use different landscape fragmentation algorithms (e.g., third-party ArcGIS Landscape Fragmentation Tool, v 2.0) to assess changes to the continuity of these different ecoregions and the landscapes that support them. Though results are preliminary, we show a slow but steady increase in the number of wells per pad, an increase in the fragmentation of ecosystems, an increase in the potential for soil loss, and possible alterations to hydrologic systems. Results indicate that small changes in infrastructure placement may reduce ecological impacts.

Keywords: oil and gas extraction, landscape fragmentation, Eagle Ford

EG-28

Thermal Controls on Porosity and Organic Matter and Porosity in the Eagle Ford Formation, South Texas

Pommer, M.E.[1], Milliken, K.M.[2]
Maxwell.Pommer@utexas.edu
1. Jackson School of Geosciences, The University of Texas at Austin, Austin, TX
2. Bureau of Economic Geology, The University of Texas at Austin, Austin, TX

Scanning electron microscopy of Ar-ion milled samples shows that character and evolution of porosity is strongly affected by type, abundance and distribution of organic matter (OM) within the Eagle Ford Formation, South Texas. Samples were collected, imaged and quantified to provide insight into pore types and distributions across a range of thermal maturities.

Observed porosity within low maturity samples correlates inversely with total organic content (TOC). Samples contain pore networks dominated by relatively large coccolith-hosted primary inter-particle (Inter_P) pores with a mean equivalent circular diameter (ECD) of ~110 nm, ranging up to ~2 µm. Primary intragranular pores are observed within coccolith fragments, coccolith-bearing fecal pellets, foraminifers, phosphate clasts, and other skeletal debris. OM-associated pores at low maturity are dominantly large pores at boundaries between organic matter and mineral surfaces with a mean ECD of ~100 nm. Smaller pores (mean ECD ~30nm) within clay-associated OM are observed, and are interpreted as primary.

In contrast, observed porosity within high maturity samples correlates positively with TOC. Samples contain pore networks that are largely dominated by secondary pores within OM. OM-hosted pores consist of smaller equant pores grading into larger pores with more complex and irregular shapes. Measured OM-hosted pores range in ECD from ~4 nm to ~400 nm with a mean of ~22 nm within high maturity samples. Mineral hosted pores are also present at higher maturities, many associated with clay minerals, but are much smaller, with a mean equivalent circular diameter of ~60 nm ranging up to ~850 nm. In addition, fecal pellets and skeletal grains are observed to contain OM that pervasively fills intra-particle pore space, which suggest that porosity is reduced through incursion of mobilized bitumen.

Both detrital kerogen and diagenetic bitumen are present at both high and low maturity, and cause porosity loss both through deformation of ductile kerogen with compaction, as well as incursion of primary pore space with mobilized diagenetic bitumen. As thermal maturation increases, bitumen is mobilized filling intraparticle pore space, and secondary pores develop within OM.

Keywords: Porosity, Bitumen, Eagle Ford, Mudrocks

EG-29

Integrated Rock Physics Modeling and Seismograms Simulation Case Study from Haynesville Shale

Ren, Q.[1] , Spikes, K.[1]
qiren@utexas.edu
1. Jackson School of Geosciences, The University of Texas at Austin, Austin, TX

The alignment of platy clay minerals and non-spherical pores are two sources of anisotropy in shale. Understanding how the shapes and size of clay minerals and pores influence elastic properties are important for characterizing unconventional reservoirs. Our work approached this problem in two steps: first, rock physics modeling by anisotropic differential effective media (DEM) model; second, full waveform seismogram simulation based on rock physics modeling. The clay mineral shapes and pore shapes were accounted in DEM modeling by introducing a distribution of each. The distributions were modeled as normal distribution under a series of different mean values. In addition, we modeled the situation of coupled clay mineral shapes and pore shapes to simulate these imbedded non-spherical pores between platy clay minerals. The size of each clay or pore inclusion modeled under normal distribution as well. This statistical treatment of the rock physics modeling accounted for the complexity of the rock and the uncertainty of the measurements and the model. With the VTI elastic stiffnesses and anisotropy parameters provided by rock physics modeling, we simulated the seismic response of shale under different reservoir properties. The case study was from Haynesville Shale. With the same mineralogy, the modeled rock stiffness decreased with pore aspect ratio and clay aspect ratio, while the rock anisotropy increased with these two parameters. These variations of stiffness and anisotropy were reflected in the synthetic seismograms. The sensitivity of the seismic response to anisotropy clearly increases at far offsets.

Keywords: rock physics modeling, anisotropic DEM, seismograms simulation, Haynesville Shale

EG-30

Constraints on the magnitude and rate of carbon dioxide dissolution at Bravo Dome natural gas field

Sathaye, Kiran.[1], Hesse, Marc.[1], Stockli D.[1], Cassidy, Martin.[2]
kiransathaye@utexas.edu
1. Jackson School of Geosciences, The University of Texas at Austin, Austin, TX
2. University of Houston

The Bravo Dome field in northeastern New Mexico contains at least 1.2Gt of magmatic CO2. Using apatite (U-Th)/He dating, we present a new estimate for the age of the gas migration of 1.2Ma. The reservoir is comprised of a CO2 gas layer overlying brine water in a sandstone reservoir. Previous estimates have used differences in the CO2/3He ratio in the gas to infer that locally, half of the CO2 originally emplaced has dissolved into the underlying brine. This study presents the first estimate of the total amount of CO2 dissolved. We incorporate gas pressure, reservoir geometry, and gas layer thickness to show that over 80% of the CO2 originally emplaced is still present in the gas layer. It is generally assumed that the dissolution of CO2 is driven by convective currents in the brine. We present an alternative hypothesis for the spatial differences of the CO2/3He ratio seen in this reservoir. Gas injection theory predicts that as gas displaces a liquid, relatively insoluble gas components will become enriched at the front of the displacement. If the emplacement occurred from west to east this would cause 3He enrichment in the eastern portion of the Bravo Dome field overlying the brine. This effect could be responsible for the spatial differences in the CO2/3He ratio.

Keywords: Thermochronology, Stable Isotope, Multiphase Flow

EG-31

Geochemical Characterization of Embryonic Fractures on West Caicos, Turks and Caicos Islands, BWI

Simon, R.[1,2], Kerans, C.[1,2], Zahm, C.[2]
Rebekah.Simon99@gmail.com
1. Jackson School of Geosciences, the University of Texas at Austin
2. Reservoir Characterization Research Laboratory, Bureau of Economic Geology

It is well-established that high-relief, steep-walled carbonate platforms, like those in Australia's Canning Basin and the Permian Reef of New Mexico and Texas, are susceptible to syndepositional deformation. However, it has only recently been understood that this early deformation may play a significant role in the evolution of the overall platform geometry, and in reservoir development. Syndepositional fractures create enhanced vertical permeability and behave as conduits for a range of fluids over time—including early diagenetic fluids, late (burial phase) diagenetic fluids, and hydrocarbons—providing extensive opportunity for dramatic chemical modification of the platform and potential reservoirs. Additionally, the early fractures are fundamental weaknesses along the platform margin that strongly influence later structural development and margin character, and frequently show evidence for multiple episodes of activation over time. On the western margin of the Caicos platform (strike: roughly N10E), Turks and Caicos Islands, a network of margin-parallel, subparallel, and perpendicular "embryonic" fractures are superbly exposed. These fractures are largely younger than 125ky on the leeward shoreline of West Caicos, and provide an exceptional opportunity to study early fractures at their first development, as well as to understand their role in early diagenesis.
In outcrop and hand specimen, at least 3 styles of embryonic fractures are observable on West Caicos: (1) simple, millimeter-wide caliche-filled fractures with variable resistance to weathering, (2) complex, anastomosing groups of millimeter-wide caliche-filled fractures with moderate to high resistance to weathering ("fracture skin") and *en echelon* structure, and (3) millimeter- to centimeter-wide caliche-filled fractures with burrows and roots, and low to moderate resistance to weathering. Type 1 fractures occur in all facies, though the physical manifestation is varied: in grainy beach facies, Type 1 fractures are commonly the longest and most continuous, but in reefal facies, the fractures often truncate against coral heads and make up a much shorter, choppier network. In comparison, Type 2 fractures are more abundant in grainy beach facies and are all but absent in the reef. Type 3 samples are extremely rare and only two were sampled, both from the beach facies. However, despite the differences in geographic distribution and physical manifestation, detailed petrographic analysis reveals a notable similarity: none of the three styles of embryonic fractures display evidence to suggest that they are truly syndepositional, and are in fact predated by at least three distinct subaerial diagenetic phases. Stable isotopic analysis ($\delta^{13}C$ and $\delta^{18}O$) and carbon-14 dating will provide numerical constraints for the evolution of this multi-generational cement/fracture network.

Ultimately, a combination of geochemical and petrographic analysis may prove that embryonic fractures, though not necessarily syndepositional, can still develop early enough to act as preferential conduits for several generations of fluid flow. Such flow may explain the condition of Lake Catherine, located in the interior of West Caicos; fluid communication through karst cave gives the waters of Lake Catherine marine salinity. Given an appropriate additional period of geologic time, it is also likely that the embryonic fracture network on West Caicos will evolve into a more robust network such as that seen in the Permian Reef of West Texas and New Mexico (Guadalupe Mountains), which shows a substantially

higher degree of variability in shape, size, fracture fill, and distribution. This variability is attributed to multiple phases of activation over a timeframe well beyond the initial syndepositional fracture development, and directly relates to the characteristic weakness created during the first instance of fracturing. Finally, this study shows that these early weaknesses on steep platform walls may in fact be so influential that they control large-scale failures of the platform margin; both the Guadalupe Mountains and the west margin of West Caicos show polygonal failure scarps that directly relate to the orientation of the fractures. These unique characteristics of syndepositionally-faulted margins have strong implications for reservoir development.

Keywords: Syndepositional Fracture, Fluid Flow, Caliche, Carbonate Platform

EG-32

Integration of seismic and mechanical properties of the Northern SACROC Unit in the Horseshoe Atoll (Pennsylvanian).
Scurry County, Texas

Sitgreaves, J.[1], Nolting, A.[1], Kerans, C.[1] Zahm, C.[2]
jeffrey.sitgreaves@gmail.com / anolting@utexas.edu
1. Jackson School of Geosciences, The University of Texas at Austin, Austin, TX
2. Bureau of Economic Geology, The University of Texas at Austin, Austin, TX

The SACROC Unit of the Horseshoe Atoll is one of the most productive reservoirs in the State of Texas. SACROC has been in production since 1948, and to date has produced just over to 1.7 billion barrels of oil (Tennyson, 2012). As part of a joint study with Kinder-Morgan, The Bureau of Economic Geology's RCRL constructed an initial reservoir characterization in 2001 as groundwork for a planned CO2 enhanced oil recovery (EOR) project. Our study revisits this characterization, and leverages advances in seismic property analysis and rock strength data to better identify potential thief zones created by the variability between facies, pore types, and mechanical properties.

The Late Pennsylvanian SACROC reservoir formed during extreme icehouse glacioeustacy. Core-based observations reveal dramatic juxtaposition of stacked ooid shoal complexes with common subaerial exposure directly overlain by deep-water carbonate buildups. This combination of primary fabric heterogeneity along with the frequent vadose and karstic diagenetic events creates super-permeability zones not highlighted in simple porosity-permeability plots. Here we employ velocity deviation analysis (Anselmetti et al, 1999) and data on unconfined compressive strength (UCS)(Zahm, 2012) to better predict these super-permeable zones. Data for the study includes a 3D seismic survey with a dominate frequency of 40 Hz, 40 wells with full log suites, continuous core from the 37-11 well that is located at the crest of the field, FMI logs, and injection surveys.

Pore networks can be defined with the use of the velocity deviation to distinguish between vuggy pore networks and interparticle porosity zones based on the behavior of velocity and porosity. The observed positive velocity deviation from the ideal Wylie time-average model identifies zones with vuggy porosity. The UCS and velocity properties of the rock are directly influenced by the pore type and amount of porosity. Touching vug porosity is the root cause for a majority of the super-permeable thief zones. The combination of velocity deviation and UCS can identify the difference between separate vug and touching vug pore structures. The relationship between the velocity/UCS and the use of injection surveys, make it possible to spatially model areas with anomalous flow behaviors. This will enhance the existing characterization and benefit the EOR efforts currently taking place in the SACROC reservoir.

Keywords: Reservoir Characterization, Carbonate Geology, Seismic and Mechanical Rock Properties

EG-33

Importance of Micropore Networks in Shallow-Water Unconventional Carbonate Reservoirs of the Cretaceous Stuart City Trend

Smith, B.P.[1], Kerans, C.[1]
bsmithguitarman@gmail.com
1. Jackson School of Geosciences, The University of Texas at Austin, Austin, TX

Recognizing the presence microporosity in carbonate reservoirs is often a critical step in the characterization process. High values for microporosity adversely affect production rates and create zones of high water saturation and need to be fully appreciated. Microporosity is commonly associated with deep-water chalks and mudrocks; however, micropore networks can be important contributors to porosity and permeability in shallow-water carbonates as well. The Albian (Cretaceous) Word Field in Lavaca County, Texas, consists of stacked subtidal cycles deposited in a lagoon behind the Stuart City Reef margin. A study of four cores and sixty thin sections determined that pore types in Word Field vary widely and are partitioned into different facies within the high-frequency cycle framework. Microporosity is related to oncoids and other coated grains, as well as the organism Lithocodium, which is preferentially located in grain-dominated packstones and grainstones near the tops of cycles. Other types of porosity include moldic porosity after fossils and interparticle porosity in lower energy peloidal facies.

Correlation along depositional strike or dip between cored intervals shows a moderate degree of heterogeneity. Additionally, changes in water depth at the system tract and sequence scales affect the thickness and frequency of different facies packages. Fully understanding the microporosity distribution involves integrating observations at the high-frequency cycle level with larger scale changes in stratigraphy throughout the field. The overall aim of the study is to improve our understanding of microporosity in shallow water carbonate and to add to our knowledge of the Stuart City trend and other Cretaceous platforms.

Keywords: carbonates, carbonate reservoir characterization, microporosity, *Lithocodium*, Stuart City, Albian, unconventional, Cretaceous carbonates, carbonate petrophysics

EG-34

An efficient algorithm for multidimensional two-point seismic ray-tracing in layered media

Sripanich, Y.[1], Fomel, S.[1]
sripanichy@utexas.edu
1. Jackson School of Geosciences, The University of Texas at Austin, Austin, TX

The issues of tracing a ray and finding its traveltime have been objects of significant interest in geophysics. An accurate set of data on both raypath and traveltime would make it possible to reconstruct a seismic image that effectively illustrate complex geological features beneath the surface. In this study, we propose a new efficient and accurate two-point ray tracing algorithm using the concept of Newton-Raphson method of locating roots to solve for the raypath corresponding to stationary traveltime according to the Ferm at's principle. The Newton-Raphson method (the Newton's method) of locating roots is chosen among others to solve this problem because of its quadratic convergence. Even though some difficulties are expected due to our choice of the Newton's method such as a failure to converge to the roots because of poor initial estimate, and difficulty in calculating the derivative of a function, the Newton's method provides a quick and efficient way to minimize the traveltime function accurately in the case where appropriate initial conditions are given.

The current version of the algorithm is functional in constant-velocity media and constant-gradient media in both 2D and 3D. To illustrate one of this algorithm's applications, its 2D version has been applied in the Kirchhoff modeling process to generate synthetic shot gathers. Future work includes extension to transversely isotropic media.

Algorithms developed in this study will be included in *Madagascar*, an open-source software package for multi-dimensional data analysis. Anyone who is interested can readily access the source code and use other existing tools in *Madagascar* to reproduce the same results I have reached or apply the algorithm to other problems of their interest.

Keywords: two-point ray tracing, Newton-Raphson method

EG-35

Low-rank one-step wave extrapolation

Sun, J.[1], Fomel, S.[1]
junzhesun@utexas.edu
1. Jackson School of Geosciences, The University of Texas at Austin, Austin, TX

We propose a method for one-step wave extrapolation using low-rank symbol approximation. We use an analytic source to construct a complex wavefield. Low-rank decomposition is employed to approximate the mixed-domain space-wavenumber wave extrapolation symbol. We demonstrate the stability improvement of a one-step scheme over a two-step scheme when waves are propagated at large time steps, thus reducing the computational cost. For wave propagation in inhomogeneous media, a velocity gradient term can be included to achieve a more accurate phase function, especially when velocity variations are large. Additionally, we develop an absorbing boundary condition which is propagation-direction-dependent and can be incorporated in the wave extrapolation operator. It allows waves to travel parallel to the boundary, thus reducing artificial reflections at wide-incident angles. We demonstrate our algorithm by propagating waves in synthetic anisotropic media. We adopt our propagator for pre-stack reverse time migration and show the imaging result.

Keywords: low-rank, wave propagation, reverse time migration

EG-36

Time-domain approach to Gaussian beams

Swindeman, R.[1], Fomel, S.[1]
ryan.swindeman@utexas.edu
1. Jackson School of Geosciences, The University of Texas at Austin, Austin, TX

Processing large amounts of seismic data while still creating an accurate image has been a well-known challenge of geophysicists for many years. Gaussian beam migration, one approach to dealing with this problem, is a flexible technique that allows us to move reflection energy back to its source. We seek to develop a new, computationally efficient algorithm to implement Gaussian beams in the time-domain. This task is accomplished by approximating the shape (center and extent) with a variety of triangles and selecting the representation which most emulates the original shape. We choose the sum of two triangles as the best result and design a program around this procedure in the Madagascar software package.

Keywords: geophysics, Gaussian, beam, time, domain, data, processing, migration

EG-37

Investigating Tortuosity and Permeability in the Carbonate-rich Niobrara Formation

Tokan-Lawal, A.[1,2], Landry, C.[2], Prodanović, M.[3], and Eichhubl, P[2]
adenike@utexas.edu
1. Jackson School of Geological Sciences, The University of Texas at Austin, TX, USA
2. Bureau of Economic Geology, The University of Texas at Austin, TX, USA
3. Petroleum and Geosystems Engineering, The University of Texas at Austin, TX, USA

Natural fractures are typically partially lined and/or filled with mineral cements, which can constrict fluid flow and create very rough fracture wall surfaces. In this study, we investigate fluid flow in the carbonate-rich, low-matrix permeability Niobrara Formation. We focus on correlating fluid flow parameters (such as permeability) with the geometric tortuosity of the fracture (pore space) and the individual fluid phases for a fractured carbonate.

We use x-ray microtomography imaging to provide information on fracture geometry. Image analysis is performed (via 3DMA Rock software), to characterize the connectivity and geometric tortuosity of the pore space and individual fluid phases at different saturations. We also use a combination of the level-set-method-based progressive-quasistatic algorithm (LSMPQS software), and Lattice Boltzmann simulation (Palabos software) to characterize the capillary dominated displacement properties and the relative permeability of the naturally cemented fractures within. Finally, we numerically investigate the effect of (uniform) cementation on the fracture permeability as well as the tortuosity of the pore space and the capillary pressure-water saturation (Pc-Sw) relationship using two different methods.

Permeability estimates in the Niobrara sample were consistent regardless of the method used. Pore space tortuosity and capillary pressure as a function of water saturation relationships both increase with cementation, and while the behavior is similar to that of cementation effects in sandstones, it is much more abrupt in fractures. This is likely because the fluid pathways are restricted to nearly planar spaces.

Keywords: Unconventional, Fluid flow, Permeability, Lattice Boltzmann, Fractures

EG-38

Characterization of the Lateral Variability in the Shoreline Facies of the Cow Creek Limestone

Voorhees, K.J.[1] Kerans, C.[1]
Kris.voorhees@utexas.edu
1. Jackson School of Geosciences, The University of Texas at Austin, Austin, TX

There is a general assumption that lateral heterogeneity of strandplain depositional systems is limited, but ancient examples with sufficient exposure to test this assumption are rare. The Aptian Cow Creek Limestone of Central Texas represents a carbonate strandplain system that prograded across 40 km from the Llano uplift southwards across the drowned Sligo shelf following OAE 1A transgression. The recent drought that has brought Lake Travis to historically low levels has unveiled continuous cliff exposures of the Cow Creek strandplain that afford the opportunity to test models of lateral and vertical heterogeneity for carbonate strandplains.

The 20 m high bluffs in the Pace Bend area reveal 10 km+ of continuous exposures of a multicyclic prograding succession of lower shoreface bivalve-oyster packstone/rudstone, upper shoreface mixed siliciclastic-carbonate lenticular to trough cross stratified grainstones with hardgrounds, coral patch reefs, and inclined foreshore grainstones. Data for this study includes 3 measured sections, detailed bedding tracings of gigapan mosaics, petrographic analysis, facies description, and paleocurrent data. Results from this work-in-progress include the first documentation from outcrop that the Cow Creek is a complex multi-cyclic prograding unit, with upward-coarsening cycles capped by conformable to bored hardground surfaces. Key lateral heterogeneities recognized to date include coral patch reefs that vary from 0.5 to 3 m within the detailed 0.5 km study window, and a shallow 2m deep tidal inlet that cuts perpendicular to the south-directed foreshore beds.

Results of this ongoing research will advance our understanding of the key elements of lateral heterogeneity in carbonate strandplains, as well as provide a better understanding for the high-frequency sequence architecture. The Cow Creek is an important element of the Lower Trinity regional aquifer, and continues to be a target for hydrocarbons in the Maverick Basin area. Integration of my results with previously published subsurface hydrocarbon and aquifer studies will build on our understanding of the Trinity system and strandplain deposits in general.

Keywords: carbonates, strandplain, Cow Creek Limestone, Pace Bend, lateral variability, sequence stratigraphy, Lake Travis, cyclicity, ourcrop analoge

EG-39

Least-squares Migration with a structure-enhancing filter

Xue, Z.[1], Fomel, S.[1]
zhiguangxue@gmail.com
1. Jackson School of Geosciences, The University of Texas at Austin, Austin, TX

To reduce the migration artifacts arising from incomplete data or simultaneous sources data, least-squares migration (LSM) can be considered, which iteratively apply modeling and migration operator pair to minimize the data misfit. In this paper, we incorporate a structure-enhancing filter into LSM, which aims at reducing artifacts while protecting structure information. Numerical tests of both post-stack and pre-stack LSM show that our approach can effectively improve imaging resolution, especially the enhancement of structural continuity.

Keywords: Least-squares migration, structure-enhancing, simultaneous sources

EG-40

Campanian estuarine reservoirs in the Oriente Basin, Ecuador

Ye Y.[1], Steel, R. J.[1], Olariu, C.[1], Good, D.[2].
pandaye@utexas.edu
1. Jackson School of Geosciences, The University of Texas at Austin, Austin, TX
2. Andes Petroleum Corporation Ecuador LTD

Campanian M1 sandstone, one of the major prospective sandstone units in the Oriente Basin, Ecuador, are derived from the eastern uplands of the Brazil Craton and dispersed northwestwards along the axis of the embryonic Andean foreland basin. Previous studies of cores and well logs have suggested a deltaic depositional system followed by the development of extensive tidal estuarine systems that infilled gradually. However, there are local problems caused by unpredictable lateral sand-mud heterogeneity. The current study uses seismic data, 11 cores and more than 300 well logs to investigate the M1 sandstone.

The M1 sandstone is always markedly sharp based, averages 25 m in thickness, shows upward increasing marine bioturbation and generally fines upward from coarse to very fine grained sandstone, all in keeping generally with a transgressive origin. In cores, the sandstones are amalgamated medium and coarse grained with prominent cross stratification (dm thick), sometimes clearly bi-directional and contains mud drapes. These suggest strong tidal or fluvial-tidal currents in estuary channels. The fine grained intervals are brackish-water intensely bioturbated and dominated by mud drapes, wavy and flaser bedding suggestive of estuary-margin intertidal flats. Associated overlying coals and coaly shales suggest supratidal conditions as the estuaries infilled. Large-scale lateral sandstone-mudstone heterogeneity has been imaged on seismic amplitude maps where a series of slightly sinuous muddy ‘lineaments’ up to 1 km wide have been mapped named “shale barriers”. Each of them is more than 15 km long and 20 – 30 meters thick. Well logs near the “shale barriers” show these are dominated by mud but contain thin sandstones immediately above the main sandstone unit. Mud thickens and sand thins toward the center of these shale barriers, with an overall decrease in total thickness of mud and sand. A core near the shale barrier shows that the main M1 sandstone is still relatively thick (30 feet), amalgamated and cross bedded. Possible explanations of the muddy ‘barriers’ are:(1) they are tidal channels that are sandy during the transgression but become abandoned and filled with mud as the late-stage estuaries infill, and (2) they are the meandering and low-energy tidal-fluvial channels which develop and are maintained in the proximal areas of the estuary. The first interpretation is favored because it explains the presence of both shale barrier and underlying sandstone.

Keywords: tide-dominated estuary, M1 sandstone, heterogeneity

EER-1

Simulating the Impacts of Hawaii's Transitioning Electrical Power System on Water Use

Dawes, C.[1]
cdawes@utexas.edu
1. Jackson School of Geosciences, The University of Texas at Austin, Austin, TX

Hawaii currently faces some of the toughest water and energy resource management problems in the United States. The famous volcanic island chain lies isolated in the center of the Pacific Ocean, the largest saltwater basin on Earth. Natural freshwater resources are therefore limited to what falls and flows on the island, specifically rainfall, streamflow and groundwater stored in aquifers, which are all vulnerable to climate change, continuous erosion and increased consumption. Hawaii's energy situation is also complicated: the islands are lush with domestic renewable energy potential. However, imported fossil fuels supply 90% of the state's energy demands, leading to the most expensive consumed electricity in the country. Moreover, thermoelectric end-users account for the largest percentage of groundwater and total freshwater use over the whole state.

The electrical system on Hawaii is unique: each island has its own grid and distinctive mix of established electrical power producers. There are no inter-island transfers of energy or water, so each island must somehow supply its particular energy and water demand. The current electrical system is also transitioning. For the past decade, Hawaii has driven renewable power production, conservation and energy efficiency improvements through local and statewide policies and incentives aimed at decreasing overall energy use and reliance on imports with the ultimate goal of becoming self-sufficient. However, several hurdles must be overcome before the whole state can meet these goals. For example, potential renewable resources differ between islands due to the uneven distribution of wind, sun, precipitation and near-surface geothermal heat over the island chain.

This study examines the current and future potential energy (specifically electrical power) resources and the associated water use for each of the major Hawaiian Islands. Using GIS tools and @Risk models to simulate different electrical capacity build outs, we can optimize the decision making and policy formation that leads to self-sufficient energy and water systems on Hawaii while decreasing costs and local externalities.

Keywords: Hawaii, Energy, Water, Transitions, Modeling

EER-2

The Magallanes Basin: A Real Solution for the Chilean Crises

Cuevas, P.[1]
pedrocuevas@utexas.edu
1. Jackson School of Geosciences, The University of Texas at Austin, Austin, TX

Nowadays, Chile is in the middle of an energy crisis, basically because of the lack of local fuel production, high electricity prices, and dirty generation.

First of all, the lack of local energy resources makes Chile an energy importing country, vulnerable against any international situation. In solid numbers, Chile imports 96% of its oil consumption, 76% of its natural gas, and 94% of its coal.

Besides, the cost of energy is the highest in the region, making Chile to lose competitiveness against its neighbors. To have an idea, the average industrial price for energy in 2011 was $ 154 USD/Mwh compared to $ 111 USD/Mwh in OCDE.

One good alternative for this last issue, is to develop Chile's recently discovered shale gas potential in Magallanes, using the new technology developments like hydraulic fracture and horizontal drilling, to produce to produce local, cheap and cleaner energy.

Moreover, the last studies on this site estimated the amount of natural gas in 1,360 billions of m3, which can meet the actual demand for nearly 300 years. However, this number does not represent a scenario under a cheap and local energy resource.

Therefore, a new scenario is proposed in order to have a better idea of the size and the economic consequences of exploiting this basin for a more realistic future demand.

Besides, the scenario simulation done in this research, concludes that the future demand of natural gas will be 182,486 teracalories, which would increase its participation on the primary energy consumption from 16% to 36%. Therefore, under this projected scenario, the Magallanes basing could supply the Chilean demand for almost 70 years.

On the other hand, this new scenario generates savings of $5,877 millions of dollars, which means a 29% reduction from the actual energy costs. Moreover, these savings are equivalent to 2.2% of the total GDP of Chile in 2012. Also, under this proposed scenario, the CO2 emission are reduced by 14,766,819 tonnes which represent 21.25% of the total CO2 emission from this country on 2012.

Finally, the results of this research concludes that the unconventional resources in the Magallanes Basin are a reliable, cheap and clean solution for the Chilean energy crises, that can return the competitiveness to the Chilean industry.

Keywords: Insert descriptive keywords here, separated by commas

MG-1

Transition from Subduction to Strike-Slip in the Southeast Caribbean: Effects on Lithospheric Structures and Overlying Basin Evolution

Alvarez T.[1], Mann, P.[2], Wood, L.[1], Vargas, C.A.[3], Latchman, J.[4]
talvarez@utexas.edu
1. Jackson School of Geosciences, The University of Texas at Austin, Austin, TX
2. Department of Earth and Atmospheric Sciences, University of Houston
3. Departamento de Geociencias, Universidad Nacional de Colombia
4. Seismic Research Centre, The University of the West Indies

Topography, basin structures and geomorphology of the southeast Caribbean-northeast South American margin are controlled by a 200-km-long transition from westward-directed subduction of South American lithosphere beneath the Caribbean plate, to east-west strike-slip motion of the Caribbean and South American plates. Our study of structures and basins present in the transitional area integrates a tomographic study of the lithospheric structures associated with lateral variations in the subduction of the South American lithosphere and orientation of the slab beneath the Caribbean plate as well as the evolution of overlying sedimentary basins imaged with deep-penetration seismic data kindly provided by the oil industry and Trinidad & Tobago government agencies. We use an earthquake dataset containing more than 700 events recorded by the eastern Caribbean regional seismograph network to build travel-time and attenuation tomography models used to image the mantle to depths of 100 km beneath transition zone. Approximately 10,000 km of 2D seismic reflection lines which are recorded to depths > 12 seconds TWT are used to interpret basin scale structures including tectono-stratigraphic sequences and structures which deform and displace sedimentary sequences. We use the observed satellite gravity to generate a gravity model for key sections traversing the tectonic transitional zone and to determine depth to basement in basins with sedimentary fill > 12 km.

Within the study area, the dip of subducted South American oceanic lithosphere imaged on tomographic images is variable from ~44 to ~24 degrees. There is a distinct low gravity, low velocity, high attenuation, northwest – southeast trending lineation located east of Trinidad which defines the location of a Mesozoic oceanic fracture zone which accommodated the opening of the Central Atlantic during the Jurassic to Middle Cretaceous. This feature is also coincident with the present-day continent-ocean boundary and acts as a lithospheric weakness during subduction. We propose that this fracture zone is a key transition point between the subduction of South American/Atlantic oceanic lithosphere; which descends into the mantle, to the northeast, and the under-thrusting of transitional to continental South American lithosphere which resists subduction to the southwest. Maps of South American basement and its overlying Cretaceous passive margin illustrates a northwesterly basement dip with a distinct change in angle of the northwest dip across the paleo-fracture zone consistent with our tomographic model. We propose that flexure of the subducting South American plate at this location exerts a critical control on the formation and evolution of the basins and the lateral distribution of Cretaceous through Pleistocene stratigraphic fill. East of the fracture zone, the overlying strata is deformed by active subduction and accretionary prism processes with a wider zone of shortening with lower overall topography, while to the west of the fracture zone there is active oblique collision with a narrower zone of shortening and greater uplift.

Keywords: Subduction zone processes, Sedimentary basin processes

MG

MG-2

A New Tectonic Model for the Breakup of India and East Antarctica

Davis, Joshua K.
buddavis@utexas.edu
Jackson School of Geosciences, The University of Texas at Austin, Austin, TX

The breakup of India (IND) and East Antarctica (EANT) and subsequent formation of the Enderby Basin is a subject of considerable debate. Deciphering the evolution of the Enderby Basin is complicated by limited data coverage, much of which is obscured by high sedimentation rates, abundant volcanic activity, and temporal proximity to the Cretaceous Quiet Zone. Currently accepted plate reconstructions hypothesize that during early basin formation, volcanic activity from the Kerguelen Plume induced a series of inboard ridge jumps. These ridge jumps detached and isolated continental crust from IND beneath the Kerguelen Plateau. However, several observations bring into question the validity of this model. Because the ridge jumps propagated northward, they would have isolated large swaths of older oceanic crust to the south, resulting in significant and improbable two way motion between IND and Madagascar (MAD). Additionally, recent compilations from the Antarctic Digital Magnetic Anomaly Project (ADMAP) reveal that the marine magnetic anomaly interpretations from the previous plate reconstructions are unsupported by basin-wide magnetic data, and are likely erroneous. Lastly, deep marine seismic studies from the conjugate IND and EANT margins show similar and distinct cross-margin features, implying that the margins are coeval, conjugate pairs. Given the improbable plate motion, lack of support from marine magnetics, and similarity of cross-margin features, we believe that the currently accepted models of IND and EANT breakup should be discarded.

I present here a new tectonic model for the breakup of IND and EANT. Seafloor spreading in this model is constrained by coeval seafloor spreading in the Somali and Mozambique basins and the ADMAP marine magnetic compilation of the Enderby Basin. In this model, break-up begins early and progresses steadily, with no two way motion between IND and MAD. The margins of IND and EANT form as conjugate pairs over a single rifting event. Along strike variability is hypothesized to be influenced by differing tectonic regimes (transtensional vs. extensional) and proximity to the Kerguelen Plume.

Keywords: Plate Reconstruction, Continental Breakup, Indian Ocean, India, East Antarctica

MG-3

Origins and evolution of the Gagua Ridge bathymetric feature: a possible example of failed subduction in the Tertiary

Daniel H Eakin[1], Luc L Lavier[1], Kirk D McIntosh[1], Harm J A Van Avendonk[1]
deakin@utexas.edu
1. Jackson School of Geosciences, The University of Texas at Austin, Austin, TX

Four E-W tomographic velocity models combined with coincident multi-channel seismic reflection data (MCS) allow us to develop a new kinematic model to describe the origin and evolution of the Gagua Ridge bathymetric feature in the West Philippine Basin. Data were acquired in the Huatung Basin offshore Taiwan to the southeast during the 2009 TAIGER program. This region is largely dominated by the eastward subduction of the South China Sea along the Manila trench to the southwest, arc-continent collision between the North Luzon volcanic arc and the passive Chinese continental margin to the northwest, and northward subduction of the West Philippine Sea Basin oceanic crust along the Ryukyu trench to the north. While the tectonic framework and development of this complex plate boundary remains enigmatic, we present tomographic evidence showing what appears to be oceanic crust to the east of Gagua Ridge underthrust to the west beneath the oceanic crust of the Huatung Basin to a depth of 15-20 km. This observation is significant as it possibly represents a failed subduction event in the past that may have coincided, competed with, and was subsequently abandoned in favor of subduction along the Manila trench. Underthrusting of this nature is likely the result of oblique compression along structures such as transform fracture zones inherited from the seafloor spreading or strike-slip plate boundaries that are capable of juxtaposing crust of differing age and thermal maturity against one another. One of the keys to obtaining a geodynamic understanding of this process and how it may have evolved in the past is to document the crustal structure of the Gagua Ridge bathymetric feature from north to south. In this area we acquired 3 wide-angle seismic datasets, T1B at 20.6°N, T2 at 21.6°N, and T4A at 22.8°N along with coincident MCS data that bisect Gagua Ridge E-W to constrain the velocity structure at depth and deformation observed near the seafloor. These models illuminate an interesting structural trend beneath Gagua Ridge, with crustal thickening and little to no apparent underthrusting in the south along T1B, to more than 15km of apparent westward underthusting along T2 and T4A to the north. These observations are supported by coincident MCS data that show significant deepening and extensional deformation of the ocean crust on the east flank of Gagua Ridge and uplift and compressional deformation of oceanic crust on the western flank. These observations are also consistent with new geodynamic modeling that indicates the initiation of subduction is likely the result of oblique convergence along relict fracture zones formed as the result of seafloor spreading. The similar geometry and orientation of the Gagua Ridge with respect to the Manila trench combined with the evidence for westward underthrusting of ocean crust suggest this feature may be an incipient subduction system that competed with, and was abandoned in favor of the Manila subduction zone to the west.

Keywords: Marine Seismic, Subduction Zone Processes, Tectonics and Magnetism, Tomography

MG-4

Parameters that may control tsunamigenic earthquakes in Northern Sumatra

Frederik, M.C.G.[1], Gulick, S.P.S.[1], Austin, J.A., Jr.[1], Udrekh[2]
Marina.frederik@utexas.edu
1. Jackson School of Geosciences, The University of Texas at Austin, Austin, TX
2.Badan Pengkajian dan Penerapan Teknologi, Jakarta, Indonesia

Recent large earthquakes, such as the Tohoku-Oki 2011 (M_w 9.0) and Sumatra-Andaman 2004 (M_w 9.1), have prompted studies to reevaluate seismicity and rupture propagation behavior at subduction zones. Large earthquakes in these zones have occurred over many decades, which limit documented reports. For subduction zones, three properties are suggested in relation to earthquakes with magnitudes 9.0 and larger: age of subducting plate (<60 m.y.), convergence rate (>8 cm/y), and accretionary margin. On the west coast of Sumatra, the Indo-Australian Plate is being subducted obliquely at a rate of 5-6 cm/yr under the Sunda block, which is part of the Eurasian Plate. The age of Indo-Australian Plate offshore of northern Sumatra is ~70 m.y. The age of incoming plate and its rate of convergence put this subduction zone as one not expected to produce M_w > 9.0. Recent events show that hypothesis to be incorrect.

Our study area is 1-7°N and 92-97°E, extending over the entire forearc from northwest of Aceh to west of Simeulue Island. Merged bathymetric data reveal that the accretionary prism offshore northern Sumatra is comprised of a plateau ~200 km wide with seafloor depths ranging from 4.5 km near the Sunda Trench to <1 km on the forearc high proximal to the Aceh (forearc) Basin. The seafloor is comprised of lineated highs and lows with distances between presumed anticlines of 2-16 km.

Five MCS profiles used to investigate the subsurface features transect the wedge from the Sunda Trench to the Aceh Basin. The incoming sediment near the Trench is up to ~4.5 km thick. Near the deformation front, faults are observed down to the décollement (~7 km depth) that suggest dewatering of sediments near the décollement. Within the wedge, faults are observed only down to ~2 km depth due to presumed highly compacted, lithified, dewatered sand- and silt-rich sediment. Analysis of the seismic profiles and bathymetry simultaneously reveal four main structural zones: 1) predominantly landward vergent folds, 2) predominantly seaward vergent folds, 3) mixed vergent folds, and 4) erosion/landslide dominated regions (likely overlying folded terrane). Extended landward vergence zone is uncommon in accretionary prisms worldwide. One suggestion is the existence of a backstop with a seaward dipping edge, where younger sediments accreted to the prism form the landward vergent folds.

Based on interpretation of the structural zones and published velocity models in this margin, we propose a backstop that extend from under the Aceh Basin to under the mixed vergence zone. The nature of the backstop may be of an older accreted sediment or the Sunda Block. With the existence of a strong inner wedge (backstop), together with the indurated sediment forming the landward vergence zone, when a major earthquake occurs under the Aceh Basin or forearc high, the rupture will propagate farther seaward toward the Sunda Trench and displace greater volumes of water than a more landward rupture, yielding a more hazardous tsunami.

Keywords: subduction zone, bathymetry, seismic reflection, landward-vergence, Sumatra, backstop

MG-5

Evolution of Wilcox Margin with focus on sediment flux and process character of the shorelines

Shunli Li[1], Cornel Olariu[1], Ronald J Steel[1]
lslcugb@gmail.com
1. Jackson School of Geosciences, The University of Texas at Austin, TX

Characteristics depositional systems at shelf and shelf edge are significant for understanding deep-water deposition. Palaeo-discharge of channel systems and type of deltaic facies at shelf edge could represent sediment flux and shoreline processes respectively. The objective of this study, Wilcox Group, is a very thick sequence terrigeous clastic deposition with thickness over of 5000 ft in northwestern Gulf of Mexico Basin. Area of study includes approximately 10 Counties around Houston embayment. In this study, Wilcox Group was subdivided into two members including Lower Wilcox and Upper Wilcox by Big Shale which is a regional and correlative marker. Combined with regional seismic profiles, well logs were collected in this area to establish stratigraphic frameworks both in dip and strike directions. Well log patterns of Lower Wilcox primarily show coarsening upward successions which indicate delta progradations with flooding surfaces. Serrated well log patterns of Upper Wilcox which represent sandstone interbedded with mudstone suggest fluvial systems and shallow water deposition on Wilcox shelf. Outcrops of Wilcox along Colorado River in Bastrop County area were measured and described in detail, which were also correlated to adjacent subsurface wells. Sedimentary facies of outcrops are mainly comprised of fluvial channels with trace fossil assemblage of skolithos (*Skolithos, Diplocraterion*, *Ophiomorpha* and *Thalassinoide*) and shallow water laminated, mottled muddy deposition. Cores in Austin County present channel sandstone with mud drapes (boundles) and bidirectional current ripples of Lower Wilcox, which indicates river-dominated Brazos Delta with moderate tidal influence at shelf edge. Trace fossils within these core show moderate to abundant bioturbation with assemblages mainly including *Planolites*, *Teichichnus*, *Macaronichus*, *Thalassinoide*, *Zoophycos* and *Chondrites*. Minor small scale hummocky cross-beddings represent storm processes occurred at pauses in sedimentation. Channel discharge was preliminarily calculated by channel parameters of width, depth and sediments density which measured at outcrops, cores and well logs. High discharge during Lower Wilcox deposition period may provide adequate sediments into deep-water area of Gulf of Mexico Basin. Sediments which were driven by high supply even at high sea level stage may acrossed shelf edge and reached deep area through incised canyons, and formed thick and widespread deep-water deposition.

Keywords: sediment flux, shoreline processes, discharge, Wilcox, Gulf of Mexico Basin

MG-6

Facies achitecture and depositional processes of the Moruga Formation, Trinidad

Peng, Y. [1], Steel, R.J. [1], Li, S. [1], Olariu, C. [1]
ypeng@utexas.edu
1. Jackson School of Geosciences, The University of Texas at Austin, Austin, TX

The migration of the paleo-Orinoco delta system has provided abundant shallow-water and deepwater sand reservoirs from mid-Miocene to Pliocene. High sediment supply of delta system, high tectonic subsidence rates on the shelf margin, and high-amplitude and frequency eustatic sea level changes provide an outstanding opportunity to evaluate the depositional processes during the outbuilding of shelf margin. The late Miocene Moruga Formation is divided into four members: the St. Hilaire Silt, the Trinity Hills Sandstone, the Las Tablas Silt and the Casa Cruz Sandstone. Outcrops located in the Moruga Bay and Guayaguayare Bay were measured in detail focusing on the Trinity Hills Sandstone and Casa Cruz Sandstone Members. Grain sizes, sedimentary structures and vertical sequences were observed and described for interpreting facies architecture and evolution of depositional systems. The Trinity Hills Sandstone Member in the Guayaguayare Bay consists of mud and silt to upper very fine sandstone with low relief wave ripples and variable scales of hummocky/swale cross beddings. Imbricated storm clasts occurred at the bottom of sandstone with hummock/swale cross bedding. Slumps were observed at several locations, which reflect high gradients of depositional geomorphology. Sand-rich channels incised into mud-rich intervals at the upper slope. The Casa Cruz Sandstone Member in the Guayaguayare Bay is characterized by silt to upper very fine sandstone interbedded with organic bearing mudstone. Wave ripples and hummocky/swale cross beddings are common within the sandstone, which indicates wave-dominated depositional processes and storm processes at pauses. The stacked coarsening-upward sequence patterns suggest delta progradations during the late Miocene.

Keywords: facies architectures, depositional processes, wave-dominated, Moruga Formation

MG-7

The Cretaceous-Paleogene boundary deposit in the Gulf of Mexico: Large-scale oceanic basin response to the Chicxulub impact

Sanford, J.[1,2], Gulick, P. S.[1,2], Snedden, J. W.[1,2]
jsanford@ig.utexas.edu
1. Jackson School of Geosciences, The University of Texas at Austin, Austin, TX
2. The University of Texas Institute for Geophysics, The University of Texas at Austin, Austin, TX

The prevailing theory for the Cretaceous-Paleogene (K-Pg) extinction event cites the Chicxulub asteroid impact on the Yucatán Peninsula as the catalyst for the global climatologic and ecologic crisis at the start of the Cenozoic. The Gulf of Mexico, due to its passive marine setting and proximity to the crater, is the premier locale in which to study the near-field geologic effect of a massive bolide impact. Additionally, hydrocarbon exploration in the last decade has yielded sufficient borehole and seismic data to evaluate the regional response of the basin to the impact from the shelf to the deep water in the Gulf of Mexico.

A thick (decimeter- to hectometer-scale) deposit of carbonate debris at the K-Pg boundary is ubiquitous in the Gulf and readily identifiable on borehole and seismic data. In cores in the southeastern Gulf, the deposit consists of primarily muddy debrites with some turbidites and suggests that debris flow was the first and most substantial regional transport mechanism in the Gulf after the impact. However, a later episode of turbidite deposition may reflect a transition from seismogenic to tsunamigenic deposition. On this basis, deposits seen in seismic and borehole data in the distal deep-water Gulf are interpreted be predominately debrite.

Mapping of the boundary deposit in the northern Gulf of Mexico reveals that the impact re-distributed over 100,000 km^3 of sediment in the northern Gulf. Deposit distribution suggests that the majority of sediment derived from coastal and shallow-water environments throughout the Gulf via seismic and tsunamic energy initiated by the impact, rather than from the crater and adjacent Yucatán Platform itself. In particular, the Texas Shelf and northern margin of the Florida Platform (i.e.. DeSoto Canyon) appear to have been primary sources of widely distributed sediment, while the Florida Platform generally appears to have undergone more localized platform collapse. Furthermore, the area of the incipient salt canopy appears to have had significant topography due to underlying salt that had a significant control on the thickness of the deposit in the north-central and northwestern Gulf. Nevertheless, the amount of sediment that was mobilized by the impact and ensuing processes was sufficient to overwhelm virtually all existing topography and depositional systems, blanketing the entire Gulf with carbonate debris in a matter of days at the start of the Cenozoic.

Keywords: K-T boundary, K-Pg boundary, Gulf of Mexico, sediment gravity flows, salt tectonics

MG-8

Preliminary analysis of the continental margin record of temperate glaciers in Southeast Alaska

Swartz, JM.[1], Walton, ML.[1], Gulick, SPS.[1]
jmarshallswartz@utexas.edu
1. Institute for Geophysics, Jackson School of Geosciences, The University of Texas at Austin, Austin, TX

Shelf-edge depositional systems in Southern Alaska have the potential to provide details regarding the depositional processes of temperate glacier systems developed within an active orogen, the St. Elias Mountains. Southern Alaska is lower in latitude (57-60°N) than most other glaciated margins, and the glacial systems have markedly different dynamics in part due to interaction with active tectonics and orogenesis. Four sea valleys crossing the Gulf of Alaska shelf have been previously identified and interpreted as glacial in origin. These valleys appear to be associated with the Bering, Malaspina/Hubbard, and Alsek glacial systems. A particular type of glacial deposit, a trough mouth fan (TMF), forms at the mouths of these glacial sea valleys and have the potential to record the dynamics of these temperate glacial systems. Using 2D multichannel seismic and multibeam bathymetry, we investigate the seafloor morphologic expression and sedimentary record associated with Southeast Alaska's unique tectonic and climate setting.

The sea valleys and associated shelf slopes have broad morphologic variability, reflective of the numerous competing depositional processes. The Bering trough (143° 30' W, 59° 48'N) is 25km wide at the shelf edge with 140m of relief. The associated slope has a gradient of 0.11 m/m, with several slumps or slides visible. The Yakutat trough (141° 30' W, 59° 7'N) has a mouth width of 32km, and 160m relief. There are smaller channels formed within the trough itself. The continental slope at the Yakutat trough shelf edge has a slope of 0.07m/m. The slope left of the Yakutat appears to have numerous fan-shaped deposits overlapping each other, but these features are seemingly unrelated to the major bathymetrically observable valleys of the shelf. In between the Yakutat and the Alsek troughs is an area of the shelf slope that is extremely steep, with a slope of 0.32 m/m. The general slope morphology is overprinted with numerous slumps, debris flows, and small incisive channels. Preliminary seismic analysis indicates significant subsurface variability similar to the surface morphology, with distinct packages of chaotic facies likely indicative of debris flows generated during glacial advances, overlain by relatively continuous layered sediments likely deposited during retreat and interglacial periods. This is consistent with previous seismic work that found multiple glacial advance and retreat surfaces within the sea valleys.

Keywords: Seismic stratigraphy, marine geology, glacial history, sedimentary processes

MG-9

Investigating ENSO Variability in the mid-Holocene using a Fossil Coral from the South Pacific

Marissa Anne Vara[1], Terrence M Quinn[1, 2], Frederick W Taylor[2], Judson W. Partin[2], Meaghan K Gorman[2, 3], Christopher R Maupin[2, 4], R. Lawrence Edwards[5], Hai Cheng[5], Mayuri Inoue[6], David Nakedau[7]
marissavara17@utexas.edu
1. Geological Science, University of Texas at Austin, Austin, TX, United States.
2. Institute of Geophysics , University of Texas at Austin, Austin, TX, United States.
3. Statoil, DPNA Baken BU, 6300 Bridge Point Parkway, Austin, TX, United States.
4. Geography, Texas A&M University , College Station, TX, United States.
5. Earth Sciences, University of Minnesota , Minneapolis, MN, United States.
6. Atmosphere and Ocean Research Institute, The University of Tokyo, Kashiwa, Japan.
7. Geohazards Section, Geology, Mines and Water Resources, Port Vila, Vanuatu.

We investigate mid-Holocene variability in the El Niño Southern Oscillation (ENSO) system using geochemical variations in a well-preserved fossil Porites lutea coral collected in 2005 at Araki Island, Vanuatu (15.62°S 166.95°E). Surface-ocean conditions (temperature and salinity) at Vanuatu respond to ENSO-related changes in the West Pacific Warm Pool (WPWP) and the South Pacific Convergence Zone (SPCZ). The coral core is ~1.64 m in length and has been U-Th dated to 7,230 ± 440 y B.P. Skeletal extension rate averages 1.5 cm per year based on analysis of X-radiographic images, which document the presence of well-defined density bands. The coral was sampled for geochemical analysis every 0.125 cm, which is approximately one sample per month. The full coral record will be approximately 90 continuous years in length once all sampling and analyses have been completed. Thus far, we have generated monthly resolved, 50-year coral δ18O and Sr/Ca records. The coral δ18O record has a mean δ18O value of -4.75 ‰ and an annual-cycle amplitude that averages 0.35 ‰. The fossil coral δ18O record contains patterns of isotopic variation that match patterns recognized as El Niño and La Niña events in modern coral δ18O records from this region. The fossil coral Sr/Ca record yields temperature estimates at ~7.2 ka that are similar to modern values.

Future work will focus in three areas: 1) extending the length of the fossil coral record to more fully explore the nature of interannual variability recorded in the present fossil coral sample; 2) generating an additional fossil coral record using another coral collected from the same reef terrace to assess reproducibility of the records; and 3) extend the assessment of past ENSO variability using paleorecords generated from fossil corals of similar age from a different location in Vanuatu.

Keywords: Paleoceanography: Corals, ENSO, Geochemical tracers

MG-10

New mapping and structural constraints on the Queen Charlotte-Fairweather Fault system, southeast Alaska

Walton, M.[1], Roland, E.[2], Gulick, S.[1], Haeussler, P.[2], Christeson, G.[1], Van Avendonk, H.[1]
maureenlwalton@utexas.edu
1. Jackson School of Geosciences, The University of Texas at Austin, Austin, TX
2. U.S. Geological Survey, Anchorage, Alaska

The dextral Queen Charlotte-Fairweather Fault lies along the western margin of Canada and southeastern Alaska, a transform plate boundary accommodating motion between the North American and Pacific Plates. The Fairweather Fault is the northern extension of the Queen Charlotte Fault and has numerous and complex splays, including the Chichagof-Baranof Fault, the Peril Strait Fault, the Chatham Strait Fault, and the Icy Point-Lituya Bay Fault. Except for a few small areas, these fault systems have not been mapped in detail. We present updated geometries and fault maps of the entirety of the strike-slip system using seismic reflection and bathymetric data, including a 2004 seismic reflection survey (EW0408), 2005 United Nations Commission on Law of the Sea multibeam bathymetry, and legacy data from the U.S. Geological Survey (USGS) and the National Geophysical Data Center.

This work is highly relevant for earthquake hazard research and mitigation in southeast Alaska. Several large (> Mw 7.0) earthquakes have occurred along this margin in the last century, impacting communities of southeastern Alaska and western Canada. Two large, recent events include 1) a Mw 7.7 earthquake that took place on 28 October 2012 near the Haida Gwaii Islands offshore of western Canada, and 2) a Mw 7.5 event which occurred on 05 January 2013, 330 km to the northwest and offshore of Craig, Alaska. Interestingly, the Haida Gwaii earthquake ruptured as a thrust event and the Craig earthquake ruptured with a near-vertical dextral strike-slip mechanism.

Since a change in Pacific Plate motion around 4 million years ago, the southern Queen Charlotte Fault system has been obliquely converging at a rate of 20 mm/year, with the boundary accommodating about 80 km of perpendicular motion over that time. This convergence explains the Haida Gwaii thrust earthquake, but leaves questions about the along-strike fault structure. Two opposing end-member theories suggest convergence is accommodated by either: 1) Pacific Plate underthrusting beneath North America; or 2) crustal shortening via smaller, localized thrust faults. The underthrusting model assumes oblique slip along fault planes that transition to a lesser dip with increasing depth, whereas the local-thrust model requires strain partitioning via a series of thrust faults proximal to and inland from the main strike-slip trace. We provide insight into this system with improved surficial fault geometries that illuminate Queen Charlotte Fault structure in the context of the two recent earthquakes. We present these data in conjunction with preliminary aftershock locations and focal mechanisms for the 05 January 2013 Craig earthquake (obtained from a joint University of Texas-USGS OBS rapid-response survey), which offer new information about the seemingly changing along-strike dip and planar structure of the southern Queen Charlotte Fault. Additionally, we can now better constrain the Queen Charlotte's northern structure in relation with the Chatham Strait and Fairweather transforms.

Keywords: Seismic reflection, earthquake, Alaska, Queen Charlotte, Haida Gwaii, fault, strike-slip, transform, tectonics, marine geophysics, plate boundary

MG-11

Detrital zircon U-Pb and U-Th/He double dating of lower Miocene samples from the Gulf of Mexico margin: insights into sediment provenance and depositional history

Xu, J.[1,2], Snedden, J.[2], Fulthorpe, C.[2], Stockli, D.[1]
jiexu@utexas.edu
1. Department of Geological Sciences, Jackson School of Geosciences, The University of Texas at Austin, Austin, TX
2. Institute for Geophysics, Jackson School of Geosciences, The University of Texas at Austin, Austin, TX

By linking provenance indicators, estimated sediment supply and depositional rate to exhumation episodes, it is possible to reconstruct timing and location of source to sink depositional pathways. The lower Miocene (LM; 23-15Ma) is an episode of voluminous sediment input to the Gulf of Mexico (GOM) from erosion of North American interior highlands (Galloway, 2009; Galloway et al. 2011). Recently, it has gained increasing attention from the oil and gas industry because of hydrocarbon potential beneath the thick salt canopy. However, inferred sediment transport pathways for this interval are based on consideration of likely river courses through known paleogeomorphological elements (Galloway et. al., 2011). Furthermore, provenance is mainly based on traditional petrographic methods (e.g. QFL diagrams), which have large uncertainties owing to degradation of sediment grains by transportation, weathering and subsurface diagenesis. Major tectonic reorganization in the western interior of North America together with rejuvenation of the Appalachian Mountains in the east further complicates LM provenance analysis. More robust data are required to understand the progressive eastward shift of source terranes and its influence on sediment dispersal to the deep-water basin, where extensive allochthonous slat canopies can hinder direct seismic observation of sediment dispersal pathways.

The dual constraint provided by crystallization age (U-Pb) and cooling age (U-Th/He) greatly increases the accuracy and precision of provenance interpretations. We therefore integrate detrital zircon (DZ) U-Pb and U-Th/He dating to reveal not only sediment provenance, but also the exhumation histories of the detrital source regions. Only limited U-Pb dating has been done in the GOM (Mackey et al., 2012 and Craddock et al., 2013) and U-Pb and U-Th/He double dating has not yet been applied there. We have collected 15 outcrop samples from Texas and Louisiana for U-Pb and U-Th/He analysis. Preliminary U-Pb results indicate that there are several major source terranes including the Oligocene volcanic field, Laramide uplift, Cordilleran Arc, Grenville, Mid-Continent, and Yavapai-Mazatzal terranes. Minor provinces including Appalachian-Ouachita, Wyoming and Superior regions are also recorded. However, by combining U-Pb ages with U-Th/He ages we identify several recycled zircons with more complex transportation, deposition and exhumation histories. Exhumation histories indicate that large numbers of zircons formed during the Sevier-Nevadan orogenies were recycled to the GOM rather than transported there directly. In addition, our data show that Grenville age zircons deposited in Louisiana were probably recycled through the Colorado Plateau from their original source in the Appalachian Mountains. In contrast, volcanic sources are readily identified because their U-Pb age is close to their U-Th/He age. DZ double dating is therefore greatly enhancing our understanding of tectonic movement, provenance changes and the evolution of sediment transport axes for the important LM interval in the GOM.

Keywords: lower Miocene, Provenance, detrital zircon, U-Pb and U-Th/He

MG-12

Geologic controls on unstable shelf-margin geometry in the Frio Formation and the Wilcox Group, South Texas

Zhang, J.[1], Ambrose, W.[1], Steel, R.[1]
Jinyu.zhang@utexas.edu
1. Jackson School of Geosciences, The University of Texas at Austin, Austin, TX

Paleogene shelf margin geometry in the northwestern Gulf of Mexico is controlled by a variety of factors that include sediment loading in deltaic depocenters, eustasy, and tectonics, all of which influence growth fault origin and development. Using cores, well logs, seismic and published literature, this study will refine current understanding of deltaic systems at unstable shelf margins with examples from the Frio Formation and Wilcox Group in South Texas. The Frio study in the Corpus Christi Bay area in South Texas, previously undertaken in a Master's thesis, suggests that patterns of deposition were strongly influenced by growth fault developments and structural deformation above mobile shale. Rapid subsidence related to growth faulting suppressing the eustatic influence is the primary process on stratigraphic development, whereas sea level change and sediment supply are subordinate.
The objectives of the ongoing Wilcox project in an area encompassing Live Oak, Bee and Goliad counties, are to (1) define sandstone spatial and temporal distribution; (2) detail the regional stratigraphic framework across major growth faults at the scale of 4^{th}-order sequences; (3) differentiate eustatic and tectonic controls; and (4)delineate the shelf-margin trajectory.

Keywords: Frio, Wilcox, South Texas, unstable shelf margin, growth fault

MG-13

Imaging Evidence for Hubbard Glacier Advances and Retreats since the Last Glacial Maximum in Disenchantment and Yakutat Bays, Alaska

Julie Zurbuchen[1], Gulick, Sean P. S. [1], LeVoir, Maureen A. [1], Goff, John A. [1], Haeussler, Peter[2]
jmzurbuchen@gmail.com
1. University of Texas Institute for Geophysics, Jackson School of Geosciences, Austin, Texas
2. U.S. Geological Survey, Anchorage, Alaska

As glaciers advance and retreat, they leave erosional surfaces, retreat sequences, morainal banks, and terminal moraines. These features can be imaged and interpreted in seismic reflection data to gain insight into ice routing, ice-sediment processes, and preserved glacial history. High-resolution 2-D multichannel seismic data gathered on the August 2012 UTIG-USGS National Earthquake Hazards Reduction Program survey of Disenchantment and Yakutat Bays have provided understanding of the advance pathways of the Hubbard Glacier and the glacial history of the bays.

These data show evidence of three unconformities appearing in the form of channels and interpreted to be glacial advance and retreat paths. The youngest observable channel in Disenchantment Bay is ~2 km wide, forming morainal banks along the edges of the bay. The depth below modern sea level in two-way travel time (twtt) shallows from 510 ms in the middle of the bay to 400 ms ~4 km north of the entrance to Yakutat Bay. The sediment contained within the youngest channel measured from the seafloor thins southward from a twtt thickness of 260 ms to 115 ms. Beneath the youngest channel lies an older, 2.2 km-wide channel which is observed at ~580 ms below sea level, and is filled with sediments ranging in thickness from 480 ms to 180 ms at the terminus. This older channel extends from Disenchantment Bay into Yakutat Bay, staying to the northeast of Yakutat Bay, then turns southward at Knight Island and shallows to 450 ms twtt before forming a terminal moraine ~10 km north of the mouth of Yakutat Bay. Evidence for the third and oldest unconformity can only be seen within a very small number of short seismic lines in Disenchantment Bay. It is the largest of the channels, at ~3 km wide and 720 ms below modern sea level.

The evidence of three nested unconformities suggests that the Hubbard Glacier has had at least three major advances in recent history. Radiocarbon dating of wooden branches in moraine deposits confirms at least two of these advances to be during the Holocene while the oldest may represent the Last Glacial Maximum. The most recent advance likely reached its terminal position at the mouth of Disenchantment Bay, never entering Yakutat Bay. Our interpretation suggests that the Hubbard Glacier has repeatedly advanced around the east side of Yakutat Bay in Knight Island Channel, possibly due to the presence of Malaspina Glacier cutting off access to the central Yakutat Bay during a time of mutual advance. Within the range of the seismic data available for the area, it seems unlikely that the Hubbard Glacier fills all of Yakutat Bay when it advances.

PS-1

Ascertaining the temporal stability of water ice in Korlev Crater, Mars

Brothers, T.C.[1], Holt, J.H[1]., Spiga, A.[2]
TCBrothers@utexas.edu
1. University of Texas Institute for Geophysics, Jackson School of Geosciences, University of Texas, Austin, TX 78758
2. Laboratoire de Météorologie Dynamique, Université Pierre et Marie Curie, Paris, France

Korolev crater is an ice-filled, ~80 km diameter, impact crater located at 73º N, 163º E on Mars. This crater is unusual because it is filled with material identified as H_2O ice [Armstrong et al., 2005] yet is located over 600 km south of the modern ice cap's edge. In fact, mapping efforts using SHAllow RADar (SHARAD) on Mars Reconnaissance Orbiter revealed the deposit's thickness to be at least 2 km [Moore et al., 2012, Brothers and Holt., 2013]. Additionally, the stratigraphy of Korolev's icy deposit has been compared to that of the ice cap, Planum Boreum. Given that Planum Boreum is hypothesized to be a recent feature, stratigraphic similarity with Korolev's ice suggests that it may be recent, not part of an ancient ice sheet or different climate regime. However, global climate modeling locates Korolev crater within a zone of instability for exposed H_2O ice.

This work will address the disagreement between global atmospheric climate modeling and observations of Korolev's ice stratigraphy using an idealized model. If modern orbital conditions of Mars do not allow for stable ice at Korolev, this implies that the ice is undergoing retreat and had a greater previous thickness. In addition, the mesoscale climate model to be used [Spiga and Forget, 2009] can be modified by changing orbital conditions to ascertain stable conditions. This tuning would aid in estimating a time period during which Korolev's ice deposit may have formed.

Equally interesting is the prospect that idealized modeling might show stable ice under current Martian conditions. If this is the case, it would lend credence to Korolev crater's central mound being coeval with ice found in Planum Boreum. Coeval ice has large implications for global Mars climate during the last few million years. Therefore, it is crucial that we understand the origin of Korolev's ice and its relationship to Mars global water cycle. Unveiling the age of ice in Korolev will determine whether the deposit is better suited for examining ancient or modern Martian atmospheric conditions, thereby focusing scientific research of circumpolar ice on Mars.

Bibliography

Armstrong J. et al. (2005) Evidence for subsurface water ice in Korolev crater, Mars. *Icarus*,174 360-3723.

Brothers, T.C. and Holt, J.H. (2013) Korolev, Mars: Growth of a 2-km-thick ice-rich dome independent of, but possibly linked to, the north polar layered deposits. *LPSC XLIV*, Abstract #3022

Moore, M.W. et al. (2012) Internal structure of the domed deposit within Korolev crater, Mars from radar sounding. *LPSC XLIII*, Abstract #2894.

Spiga, A. and Forget, F. (2009) A new model to simulate the Martian mesoscale and microscale atmospheric circulation: Validation and first results. *Journal of Geophysical Research*, 114, doi:10.1029/2008JE003242

Keywords: Mars, Korolev, ice, modeling, atmosphere

PS-2

Neptune and Triton: A Study in Future Exploration

Day, M.[1], Malaska, M.[2], Hosseini, S.[3], Alibay, F.[4], Clegg, R.[5], Craig, P.[6], Fernandes, P.[7], Fougere, N.[8], Girazian, Z.[9], Hutchins, M.[10], Leonard, J.[11], McGranaghan, R.[11], Patthoff, A.[2], Ries, P.[2], Scully, J.[12], Uckert, K.[13], Budney, C.[2], Mitchell, K.[2]
mdday@utexas.edu
1. Jackson School of Geociences, University of Texas at Austin, Austin, TX
2. Jet Propulsion Laboratory, Pasadena, CA
3. University of California, Davis, Davis, CA
4. Massachusetts Institute of Technology, Cambridge, MA
5. Washington University in St. Louis, St. Louis, MO
6. Johnson Space Center , Houston, TX
7. Dartmouth College, Hanover, NH
8. University of Michigan, Ann Arbor , MI
9. Boston University, Boston, MA
10. University of Washington, Seattle, WA
11. University of Colorado at Boulder, Boulder, CO
12. University of California, Los Angeles, Los Angeles, CA
13. New Mexico State University, Las Cruces , NM

Neptune provides a unique natural laboratory for studying the dynamics of ice giants. Last visited by Voyager 2 in 1989, Neptune and its moon Triton hold important clues to the evolution of the solar system. The Voyager 2 flyby revealed Neptune to be a dynamic world with large storms, unparalleled wind speeds, and an unusual magnetic field. Triton, Neptune's largest satellite, is believed to be a captured Kuiper Belt Object with a thin atmosphere and possible sub-surface ocean. Further study of the farthest planet in our solar system could offer new insights into the dynamics of ice-giant exoplanets, and help us understand their complex atmospheres. The diverse science questions associated with Neptune and Triton motivate the complex and exciting mission proposed in this study.

The proposed mission follows the guidelines of the 2013-2022 Planetary Science Decadal Survey, and optimizes the number of high priority science goals achieved, while still maintaining low mission costs. High priority science goals include understanding the structure, composition, and dynamics of Neptune's atmosphere and magnetosphere, as well as analyzing the surface of Triton. With a New Frontiers budget of $1.5 billion (FY2015), the mission hosts an atmospheric probe and suite of instruments equipped with technologies significantly more advanced than those carried by Voyager 2. Additionally, the mission offers improved spatial coverage and higher resolution measurements than any previously achieved at Neptune. The proposed spacecraft would execute a flyby of Neptune and Triton. Further study of Neptune and Triton will provide exciting insights into what lies on the edge of our solar system and beyond.

Keywords: Neptune, Triton, mission, exploration

PS-3

Estimating Radar Reflector Dielectric Properties Using SHARAD Data

Lalich, D.[1], Holt, J.W.[1]
dlalich90@gmail.com
1. Institute for Geophysics, The University of Texas at Austin, Austin, TX

The Martian polar caps are thought to represent a detailed history of the planet's late Amazonian paleoclimate. In particular, the North Polar Layered Deposits (NPLD), which are comprised of many sub-parallel layers of water ice with varying dust content, are thought to contain a climate signal related to the hydrologic cycle of Mars. Many internal reflections are visible in radar sounding data from the Shallow Radar (SHARAD) instrument on the Mars Reconnaissance Orbiter (MRO), presumably resulting from variations in dust content with depth. Using these reflections and a simple plane wave propagation model, it is possible to estimate the dielectric properties of the layers. These estimates could be used to determine dust concentration as a function of depth in the NPLD. This would provide necessary constraints for climate models that aim to explain the presence and evolution of the polar cap. Although the bulk properties of the NPLD are well understood, little has been done to characterize individual layers. There are two main hypotheses for layer formation in the NPLD. The first is that changing rates of dust and ice deposition through time result in layer properties different enough to cause reflections. The second hypothesis is that lag deposits of nearly pure dust are left behind during periods of sublimation and then cemented under new ice layers. The two hypotheses predict distinct layer dielectric properties.

Using the model of Lauro et al. (2012) it is possible to use the power reflected at the subsurface interface relative to the power reflected at the surface in order to calculate the real part of the dielectric constant at the subsurface boundary. Using this technique we have mapped estimated dielectric constants of multiple subsurface layers in the Gemina Lingula region of the NPLD. Estimated values fall well outside of the range expected for ice-dominated layers and instead match those predicted for dust lags. With minor adjustments to the model as well as increased coverage in both depth (time) and geographic extent, we hope to expand these results to the NPLD as a whole.

Keywords: Mars, Ice, Radar

PS-4

A comparative study of Martian lobate debris aprons in west and east Deuteronilus Mensae: surface morphologic and flow-line topographic analysis to infer surficial and internal radar characteristics.

Petersen, E.[1], Holt, J.[1], Berney, J.[2]
eric_petersen@utexas.edu
1. Institute for Geophysics, The University of Texas at Austin, Austin, TX
2. Bureau of Economic Geology, The University of Texas at Austin, Austin, TX

Lobate debris aprons (LDA) are Martian surface features first identified as ice-related due to their characteristic convex-up topographic profiles and viscous flow morphologies (e.g. Squyres et al, 1978, Lucchitta et al, 1984). They are typically found extending out from the base of escarpments and mesas in both the northern and southern mid-latitudes, particularly in the high-relief dichotomy boundary region between Mars' northern lowlands and southern uplands.
Orbital radar sounding of LDAs via the Mars Reconnaissance Orbiter (MRO) Shallow Radar (SHARAD) instrument has revealed unambiguous subsurface reflectors, analysis of which has shown that many of these LDAs are composed of nearly pure water ice thermally insulated under a blanket of rock and dust debris ~1-10m thick (e.g. Holt et al 2008). Previous studies in geomorphology (e.g. Head et al 2006), climate modeling (e.g. Madeleine et al 2009), flow modeling (e.g. Fastook et al 2011), and radar stratigraphy (Quartini et al 2011) have shown LDAs to be remnants of multiple obliquity-driven glacial cycles on Mars and thus valuable indicators of Martian Amazonian palaeoclimate.
SHARAD data on LDAs in the dichotomy boundary region of Deuteronilus Mensae exhibits a spectrum in the strength of observed subsurface reflectors, from strong and clear to more weak and ambiguous or nonexistent returns. In general, west Deuteronilus is dominated by unambiguous returns, while east Deuteronilus only contains relatively few weak returns. In this study, we explore the possibility that all observed LDAs exhibit a basal interface, yet the eastern LDAs do not permit the radar to observe it via one or both of two proposed mechanisms. The first mechanism is that the debris cover is more completely radar reflective or more highly radar scattering in the eastern LDAs, a hypothesis made appealing by the differing geologic ages of highland surfaces between the east and west. The second mechanism is through varying dust-ice fraction, which will control the attenuation of the radar signal. Dust-ice fraction is also significant in determining the ice rheology, thus in turn the flow history and resultant topographic profile. This study tests the likelihood that these two mechanisms play a role in observed radar differences by examining differences in debris surface properties, flow-parallel topographic profiles, and LDA geometries between study site LDAs in eastern and western Deuteronilus Mensae. High-resolution imagery obtained from the MRO HiRise and CTX camera systems is used to characterize LDA surfaces at each site to compare surface roughness estimates, albedo, and geomorphic characteristics. Topography data obtained from Mars Express' High Resolution Stereo Camera (HRSC) and Mars Global Surveyer's Mars Orbiter Laser Altimeter (MOLA) are used to extract flow-parallel topographic profiles to compare between sites and with the results of idealized flow models found in the literature (e.g. Parsons et al 2011). From these profiles, extents and thicknesses of LDAs are also estimated.
SHARAD radar interpretations are tested for correlation with surface analysis to test for debris-cover signal loss and topography/geometry to test for internal attenuation within the LDA. Results are discussed in light of LDA structure/composition and implications for global and local climate history. One question we address in the discussion is the evidence for LDAs as remnants of regional ice sheet formation and deflation vs. LDAs as remnants of smaller, localized glacial events.

Keywords: Mars, geophysics, radar, palaeoclimate, lobate debris aprons, obliquity, cryosphere, glaciology

SETP-1

Protracted depositional and provenance record of Cenozoic orogenesis in northern Tibet: New evidence from the Qaidam basin

Bush, Meredith A.[1], Horton, Brian K. [1,2], Saylor, Joel E. [3], Nie Junsheng [4]
meredith.a.bush@utexas.edu
1. Department of Geological Sciences, Jackson School of Geosciences, University of Texas at Austin, Austin, Texas, 78712, USA
2. Institute for Geophysics, Jackson School of Geosciences, University of Texas at Austin, Austin, Texas, 78712, USA
3. Department of Earth and Atmospheric Sciences, University of Houston, Houston, Texas, 77204, USA
4. Key Lab of Western China's Environmental Systems (Ministry of Education), Lanzhou University, Lanzhou, China.

Integrated analysis of the sedimentology, stratigraphy and provenance record of the Qaidam basin on the northern Tibetan plateau reveals a long-term record of Cenozoic deformation associated with faulting and structural reactivation in response to the Indo-Asian collision. Multiple, independent lines of evidence point to a major shift in source composition is detected between Eocene and Miocene strata. The shift is seen in paleocurrent measurements (clast imbrication and trough cross-stratification), detrital zircon U-Pb geochronology, conglomerate clast counts, and sandstone petrography. Depositional systems of the >6 km-thick Xitieshan section (37°32' N 95°10'E) (include sand-dominated meandering rivers with extensive pedogenically modified alluvial plains, marginal lacustrine, and gravelly braided river systems. The section shows two major upward coarsening sequences from mudrock-dominated lithofacies to >1 km of conglomeratic facies, with smaller-scale internal shifts between various alluvial systems. Sedimentological and stratigraphic patterns reveal at least two phases of enhanced exhumation and sediment delivery during the Cenozoic.

Changing depositional systems and source areas are interpreted as a response to the reactivation of Paleozoic suture zones in the Qilian Shan (to the north) and Kunlun Shan (to the south), which served as the circum-basin catchment areas and primary sources of extrabasinal grains throughout the Cenozoic. Strike-slip deformation along the Altyn Tagh fault system (to the west) help promote a general eastward migration of the Qaidam basin depocenter. This study demonstrates that deposition in the Qaidam Basin has been maintained throughout the Cenozoic largely by topographic isolation through uplift of resistant barriers. Possible geodynamic mechanisms for such long-term stability of the Qaidam Basin as a topographically closed basin with high-relief walls include (i) deep crustal/ lithospheric viscous processes (crustal flow, mantle convection, injection) caused by Moho topography and/or (ii) heterogeneous and anisotropic rheological conditions associated with inherited terranes and resultant changes in elastic thickness of the crust (rigidity).

Keywords: Basin analysis, sedimentology, tectonics, Qaidam basin, Tibetan plateau, Cenozoic, detrital zircon geochronology

SETP-2

Impact of meteoric fluid flow on the thermal evolution of the Gotthard Massif; insights from Alpine railway tunnels

Arnost, D.R.[1], Stockli, D.F.[1], Antognini, M.[2], Hesse, M.[1]
danielarnost@utexas.edu
1. Jackson School of Geosciences, The University of Texas at Austin, Austin, TX
2. Museo Cantonale Di Storia Naturale, Ticino, Switzerland

The Gotthard Base Tunnel provides a unique window into the subsurface of the Swiss Alps and into the complex thermal evolution of the Gotthard Massif. The 57 km tunnel trends north-south and provides an orogen perpendicular cross section through the backbone of the Swiss Alps, the Aar and Gotthard massifs. The modeled temperature profile in the tunnel mimics topography; increasing from 11°C at the north entrance to 42°C in the middle where overburden exceeds 2300 meters. A 15°C negative temperature anomaly exists 37 km south of the Erstfeld portal at the intersection of the Piora Zone aquifer. The Piora Zone is a syncline comprised of a heavily deformed and kartsified Triassic dolomite that overlies the gneissic basement of the Gotthard Massif. This aquifer is a conduit that funnels cold Alpine meteoric water deep into the massif. The water absorbs heat from the adjacent bedrock, creating an advective thermal regime and a local negative temperature anomaly.

Apatite (AHe) and zircon (ZHe) (U-Th)/He ages will be measured for 30 samples collected through the length of the tunnel through the Piora Zone, as well as corresponding surface transects, in order to trace the extent to which meteoric fluid has depressed the underlying isotherms throughout the exhumation history of the complex. Samples adjacent to the Piora Zone have been analyzed and show AHe ages of ~2.0 Ma, which represent cooling of the massif through a 70°C isotherm, unperturbed by the Piora zone aquifer. Ages within the Piora Zone that are anomalously older will indicate that meteoric fluid has depressed isotherms substantially enough to affect the closure of apatite and zircon during exhumational cooling. The resulting data will reveal the topologic evolution of the AHe and ZHe closure temperature isotherms through times t_1 (tunnel samples) and t_2, (surface samples) shaped by the coupled effect of meteoric fluid-flow and topography.

Keywords: Thermochronometry, Alps, apatite, zircon

SETP-3

Paleogeographic and tectonic implications of the Paleogene Missouri River headwater system in SW Montana

Barber, D.E.[1], Schwartz, R.K.[2]
douglasbarber@utexas.edu
1. Jackson School of Geosciences, The University of Texas at Austin, Austin, TX
2. Department of Geology, Allegheny College, Meadville, PA

Recent work on the Renova Formation in SW Montana has documented a Paleogene (>50 Ma) intermontane basin system and drainage network similar in configuration to that of the modern system in a region that includes the Divide, Beaverhead, Jefferson, Gallatin, and Radersburg-Townsend intermontane basins. That region constitutes much of the modern and Paleogene, northward-flowing, Missouri River headwater drainage. In this study, facies, paleocurrent, compositional, and detrital zircon U-Pb age analyses have been expanded in order to evaluate the headwardmost paleodrainage system with regard to provenance, paleogeography, and tectonism. Although Paleogene erosion and deposition overlapped terminal Sevier-Laramide contraction and incipient Tertiary extension, this southern study area has been overprinted by Basin-and-Range (~16 Ma) and Yellowstone hotspot trackway (~6 Ma) uplift and extension.

A large-scale, cobble to boulder, Eocene fluvial conglomerate system in the Beaverhead basin demonstrates northward paleoflow and serves as evidence of a major influx of Proterozoic clasts from tributaries in the south and southwest. Other detrital components and zircon provenance data document minor to moderate sediment supply from exposures of Cretaceous plutons in the Pioneer Mountains, Archean basement, and early Paleogene volcanics. Fluvial conglomerates within the Frying Pan, Grasshopper, Medicine Lodge, and Horse Prairie basins substantiate primary sources of Proterozoic strata in the SWMT-central Idaho region as well as more proximal recycling from thrust sheets of the Late Cretaceous/Paleocene Beaverhead Formation conglomerate. This, and scattered exposures of basin margin alluvial facies, indicate a mountainous regional topography with drainage into the paleo-Beaverhead basin most likely through a paleovalley in the Beaverhead Canyon region as well as southeastward from the southern end of the Pioneer Mountains. Fluvial paleoflow data for the headwater basins indicate axial orientations similar to those of the modern basins. Overall, Late Cretaceous to early Eocene fluvial systems are interpreted to have carved intermontane-scale paleovalleys with reliefs on the 100-1000 m scale into the Sevier orogenic wedge along zones of structural and stratigraphic weakness to form the paleo-Missouri River headwater system.

Keywords: SW Montana, Paleogene Renova Formation, detrital zircon U-Pb geochronology, provenance, paleodispersal, sedimentology, tectonics

SETP-4

Challenging the assumptions of Lu-Hf dating in spinel peridotites

Benjamin L. Byerly[1], John C. Lassiter[1]
benbyerly@utexas.edu
1. Jackson School of Geosciences, The University of Texas at Austin, Austin, TX

Lu-Hf "pseudoisochrons" using peridotite-derived clinopyroxene separates are commonly used to constrain timing of melt depletion and lithosphere formation. However, cpx-based pseudoisochrons are only valid if 1) almost all Hf and Lu is hosted in the cpx, or 2) the system is below the mineral closure temperature. We tested these assumptions by examining Lu and Hf partitioning and Hf-isotope variations in cpx, opx, and bulk peridotite in xenoliths from the eastern Colorado Plateau and Rio Grande Rift. The samples primarily derive from Proterozoic SCLM, span a range of fertility (spinel Cr# range from 0.1-0.5), and have equilibration temperatures ranging from 950-1050°C, similar to temperatures reported for other xenoliths utilized in Lu-Hf isotope studies.

Cpx have Hf and Lu concentrations ranging from 40-1000 ppb and 80-290 ppb, respectively. Opx have much lower Hf and Lu concentrations (5-60 ppb and 21-51 ppb). Concentrations of Lu, Hf, and other trace elements are well correlated between cpx and opx, indicating mineral equilibrium. $D_{Lu}^{cpx/opx}$ and $D_{Hf}^{cpx/opx}$ range from 3.5-6.1 and 7.0-20, and are negatively correlated with cpx MgO content and other indices of peridotite fertility (e.g., spinel Cr#). Our results agree with (and extend the compositional range of) partition coefficients estimated following the formulation of [1]. The fraction of Lu and Hf hosted in opx increases in highly refractory samples. Although Lu/Hf in cpx is close to WR Lu/Hf in fertile samples, in refractory samples it is much lower.

Opx have systematically higher Lu/Hf than cpx, but in most samples have identical Hf isotopes. Some opx and WR have lower $^{176}Hf/^{177}Hf$, similar to the host magma, likely reflecting melt contamination. The identical Hf isotopes in cpx and opx indicate that xenoliths evolved above the Lu-Hf closure temperature. Therefore, cpx (and opx) $^{176}Hf/^{177}Hf$ is supported by the bulk-xenolith Lu/Hf ratio, not the mineral ratio.

Use of cpx Lu/Hf in pseudoisochrons yields systematically older ages and higher initial ε_{Hf} values than when WR Lu/Hf is used. For example, xenoliths from the North China Craton [2] have a cpx pseudoisochron age of 1.7 Ga (initial ε_{Hf} of +19), whereas a pseudoisochron using "calculated" WR Lu/Hf yields a much younger age of 0.9 Ga (and more reasonable initial ε_{Hf} of +14). Most studies report anomalously high initial ε_{Hf}, which may be the result of using cpx Lu/Hf when WR Lu/Hf is more appropriate.

[1] Witt-Eickschen, G., O'Neill, H.S.C., (2005). Chem. Geo., 221, 65-101.
[2] Liu, J., et al., (2012). Chem. Geo., 332-333, 1-14.

Keywords: Peridotite, upper mantle, lithosphere, Lu-Hf, melt-depletion, pseudoisochron

SETP-5

Os isotopic composition of steels: Constraints on sources of Os in steel & crustal isotopic evolution of iron ores.

Chatterjee, R.[1], Lassiter, J.[1]
rudra025@gmail.com
1. Jackson School of Geosciences, The University of Texas at Austin, Austin, TX

Metal contamination during sample processing is a potential concern in Os-isotope studies. We examined Os concentrations and Os isotopes in industrial steels. Samples include high Cr stainless steels (>10.5% Cr), low alloy steels (>=92% Fe) and high alloy steels (<92% Fe). The chief components used to make steel are iron ore, chromites and coke. Coke is derived from coals that have low Os concentration and highly radiogenic isotopic composition (~36±5 ppt, $^{187}Os/^{188}Os$ = 1.84±47) [1]. Chromites in steels are mined from chromitites, which have high average Os concentrations and mantle-like $^{187}Os/^{188}Os$ ratios (~87±8 ppb Os, $^{187}Os/^{188}Os \approx 0.127\pm5$) [2]. Iron ores used in US steel manufacturing derive chiefly from magnetites mined from iron-bearing formations such as Banded Iron Formations (BIF), which have median Os concentration of ~ 81±36 ppt and radiogenic $^{187}Os/^{188}Os \approx 0.88\pm15$ [3].

Os concentrations in the measured steels span a wide range, from 0.03 to 22 ppb. The $^{187}Os/^{188}Os$ ratios vary from 0.144-0.66. Such high Os concentrations and radiogenic isotopic compositions confirm that metal contamination can affect Os-isotope compositions during sample processing, particularly for low-[Os] samples. Os concentrations in steels are positively correlated with Cr content, suggesting that chromite-derived Os dominates the Os budget in stainless steels. $^{187}Os/^{188}Os$ is negatively correlated with Cr content, ranging from 0.144-0.195 in high-Cr (>10.5 % Cr) steels but from 0.279-0.66 in low-Cr steels. In addition, there is a positive correlation between 1/Os and $^{187}Os/^{188}Os$, consistent with two-component mixing of Os derived from iron ore/coke and chromites. Lower Os concentrations in steels than expected from simple mixing of iron ore/coke and chromitite suggest some volatile Os loss during smelting.

Although the current data is limited, the $^{186}Os/^{188}Os$-$^{187}Os/^{188}Os$ trend defined by the steel analyses can be utilized to extrapolate compositions of the end-member chromite and BIF components. $^{186}Os/^{188}Os$ values in steels range from 0.119834±5 to 0.119840±4, indistinguishable from the upper mantle. Extrapolation of the $^{186}Os/^{188}Os$-$^{187}Os/^{188}Os$ trend to $^{187}Os/^{188}Os$ values typical for chromites results in an estimated $^{186}Os/^{188}Os$ value of 0.119837±2, within error of values previously reported for chromites [4,5].

Extrapolation of the chromite-steel trend to the highly radiogenic (continental crust-like) ^{187}Os values found in BIFs results in greater uncertainty, but the extrapolated value (0.119834±9) is also indistinguishable from the upper mantle. We estimate an upper bound for the initial $\varepsilon^{186}Os$ of the 1.8 Ga BIF source of magnetite ore of ~0.3, similar to initial $\varepsilon^{186}Os$ in black shales (0.3-0.5) and freshwater Mn-nodule (1.6), but lower than in loess (1-2.4) [6]. Aqueous deposits and precipitates may sample Os derived from crustal sources with systematically lower time-integrated Pt/Os than the sources for loess.

References:
[1] Baioumy H.M et al., Chem Geo 2011; [2] Walker R.J et al., GCA 2002;
[3] Ripley E.M et al., Chem Geo 2008; [4] Walker R.J et al., EPSL 2005;
[5] Brandon A.D et al., Science 1998; [6] McDaniel D.K et al., GCA 2004

Keywords: Os isotopes, steels, iron-ores, composition of the upper continental crust

SETP-6

Constraints on the Composition and Hydrothermal Alteration History of the Pacific Lower Crust beneath the Hawaiian Islands: Geochemical Investigation of Gabbroic Xenoliths from Hualalai Volcano

Gao, R.[1], Lassiter, J. C.[1]
1. Jackson School of Geosciences, The University of Texas at Austin, Austin, TX

Understanding the composition and hydrothermal alteration history of the lower oceanic crust (LOC) can help constrain deep hydrothermal circulation at mid-ocean ridges, which may have a substantial impact on the thermal regime and magmatic processes at spreading centers. Previous studies of LOC primarily examined ophiolites or layer-3 gabbros exposed at the seafloor through faulting. These potentially have experienced secondary hydrothermal alteration in response to faulting, uplift and exposure. We examined major and trace element and isotopic compositions of a suite of gabbroic xenoliths derived from the 1800-1801 Kapulehu flow, Hualalai, Hawaii to constrain the composition and "primary" hydrothermal alteration history of the in situ Pacific crust beneath the Hawaiian Islands (HI). Although most Hualalai gabbros have trace element and isotopic compositions consistent with derivation from Hualalai magmas, a subset has characteristics indicative of an origin from MORB-related melts. These gabbros contain LREE-depleted clinopyroxene, have Sr-Nd-Hf isotopic compositions that overlap the range of EPR basalts, and are geochemically distinct from Hualalai-related xenoliths and lavas.

Despite the limited range recorded, plagioclase and clinopyroxene oxygen isotope compositions correlate well for both MORB-related and Hualalai-related gabbroic xenoliths. This suggests clinopyroxene and plagioclase are in equilibrium. The Δplag-cpx (~0.6-0.9‰) is consistent with closure temperatures of ~1170-1220℃.δ18Ocpx (+4.9-5.3‰) of the MORB-related gabbros are negatively correlated with cpx 87Sr/86Sr, but not with 143Nd/144Nd or La/Sm. In contrast, δ18Oplag does not correlate with plag 87Sr/86Sr. Cpx Sr-isotopes may be affected by seawater alteration, which is not as apparent in plag due to higher Sr concentrations. However, the MORB-related gabbros have δ18O values that are largely in the range for normal, fresh MORB (δ18Omelt/NMORB = +5.7-6.0‰, Δmelt-cpx~0.7‰). This suggests that only limited hydrothermal circulation penetrated to the depth of the layer-3 LOC gabbros beneath the HI, which resulted in only minor hydrothermal alteration. This is in contrast with observations from several ophiolite sequences and fault-exposed gabbros, which show significantly greater hydrothermal alteration and larger shifts in δ18O from normal mantle values (e.g., δ18O down to +3.5‰; c.f., [1]). The greater alteration recorded in these samples may result from hydrothermal circulation triggered by faulting/uplift associated with their exposure. The relatively uniform and "normal" δ18O values of the MORB-related gabbros also suggest that assimilation of Pacific crust by Hawaiian magmas ponding within the lower crust is unlikely to produce significant shifts in the magma oxygen isotope composition, and is therefore unlikely to account for the low δ18O values recorded in some Kea-trend lavas as previously proposed (c.f., [2]).

[1] Gregory, R. T. & Taylor Jr, H. P., 1981, J. Geophys. Res., 86, 2737-2755.
[2] Eiler, J. M., Farley, K. A., Valley, J. W., Hofmann, A. W. and Stolper, E. M, 1996, Earth Planet. Sci. Lett., 144, 453-468.

Keywords: hydrothermal alteration, geochemistry, lower oceanic crust, xenolith

SETP-7

Paired oxygen and hafnium isotopic analysis of zircon from gabbros: Identifying potential Mesozoic mantle heterogeneity in the Sierra Nevada arc

Gevedon, M.[1] and Clemens-Knott, D.[2]
mgevedonl@utexas.edu
1. Jackson School of Geosciences, The University of Texas at Austin, Austin, TX
2. California State University Fullerton

The composition of the mantle below the Mesozoic Sierra Nevada arc is a topic of debate; the presence of enriched mantle has major implications for modeling the magnitude and mechanisms of the Cordilleran crustal growth event. Multiple lines of whole-rock geochemical and isotopic evidence indicate the presence of depleted mantle below the western arc. Similar whole-rock isotopic studies suggest a more complex origin of eastern Sierra magmas, and the presence of an enriched mantle source.

This study represents a significant contribution to the enriched-mantle debate because (A) the new isotopic data are from gabbros, which closely represent the composition of mantle-derived parental magma; (B) ages determined during this study are late Jurassic and Early Cretaceous, making these rocks coeval with arc magmatism; and (C) zircon are better suited for isotopic studies because they are not susceptible to open-system process that impact and potentially compromise whole-rock analyses.

Coupled zircon hafnium-oxygen isotopes provide mantle signatures that suggest arc magma generation in two distinct source regions, with western samples derived from depleted mantle and eastern samples possibly extracted from enriched mantle. Three potential interpretations are proposed for the eastern gabbros: extraction from depleted mantle with subsequent crustal assimilation; extraction from an enriched mantle source region; or derivation from a tectonically assembled deep crustal mafic magma source.

Keywords: Sierra Nevada, enriched mantle, hafnium, oxygen isotopes, zircon , gabbro.

SETP-8

Investigation of Quaternary slip rates along the Banning strand of the southern San Andreas Fault near San Gorgonio Pass

P.O. Gold[1], W.M. Behr[1], K. Kendrick[2], T. Rockwell[3], D. Rood[4,5], W. Sharp[6]
Peter.gold@utexas.edu
1. Department of Geological Sciences, University of Texas, Austin
2. United States Geological Survey, Pasadena
3. Department of Geological Sciences, San Diego State University
4. AMS Laboratory, Scottish Universities Environmental Research Center
5. Earth Research Institute, University of California, Santa Barbara
6. Berkeley Geochronology Center

Present-day Pacific-North American relative plate motion in southern California is shared primarily between the San Jacinto and San Andreas faults. At the north end of the Coachella Valley, the San Andreas fault splits into the Banning and Mission Creek strands, which are sub-parallel to each other within the Indio Hills. Northwest of the Indio Hills, the Mission Creek fault diverges from the Banning and continues northwest toward the southeastern San Bernardino Mountains, but loses surface expression beneath Quaternary alluvial deposits in Morongo Wash. The Banning fault, upon exiting the Indio Hills, is deflected toward the west and transitions into a structurally complex fault zone at San Gorgonio Pass, where it is delineated by thrust scarps in Holocene alluvium. The slip rates of the Banning and Mission Creek fault strands northwest of the Indio Hills and southeast of San Gorgonio Pass are presently unconstrained, but understanding how slip is partitioned between these two strands is critical to southern California earthquake forecasting efforts. Here we present preliminary slip rate data for the Banning fault ~2 km southeast of San Gorgonio Pass at Devers Hill. Using the B4 LiDAR as a base, we have mapped the extents of three truncated and offset alluvial fan deposits, which we have differentiated based on both field and remote (LiDAR- and air photo-based) observations of texture: in particular, the distribution of different clast sizes, pavement and soil development, and color and appearance. To confirm across-fault correlation of the displaced deposits, we have measured 26 cosmogenic Be-10 ages from boulders and cobble samples taken from each of the three fan surfaces on both sides of the fault. One debris flow deposit (Q2a) has been dated to ~80 ka, and appears to be offset 1.6-2.2 km, though confirming this reconstruction will depend on future excavations and uranium-series dating of soil carbonate. A second debris flow deposit (Q2b), for which ages are pending, has been displaced 1-1.6 km. Together, these measurements suggest a late Quaternary slip rate for the Banning strand of the San Andreas fault of about 12-24 mm/yr. Our preliminary slip rate measurement for the Banning strand just southeast of San Gorgonio Pass is consistent with the slip rate of the San Bernardino section of the San Andreas fault to the northwest, and suggests that averaged over late Quaternary timescales (~80 ka), displacement along the San Andreas south of San Gorgonio Pass may be more focused on the Banning strand than the Mission Creek strand.

Keywords: San Andreas Fault, slip rate, San Gorgonio Pass, Coachella Valley

SETP-9

Using Baffin Island zircons to understand radiation effects on zircon (U-Th)/He ages

A. Goldsmith[1], C.G. Creason[2], D.F. Stockli[1], R.A. Ketcham[1]
atom.goldsmith@utexas.edu
1. Jackson School of Geosciences, The University of Texas at Austin, Austin, TX
2. Dalhousie University, Halifax, Nova Scotia, Canada

Zircon (U-Th)/He thermochronometry (ZHe) is a method of determining low-temperature thermal histories by measuring the concentrations of U, Th and He in zircon. Because the diffusion of He from the crystal is a function of temperature and time, the combined ratios of these elements contain valuable information about cooling of the hostrock. Helium diffusion in zircon, however, is more complex than is currently understood, in that it is significantly and systematically affected by damage to the crystal lattice caused by the α-decay of U and Th, and the spontaneous fission of ^{238}U. Therefore, a thorough and quantitative understanding of the effects of radiation damage on He diffusion kinetics is critical to the accurate modelling of thermal histories. This is particularly useful for cases in which zircons have experienced significant radiation doses, or prolonged residence at temperatures above which radiation damage is annealed. This study uses (U-Th)/He thermochronology in zircon from Hall Peninsula, Baffin Island, which displays a negative correlation with radioactive element concentration, in combination with Raman spectroscopy and laser-ablation inductively coupled plasma–mass spectrometry, to quantify the effects of radiation dose on helium diffusivity. The ages produced from this study are anticipated to show the full range of variability in He diffusivity from radiation dose. These data and others will help in identifying the thresholds of radiation dose required for significant alteration of He diffusivity, and in developing a new and more accurate model for ZHe thermochronology.

Keywords: zircon, (U-Th)/He, Baffin Island

SETP-10

Temporal Constraints on Multiple Rifting Stages of a Hyper-Extended continental Margin using coupled bedrock and detrital thermochronometry, Mauléon Basin, Western Pyrenees

Hart, N.[1], Stockli, D.[1,2], Lavier, L.[1,2], Hayman, N.[1,2]
hartnic4@utexas.edu
1. Jackson School of Geosciences, The University of Texas at Austin, Austin, TX
2. Institute for Geophysics, The University of Texas at Austin, Austin, TX

Multi-mineral double-dating of detrital and bedrock units from a hyper-extended continental margin have the potential to show a detailed progression and timing of continental rifting. Modern thermochronometric dating techniques have a range of applications in quantifying tectonic and sedimentary processes at rifted continental margins. Zircon (U-Th)/He (ZHe) and detrital zircon U-Pb dating, constrain sediment provenance and the temporal and thermal evolution of tectonically active source areas. Additionally, hyper-extended margin basins, such as the Mauléon basin, hold inverted unroofing sequences with up-section variation in lag time that record changes in sediment source or exhumation rates as different lithospheric levels are exhumed, eroded and deposited during progressive continental break-up. These sediments deposited in syn-rift basins typically archive a more complete history of margin evolution than bedrock alone that is prone to thermal overprinting or erosion. Furthermore, zircon and rutile U-Pb-He and detrital U-Pb-He double dating studies have shown the power of coupling these data with other geochemical characteristics to further refine provenance signatures and reconstruct the complete tectonic evolution of hyper-extended continental margins.
The Mauléon Basin of the Western Pyrenees is an ideal field site due to extreme crustal thinning during Cretaceous rifting followed by Pyrenean reactivation. Reactivation and deformation were minimized in the west, so many pre- and syn-rift structures are preserved and can be compared to post-rift units and structures. Initial results show that there has not been complete resetting in this region after Cretaceous rifting, therefore parts of the rifting events have been preserved by the zircon U-Pb and (U-Th)/He systems. This study is the first major chronologic study of bedrock and detrital units completed in the Mauléon Basin and will contribute new insights into continental rifting, the evolution and structure of the Mauléon Basin and the Western Pyrenees and also plate reconstructions and kinematics of the Iberian and European plates.

Keywords: Pyrenees, Zircon, U-Pb, (U-Th)/He, Double-dating, Extensional tectonics

SETP-11

3-D fracture network tracing and influence on flow

Hildebrandt, J.[1], Ketcham, R.[1]
the.jordan.hildebrandt@utexas.edu
1. Jackson School of Geosciences, The University of Texas at Austin, Austin, TX

X-ray computed tomography (CT) is a nondestructive imaging method that shows differences in X-ray attenuation, which is a proxy for density. Sensitivity to density differences makes CT a good choice for imaging open natural fractures because of the significant density contrast between air and rock. The image data, however, are prone to artifacts and blurring, which makes taking accurate measurements challenging. To counteract this problem, a tool has been created to quantify the spatial resolution of the data with a point-spread function (PSF). The PSF tool permits accurate measurement of fine-scale features in CT data – critical for measuring fractures, which are often thinner in one dimension than the PSF size, in turn influencing measurement of aperture. A network tracing algorithm is paired with the PSF to characterize accurately a full fracture network in 3-D.

To date, only single, isolated, relatively flat fractures have been characterized thoroughly in 3-D for CT data, and most numerical modeling has been conducted on 2D subsets. Additionally, research involving fracture networks is currently limited to simplified numerical models and simulations. This new work extends CT fracture characterization to full 3-D networks, thus providing a robust source of real network data for studying the difference between fracture networks and single fractures. Here, the focus is on the influence of a network on flow through the system.

With its large number of thin fractures and complex, anastomosing bifurcations, a Packsaddle schist sample was selected as a testing ground for the network tracing algorithms to be developed. We further hypothesize that the bifurcation in the sample will create different equivalent hydraulic apertures based on the directionality of the predominant current flow through the sample, and the distribution of aperture across intersections.

Keywords: x-ray computed tomography, fracture networks, point spread function

SETP, EG-12

Reactive melt transport in binary solid solution

Jordan, J.[1], Hesse, M.[1]
1. Jackson School of Geosciences, The University of Texas at Austin, Austin, TX

Partial melting and melt migration are instrumental in determining the large-scale physical and chemical characteristics of terrestrial planets and smaller, rocky celestial bodies. The study of MORBS and ocean island basalts provide insight into rocky planets with chemically differentiated interiors. However, ocean island basalts and MORBs and their compositions cannot be interpreted in terms of their source material without an understanding of partial melting and reactive transport through the crust and the mantle.

The essential role of lithological heterogeneities during partial melting of the mantle is increasingly recognized. How far can enriched melts propagate while interacting with the ambient mantle? Can the melt flow emanating from a fertile heterogeneity be localized through a reactive infiltration feedback in a model without exogenous factors or contrived initial conditions? How far can an enriched melt pulse travel in a partially molten system without forced, buoyancy driven migration?

A full understanding of the role of heterogeneities requires reactive melt transport models that account for the phase behavior of major elements in solid solution. Previous work on reactive transport in the mantle focuses on trace element partitioning, we present the first nonlinear chromatographic analysis of reactive melt transport in systems with binary solid solution. Based on the enthalpy method (Katz 2008) we analyze the evolution of simple systems with a focus on ion exchange and melting due to the transport of enthalpy, not decompression. From this we hope to shed insight into the dynamics of reactive transport within molten solid solution without the aid of adiabatic, decompression melting. We model the isenthalpic end member of melting conserving bulk rock composition and enthalpy in time dependent balance equations. We present self-similar solutions and reactive front speeds relative to the transport of molten material in a porous solid solution.

Keywords: Thermodynamics, phase behavior, reactive transport, melting processes, deep Earth processes, mantle dynamics

SETP-13

Deciphering P-T Conditions of Metamorphic Rocks from the Southern Menderes Massif of SW Turkey

Atakturk, K.[1], Catlos, E.J.[1], Diniz,E.[2], Cemen, I.[3]
Atakturk@utexas.edu
1. Jackson School of Geosciences, The University of Texas at Austin, Austin, TX
2. Pickens School of Geology, Oklahoma State University, Stillwater, OK
3. Geological Sciences, University of Alabama, Tuscaloosa, AL

The Aegean region contains numerous metamorphic core complexes that reflect post-collision extensional tectonics. The largest of these is the Menderes Massif of Turkey, which covers an area of ~40,000km^2. At its southern border is the Selimiye Shear Zone, a key location for understanding the Menderes system. Only limited and scattered pressure-temperature (P-T) data exists in the Southern Menderes Massif (SMM), and here we report conditions to supplement information regarding its evolution. Rocks were collected perpendicular to strike along 7 spaced transects in the SMM. We analyzed garnets in the samples using electron beam microscopy and obtained high-resolution back-scattered electron (BSE) images, X-ray element (Fe, Mg, Mn, Ca and Y) maps, and quantitative compositional data. The results show the garnets record a complex metamorphic history. Sixteen garnet X-ray element maps from separate samples show zoning consistent with multiple stages of growth, diffusion, and retrogression. The zoning is often clearly visible in high contrast BSE images and indicates the rocks experienced conditions inconsistent with a simple, single stage metamorphic history. We applied common thermobarometers to generate preliminary P-T conditions. The rocks record ~400-600°C and unrealistically high pressures (>10-20 kbar). Data reported here support the hypothesis that polymetamorphism is recorded in SMM rocks in close proximity to the Selimiye Shear Zone. To model the thermal evolution of the region accurately requires an understanding of the peak P-T the rocks experienced and the time at which they were at those conditions. Future work will include dating monazite inclusions in garnet to understand the timing of metamorphic stages in the SMM.

Keywords: Metamorphic, garnet, P-T, geochronology, monazite, zircon

SETP-14

Exploring the Changes of Tourmaline in the Himalayan Main Central Thrust Zone, Mt. Everest Transect, Nepal

Kenigsberg, A. R.[1], Catlos, E. J.[1]
arkenigsberg@gmail.com
1. Jackson School of Geosciences, The University of Texas at Austin, Austin, TX

Tourmaline is a useful mineral to decipher the metamorphic processes operating in the Himalayas. The Main Central Thrust (MCT), located at the base of the Himalayan break in slope, places lower-grade rocks of the Lesser Himalayan Formation beneath high-grade rocks of the Greater Himalayan Crystallines. The MCT has accommodated as much as 300 km of convergence between India and Asia and is a broad distributed shear zone. Because of this, an exact location of the MCT can be difficult to discern in the field. The long-term goal of this project is to analyze Himalayan tourmaline using a petrographic microscope, an electron microprobe for compositions, and a small-radius ion microprobe to obtain boron isotopes, to develop a model of how the mineral formed and/or was affected by deformation within and across the MCT shear zone. The overall objective is to correlate tourmaline chemical composition, grain size, color, inclusions, zoning, and abundance to the environment in which it formed. This is significant to address because the fault figures prominently in a number of models for a continent-continent plate tectonic setting and knowing how rocks and minerals within and across the fault zone deformed furthers our understanding of plate convergence, Himalayan tectonics, and the response of tourmaline to large-scale deformation. Tourmaline grains were identified in 16 thin sections from a transect across the MCT in eastern Nepal (Everest Transect). The number of tourmaline grains identified in a single thin section varied from 2 to > 100. Greater Himalayan Crystallines thin section sample ET-03 had significantly more tourmaline than any other. However, Greater Himalayan Crystalline tourmaline in general tend to be larger in size, many greater than 200 microns, but less abundant than the tourmaline found in the Lower Lesser Himalaya.

Keywords: Tourmaline, Himalaya, Main Central Thrust

SETP-15

Timing of high-pressure metamorphism in the Nevado-Filabride Complex of the Betic Cordillera, Spain: implications for subduction in the Western Mediterranean

Kirchner, K.[1], Behr, W. [1], Loewy, S.[1], Platt, J.[2]
korykirchner@utexas.edu
1. Jackson School of Geosciences, The University of Texas at Austin, Austin, TX
2. University of Southern California, Los Angeles, CA

The Betic Cordillera of southern Spain is an orogen formed in response to millions of years of convergence between Africa and Iberia, from the late Mesozoic to the present. The orogen consists of three main tectonic complexes, two of which have been subducted to depth, then exhumed back to the surface over short timescales. Subduction in the structurally higher of these complexes is relatively well constrained to the Eocene, but the timing of high-pressure metamorphism in the structurally lower complex, known as the Nevado-Filabride Complex, has been a topic of debate for several years due to conflicting geochronological data. Several proposed tectonic evolution models for the Nevado-Filabride Complex are based on ages of single mineral phases. For example, models based primarily on 40Ar/39Ar dating on white mica in high-pressure schists require that the Nevado-Filabride and the overlying tectonic unit were coevally subjected to high-pressure metamorphism in the Eocene, and subsequently exhumed at different rates. More recent models, based on Lu-Hf dating on prograde garnets in eclogites, separate the timing of high-pressure metamorphism of the Nevado-Filabride Complex from the overlying tectonic unit by at least 10 m.y. We examine the viability of these models using multimineral Rb/Sr dating of blueschist and eclogite facies rocks in the Nevado-Filabride Complex. The multimineral isochron method uses the whole high-pressure mineral assemblage rather than a single phase, which may not be in equilibrium. The results will allow us to distinguish between these two conflicting tectonic models and to clarify the tectonic history of the Western Mediterranean region.

Keywords: Spain, Nevado-Filabride Complex, high-pressure metamorphism, Rb-Sr.

SETP-16

Structural Analysis of NNE-SSW Ridges in the Western Desert, Egypt Using Remote Sensing Data

Laciano, P.[1], Tewksbury, B.[2]
peter.laciano@utexas.edu
1. Jackson School of Geosciences, The University of Texas at Austin, Austin, TX
2. Hamilton College, Clinton, NY

The Western Desert is a remote, arid region covering almost 700,000 km^2 west of the Nile River in Egypt. Recently released high-resolution satellite imagery from Google Earth revealed widespread structural features in the Stable Platform of the Western Desert. One specific area of the Stable Platform, the Drunka-Serai region, which spans a 20,000 km^2 area west of the Nile Valley city of Sohag, features a system of NNE-SSW oriented ridges. These ridges appear to be oblique-slip faults formed in a transtensional stress regime during the Oligocene/Miocene Red Sea rifting event. N-S basement faults were reactivated by this event and propagated through the overlying sedimentary cover as Riedel shears, en echelon segments, and folds within the fault zone. Future work on the ground can help confirm and build on these remote sensing interpretations.

Keywords: Structural geology, remote sensing, Google Earth, Egypt, Red Sea rifting, Stable Platform, basement reactivation

SETP-17

Investigating the Pathways and P-T-X Conditions of Hydrothermal Fluid Flow Responsible for Mineralization in the Ertsberg East Cu-Au Skarn, Papua, Indonesia

Ledvina, M.[1], Kyle, J.R.[1]
Ledvina@utexas.edu
1. Jackson School of Geosciences, The University of Texas at Austin, Austin, TX

The Ertsberg East Skarn System (EESS), a 3Gt ore body at 0.59% Cu and 0.49ppm Au, is located in the Ertsberg-Grasberg mining district, a 50km^2 region of world class Cu-Au porphyry and skarn deposits perched in the highlands of Papua, Indonesia. The region is tectonically complex: subduction of the Australian plate beneath the Pacific plate ca. 12Ma uplifted a succession of Upper Cretaceous siliciclastics to Lower Tertiary carbonate strata which act as host rocks for the skarn ore bodies. The transition to a strike-slip margin ca. 4Ma is associated with magmatism and episodic hydrothermal fluid flow which resulted in skarn mineralization. While the neighboring Grasberg deposit is believed to have formed by a throttling cupola mechanism, where hydrothermal fluids collect at the top of a batholith and are periodically released into a pluton, the origin and transport mechanism for fluids that formed the EESS are unknown.

Several structural and stratigraphic pathways have been proposed as fluid conduits connecting a deep fluid source with the reactive carbonate strata, but controls on the P-T-X conditions of calc-silicate alteration and Cu-Au mineralization are essential to describing skarn formation. Cu-Au mineralization in the EESS is stratigraphically controlled in the exoskarn, but also occurs within hydrothermal quartz veins across the endoskarn, hornfels, and exoskarn facies. This relationship suggests that quartz veining and silicification record the evolution of fluids during calc-silicate alteration and Cu-Au mineralization. ESEM-Cathodoluminescence imagining reveals zonation textures and cross-cutting relationships in vein quartz that results from changes in the P-T-X conditions throughout multiple generations of Si-saturated fluid input. When partnered with fluid inclusion analysis and Quartz Ti-thermometry it may be possible to quantify fluctuations in the depositional conditions of Cu-Au skarn formation with time to identify the pathways of mineralizing fluid migration.

Keywords: Skarn, Hydrothermal Fluids, Cu-Au Mineralization, Quartz Veins, Cathodoluminescence

SETP-18

Novel Coupled Thermochronometric Geochemical Investigation of Fluid Flow and Geothermal Systems in Extensional Tectonic Settings, Dixie Valley, Nevada

MacNamee, A.[1], Stockli, D.[1]
amacnamee@utexas.edu
1. Jackson School of Geosciences, The University of Texas at Austin, Austin, TX

The Dixie Valley area of Nevada lies within the Basin and Range province and is characterized by extensional tectonics, thin crust, elevated heat flow, and seismic belts. The extensional tectonic setting has created a complex interplay between normal faults and strike-slip faults such that these structures form fault-controlled dilational corners. These corners are areas of heightened extension, resulting in increased fracture permeability, and can therefore host blind geothermal prospects. The source of heat for these geothermal anomalies is the related to deep circulation of fluids associated with these structural features. However, the relationship between the thermal background and the structural setting is not well understood. Moreover, it is unclear what role structural features play in the control and occurrence of geothermal anomalies.

Apatite (AHe) and zircon (ZHe) (U-Th)/He analyses were employed to address these geologic problems. 75 samples were collected along the footwall of the Stillwater range front normal fault and in elevation transects. ZHe ages range from 2.8 ± 2.1 Ma to 72.8 ± 4.7 Ma, but cluster around ~20 to 30 Ma. An exhumed fossil partial retention zone is apparent in the White Rock Canyon area ZHe transect data. AHe ages range from 0.5 ± 0.2 Ma to 7.5 ± 4.8 Ma and are generally younger with decreased elevation. These ages also show a younging trend with increased proximity to fault apices. In the Dixie Comstock area, AHe ages decrease toward the nearest shallow geothermal anomaly. An elevation transect in this same area shows the onset of rapid exhumation of the range front began at ~4 Ma at a minimum rate of ~0.12 mm/yr. Samples of significantly younger AHe age are likely fully or partially reset due reheating by geothermal fluids. 4He/3He thermochronologic analysis is expected to further constrain a continuous time-temperature history of samples at temperatures as low as 20°C.

Keywords: (U-Th)/He dating, geothermal, fluids, Dixie Valley, Stillwater Mountains

SETP-19

Thrusting sequence and basin evolution of the Zagros orogenic belt, NE Iraq, Kurdistan

Koshnaw, R. I.[1], Stockli, D. F.[1], Horton, B. K.[1]
renas.i.mohammed@utexas.edu
1. Jackson School of Geosciences, The University of Texas at Austin, Austin, TX

The Zagros fold-thrust belt and foreland basin is a 2000 km long orogen in the Middle East that formed during the Cenozoic Arabia-Eurasia collision; however, the precise shortening time is still ambiguous. The study area within the Kirkuk embayment contains a thick Phanerozoic sedimentary cover up to 14 km with a well-exposed succession of Cenozoic clastic foreland-basin fill. The research-focused Neogene sediments include the Lower Fars(M. Miocene), Upper Fars(U.Miocene), Lower Bakhtiari (Mio-Pliocene), and Upper Bakhtiari (Plio-Pleistocene) Formations. Previous studies have utilized the geo-/themochronologic and magnetostratigraphic techniques in the Iranian Zagros to quantify the duration of deformation, erosion and deposition. Understanding the evolution of the northwestern extremity of the Zagros orogeny in Iraqi Kurdistan will give a complete picture of the entire Zagros fold-thrust belt and foreland basin evolution.

The goal of this study is to test hypotheses of whether the fold-thrust belt advanced sequentially into the foreland or there were out-of-sequence deformation events. Also, this study investigates the possible sources for the basin fill. Were the sediments sourced from the adjacent nearby mountains or from extrabasinal sources? In other words, what is the influence of axial and transversal interplay in filling of a foreland basin?

This study utilizes a variety of basin analysis techniques,, such as low-temperature thermochronometry, geochronology, and magnetostratigraphy. Apatite (U-Th)/He ages reveal that the High Zagros Fault thrusted at ca. 12 Ma and frontal thrusts at ca. 8 Ma. At 6 Ma, a thick-skinned deformation has occurred and generated a structural step of ca. 700 m high. Detrital zircon U-Pb analysis shows that highest sediment input were derived from the Urmieh-Dokhtar Volcanic Zone and Sanandaj-Sirjan Zone in Iran, as well as from Bitlis terrane in SE Turkey. The along strike variation of detrital zircon ages indicates that older grains population increase toward the NW of Kirkuk embayment, which indicate a systematic unroofing of source bedrock.

In summary, the deformation of the Zagros orogenic belt in Iraqi Kurdistan is characterized by an out-of-sequence thick-skin deformation that enhanced the accommodation space. Paleodispersal pattern from paleocurrent and detrital zircon U-Pb age analyses indicate the N and NNW as major source of the sediments. However, in thicker parts of the Neogene basin in SE Kurdistan the U-Pb data indicates NE and E as source while the paleocurrent refer to NNW as a source direction.
This research is providing more constraint on the onset of Arabia-Eurasia collision and significantly assists in reconstructing the tectonic history of Middle East. Economically, defining the time of deformation and structural styles have crucial impact on the current ongoing hydrocarbon exploration processes in the northern region of Iraq, Kurdistan.

Keywords: Zagros foreland basin, fold-thrust belt, thermochronology, geochronology,

SETP-20

Cenozoic deformation history of the central Andes, southern Peru: structural inversion, basin dynamics and Altiplano uplift

Perez, N.D.[1], Horton, B.K.[1]
nicholas.d.perez@gmail.com
1. Jackson School of Geosciences, The University of Texas at Austin, Austin, TX

Pre-Andean extensional systems influenced subsequent shortening patterns and foreland basin evolution during Cenozoic construction of the central Andean plateau. However, the style and timing of inversion, location of major controlling structures, foreland basin response to shortening and plateau uplift remain poorly defined. New measured stratigraphic sections, sediment provenance, field mapping, structural transects, and thermochronology from the Altiplano, Eastern Cordillera and Subandes of southern Peru provide insights into how pre-existing Permo-Triassic rift structures influenced the geometry, kinematics and magnitude of Andean shortening and foreland basin partitioning.

We present a regional balanced cross section spanning the Altiplano to Subandes as the structural framework for three new results linking inversion tectonics and Cenozoic basin evolution. 1) Inversion of pre-existing normal faults controlled major structures in the Eastern Cordillera fold-thrust belt. Subcrop maps and structural restorations demonstrate the location of pre-existing structures inverted as thrust faults. We have constrained the timing of inversion along two of these structures (pre-Andean intrusive basement and the Ayaviri backthrust) using (U-Th)/He apatite thermochronology and newly dated growth strata. Previous workers have suggested that earliest exhumational cooling (at ~38 Ma, from $^{40}Ar/^{39}Ar$ results for pre-Andean basement) is linked to Eocene shortening. Our new low-temperature (U-Th)/He results suggest continued cooling at ~16-20 Ma. These datasets suggest long-lived or multiphase inversion. Growth strata along the Ayaviri backthrust, an inverted normal fault defining the Altiplano-Eastern Cordillera boundary, demonstrates motion at ~28 Ma. Together, these results suggest that inversion may promote coeval, spatially distributed shortening. 2) The Ayaviri basin in the Peruvian Altiplano preserves an Oligocene-Miocene record of proximal sediment shed from a growing thrust wedge in the Eastern Cordillera. Basin evolution was controlled by thrust tectonics, yet was strongly influenced by the proximity of the Andean volcanic arc. U-Pb detrital zircon samples demonstrate a consistent supply of syndepositional volcanic zircons throughout basin filling. Sediment provenance, newly dated growth strata and U-Pb zircon geochronology are employed to document basin reorganization at ~16.4 Ma attributable to out-of-sequence thrusting and structural partitioning of the basin. 3) The Cenozoic foreland basin exposed in the Subandean fold-thrust belt also preserves the sedimentary record of Eastern Cordillera shortening. However, the detrital zircon record from synorogenic basin fill lacks the abundant Cenozoic volcanic zircons emblematic of the Ayaviri Basin. Other unique detrital zircon spectra further distinguish the Subandean and Altiplano basins.

We interpret these results as evidence for early, potentially long-lived inversion of pre-existing normal faults that created the incipient Eastern Cordillera as a topographic barrier separating the Altiplano and Subandean basins. Continued Eastern Cordillera shortening sustained flexural subsidence throughout the Cenozoic filling of these basins. These results demonstrate that the northern Altiplano deformational and basin history has been strongly influenced by the inherited structural architecture. This improved record of the timing and distribution of shortening has implications for when and how crustal thickening contributed to Altiplano uplift.

Keywords: Central Andes, Altiplano, tectonics, foreland basin, fold-thrust belt

SETP-21

Understanding the role of strike-slip faulting as oceans close, north central Turkey

Pettit, B.[1], Catlos, E. [1], Elliot, B. [1]
bridgetpettit@utexas.edu
1. Jackson School of Geosciences, The University of Texas at Austin, Austin, TX

The goal of this project is to compile and interpret remotely sensed imagery and produce maps intended to lessen hazards associated with Turkey's North Anatolian Shear Zone (NASZ). These hazards include landslides and rock falls due to seismic activity. The NASZ contains the North Anatolian Fault, a right lateral strike slip fault extending approximately 1200 km in length. The NASZ is speculated to have accommodated from 25 to 110 km of displacement, depending on location. In the proposed field area, the shear zone is comprised of five major strands: Erbaa, Tosya-Ladik, Niksar-Kalekoy, Erzincan, and Tasova-Tekke faults with a combined estimated displacement of ~80 km. These strands, although named after villages and towns along the NASZ, do not have consistent names in the geological literature. The range of names highlights the fact that many details of these structures are unknown. By looking at surface expressions, it is possible to identify the extent of each fault and their relationship to one another; the resulting maps will help understand the tectonic history and identify geohazards of the region. In order to produce these maps, I developed objectives that will guide this research. The first is to compile aerial photographs, Digital Elevation Models (DEMs), geological maps, and strike and dip data of the field area. The next step is to propose locations, extent, and type of faulting based on data visible on the maps. The final step is to visit the proposed locations in outcrop and update the map according to the results. As an outcome, a series of maps focused in the region around the town of Amasya will be developed.

Keywords: North Anatolian Shear Zone (NASZ), Turkey, geohazards

SETP-22

Late extension inception and rapid fault-slip at the southern edge of the lower Colorado River extensional corridor: Harquahala Mountains core complex, west-central Arizona

Prior, M.P[1]., Stockli, D.F.[1]
mprior@utexas.edu
1. Jackson School of Geosciences, The University of Texas at Austin, Austin, TX

The Harquahala Mountains metamorphic core complex of west-central Arizona is located within the lower Colorado River extensional corridor (CREC) and bound by a low-angle normal fault, the Eagle Eye detachment (EED). The Harquahala core complex is the southernmost exposure of Tertiary mylonites exhumed along the regional low-angle normal fault system that connects the lower plate of the Chemehuevi, Whipple, Buckskin-Rawhide, and the Harcuvar Mountains, making it a key location to understand the timing and pattern of extension within the lower CREC as a complete system. A ~45 km transect of samples for (U-Th)/He dating (n=16) was collected from the Harquahala footwall along the regional extension direction of ~060° to determine the cooling history associated with core complex exhumation and slip along the Eagle Eye detachment. Zircon (U-Th)/He ages (ZHe) were plotted versus distance from the EED and display 3 main characteristics: 1) samples furthest away yield older, pre-extension cooling ages of ~43 Ma, 2) a decrease in ZHe ages through a preserved partial retention zone (PRZ), and 3) ten nearly invariant ages that decrease from 17.6 ± 0.3 to ~15-16 Ma over the last 22 km and record cooling due to slip on the EED. Initial apatite (U-Th)/He ages are systematically younger than ZHe ages and display the same pattern. The preserved inflection point between the PRZ ages and ZHe ages recording fault slip indicates extension began at ~17-18 Ma within the Harquahala Mountains, several million years later than the ~20-24 Ma estimates from other core complexes in the lower CREC. Nearly invariant ZHe ages attributed to fault-related cooling suggest rapid time-averaged slip rates of ~10-16 km/m.y. from 17.6 ± 0.3 Ma to ~15-16 Ma. Extension continued in the Harquahala Mountains to at least ~12-13 Ma based on an apatite (U-Th)/He age of 12.6 ± 0.3 Ma ~1 km from the Eagle Eye detachment. These results indicate extension began several million years later in the Harquahala Mountains than other core complexes in the lower CREC and was accommodated by rapid fault-slip along the Eagle Eye detachment.

Keywords: Harquahala Mountains, low-angle normal faults, metamorphic core complex, (U-Th)/He dating, slip rates

SETP-23

(U-Th)/He and U-Pb double dating constraints on the interplay between thrust deformation and basin development, Sevier foreland basin, Utah

Pujols, E.[1], Stockli, D.[1], Horton, B.[1] , Steel, R. [1] , Constenius, K. [2]
edgardopujols@utexas.edu
1. Jackson School of Geosciences, The University of Texas at Austin, Austin, TX
2. Independent researcher

As in many thrust belts and corresponding foreland basins, the temporal progression, feedbacks, and linkage between deformation and exhumation of the fold-and-thrust belt and its influences on the proximal to distal foreland basin successions are poorly constraint, but of fundamental importance to understand thrust-sedimentation linkage, syn-tectonic basin architecture, detrital provenance, and hydrocarbon maturation and migration. This research is employing zircon (U-Th)-(Pb-He) double dating on pre- and syn-tectonic sediments along the Sevier thrust front and basin to provide an unprecedented geochemical frame, which will be used to temporally and spatially link the Sevier foreland basin stratigraphy to nearby sources. These new data will shed light on the in-depth connectivity and feedback relationships between foreland basin and thrust belt dynamics, the temporal aspect of thrusting and clastic progradation, sediment sources, basin subsidence, and stratigraphic architecture. The current DZ (detrital zircon) U-Pb signatures obtained from Precambrian units in the hinterland are mostly dominated by Grenville ages (~1 -1.15Ga.) and older anorogenic granites intruded in the Yavapai-Mazatzal craton (~ 1.4-1.6Ga.). The youngest Cambrian units are dominated by Yavapai-Mazatzal (~1.6 -1.8Ga.) and Trans-Hudson ages (~1.8 -1.9Ga.). (U-Th)/He ages in Canyon Range so far show a zircon partial retention zone exposed in Caddy Canyon Fm. with ages as young as Santonian. The Canyon Range Conglomerates recorded in sequence the unroofing of the thrust-belt and show (U-Th)/He ages ranging from Late Cretaceous to Permian. Additionally, the Canyon Range Conglomerates contain (U-Th)/He ages equivalent to their biostratigraphic age suggesting very short lag times and fast hinterland exhumation. These syn-depositional ages are in direct conflict with current models of exhumation in Canyon Range area since they show only a few kilometers (<3km) of exhumation when at least six kilometers are needed to explain our results. In the Sevier foreland basin (Book Cliff) (U-Th)/(He-Pb) plots from Turonian units are dominated by Late Cretaceous volcanic ages and an attenuated older signature. From lower Bluegate to the Castlegate units, volcanic signatures are also present, but with a stronger Precambrian signature, probably introduced by early stages of unroofing.

Keywords: Foreland basin dynamics, thrusting, (U-Th)/(He-Pb) double dating

SETP-24

Understanding the thermal and tectonic evolution of Marie Byrd Land from a reanalysis of airborne geophysical data in the West Antarctic Rift System

Quartini, E. [1], Powell, E.M. [1], Richter, T. [1], Damiani, T.[2], Burris, S.G.[3], Young, D.A.[1], Blankenship, D.D. [1]
enrica@ig.utexas.edu
1. UTIG, The University of Texas at Austin, Austin, TX
2. NOAA, National Geodetic Survey, Silver Spring, MD
3. Rice University, Houston, TX

The West Antarctic Rift System (WARS) is a region characterized by a significant topographic range, a complex tectonic history, and active subglacial volcanism. Those elements exert a large influence on the stability of the West Antarctic Ice Sheet, which flows within the cradle-shaped rift system and is currently grounded well below sea level. This potentially unstable configuration is the motivation for gaining a better understanding of the ice sheet boundary conditions dictated by rift evolution and how they impact the ice flow. In this study we focus on characterizing the distribution of and transition between sedimentary basins and inferred geothermal heat flux from the flanks to the floor of the rift system. We do so through analysis of gravity data both for sources within the deep lithosphere and near surface targets in the crust.

A compilation of gravity datasets over West and Central Antarctica and the analysis thereof is presented. In particular we use gravity data collected during several airborne geophysical surveys: CASERTZ (1994-1997), SOAR/WMB (1997-1998), AGASEA (2004-2005), ICEBRIDGE (2008–2011), and GIMBLE (2012-2013). New processing and data reduction methodologies are applied to the older gravity surveys to improve the high frequency signal content and to make these surveys compatible with modern works (i.e. AGASEA, ICEBRIDGE, GIMBLE). The high frequency signal provides better resolution of small-scale features within survey blocks but long-wavelength integrity is retained by registering the airborne free-air disturbance within those blocks to the gravity disturbance derived from the GOCE global satellite gravity field. This allows for consistent long wavelength interpretation across the merged surveys and provides improved gravity analysis of the deep lithosphere while retaining the capacity to study smaller scale features.

A crustal model for the area is produced using the Bouguer anomaly and spectral analyses of the Bouguer anomaly and free-air disturbance. Airy isostatic corrections are applied to the Bouguer anomaly where permissible to set the foundation for the identification and discrimination of sedimentary basins and intrusive/extrusive complexes beneath the West Antarctic Ice Sheet. This analysis also provides a framework for interpreting POLENET seismic studies in the region. Successful integration of the gravity and seismic results will ultimately be necessary for understanding the thermal evolution of Marie Byrd Land and its context within the West Antarctic Rift System.

Keywords: gravity anomalies, volcanism, Antarctica

SETP-25

The effect of water and stress magnitude on lattice-preferred orientation of olivine in naturally deformed peridotites

Bernard, R.[1], Behr, W.[1]
rachelbernard@utexas.edu
1. Jackson School of Geosciences, The University of Texas at Austin, Austin, TX

Seismic anisotropy in the upper mantle is produced primarily by lattice-preferred orientations (LPO) in olivine formed during ductile deformation. Because seismic anisotropy is one of the principal means of characterizing upper mantle flow directions, it is critical to understand how LPO is affected by deformation conditions, including temperature (T), pressure (P), water content and strain magnitude. The factors controlling LPO development in olivine have been investigated experimentally for several decades. Most recently, high T&P laboratory experiments by Jung et al. (6) demonstrated that water content and stress magnitude each play key roles in the development of LPO in olivine under experimental conditions. This experimental work not only reproduced the fabric most commonly observed in olivine in natural rocks (known as A-type), but also identified several new types of LPO that form under different water and stress conditions (B-type through E-type). The existence and occurrence of these less common fabric types in natural rocks have important implications for seismic anisotropy interpretation, which has traditionally assumed only the existence of A-type fabric.

Although the Jung et al. study was the first to document several different fabric types in olivine, the experiments were conducted at ~7 orders of magnitude faster strain rates and under much narrower PT conditions than typically present in Earth's mantle, so it is unclear whether their results can be directly extrapolated to natural peridotites. While LPO has been documented for many peridotite localities around the world, there is a dearth of studies that have connected these fabrics to measured water contents or stress magnitudes. A few have looked at both water content and LPO in naturally deformed peridotites: some agree with the experimental results of Jung et al., but some do not, suggesting that other variables, such as T or P may affect the LPO of olivine as well. The motivation of my research is to systematically test the experimentally-derived hypothesis that water content and stress magnitude primarily control LPO development in olivine. To do this, I will examine water content, stress magnitude, and olivine LPO in several naturally deformed peridotites derived from a wide range of conditions of Earth's upper mantle.

Keywords: Peridotites, xenoliths, olivine, stress, anisotropy

SETP-26

Experimental Study of Sedimentationin Pyroclastic Density Currents

Ramirez, G.[1,2], Andrews, B.[2], Dennen, R.[2]
ger426@utexas.edu
1. Jackson School of Geosciences, The University of Texas at Austin, Austin, TX
2. Department of Mineral Sciences, Smithsonian National Museum of Natural History, Washington, DC

Large, unconfined, particle laden density current experiments provide insight into the dynamics of dilute pyroclastic density currents (PDCs). Experiments were run in a sealed, air-filled tank measuring 8.5 m long by 6.1 m wide by 2.6 m tall. Currents were generated by feeding mixture of heated particles (5 mm aluminum oxide, 25 mm talc, 27 mm walnut shell, 76 mm glass beads) down a chute at controlled rates to produce dilute, turbulent gravity currents. Comparison of experimental currents with natural PDCs shows good agreement between Froude, densimetric and thermal Richardson, and particle Stokes and settling numbers; experimental currents have lower Reynolds numbers than natural PDCs, but are fully turbulent. Ambient temperature and warm currents have several distinct differences:

-warm currents have shorter run out distances, narrow map view distributions of currents and deposits, thicken with distance from the source, and lift off to form coignimbrite plumes;
-ambient temperature currents typically travel farther, spread out radially, do not thicken greatly with transport distance, and do not form coignimbrite plumes.

Isopach maps of the deposits show predictable trends in sedimentation versus distance in response to eruption parameters (eruption rate, duration, temperature, and initial current mass), but all sedimentation curves can be fit with 2nd order polynomials (R2>0.9). Proximal sedimentation is similar in comparable warm and ambient temperature currents, but distal sedimentation (beyond the current runout) is present in warm currents reflecting deposition from coignimbrite plumes.

Keywords: volcanology, volcanic deposits, pyroclastic density currents

SETP-27

Dating the Menghai Batholith, southern China

Reyes, E.[1], Brookfield, M.[2], Shin, T.A.[1],Catlos, E.J.,[1] Stockli, D.[1]
enrique.reyes@utexas.edu
1. Jackson School of Geosciences, The University of Texas at Austin, Austin, TX
2. School for the Environment, University of Massachusetts at Boston, 100 Morrissey Blvd, Boston, MA 02125

Paleogeographic reconstructions are used to determine the evolution and migration of Earth's continents, identify important economic resources that formed during specific times in Earth's history, and assess geological hazards that result due to reactivation of older faults or mass movement of rocks. The goal of this study is to improve our understanding of the complex tectonic history of southern China by constraining the timing of crystallization and uplift of the Menghai batholith. We aim to obtain U-Pb zircon ages and apatite U-Th/He ages from 8 samples of the batholith to decipher its tectonic and magmatic history and relationship to surrounding areas. The batholith is part of the Lancangjiang belt, a principle boundary between Gondwana and Eurasia, on the eastern side of China's Shan Plateau, and encompasses the southern extension of the Lincang Granite group. A few U-Pb zircon ages have been reported for the Lincang granite, timing emplacement during the Upper Triassic. No reliable U-Pb or U-Th/He ages exist for the Menghai batholith. Zircon and apatite grains have been separated from rock samples from the study area to be dated using Laser Ablation-Inductively Coupled Mass Spectrometry and noble-gas thermometry. In addition, petrographical work and geochemical analyses will be done to assess granite compositions and microstructures. Overall, reliable age data from the Menghai batholith will aid in determining the tectonic and magmatic history of the region, including understanding the dynamics of ancient Tethyan ocean closure in southern China and more recent Himalayan uplift.

Keywords: granitoids, exhumation, thermochronology, zircon, apatite, batholith, microstructures

SETP-28

Remote Sensing for Tectonic Geomorphology and Relative Slip of the Banning and Mission Creek faults, California

Salin, Aaron[1], Behr, W.M[1], Gold, P.O.[1]
a.salin@utexas.edu
1. Jackson School of Geosciences, The University of Texas at Austin, Austin, TX

With southern California primed for an earthquake, it is necessary to understand how the complex southern San Andreas Fault system ruptures and distributes slip. The restraining bend structure in San Gorgonio Pass is hypothesized to restrict earthquakes. The Banning and Mission Creek strands of the San Andreas fault in the northern Coachella Valley feed into San Gorgonio Pass after splitting from the single Coachella Valley strand to the south. The distribution of slip along these two strands is currently debated, but is critical for evaluating whether ruptures can propagate through the San Gorgonio Pass structural complexity. We use high resolution airborne LiDAR data and satellite imagery to resolve meter-scale offset features on these two strands to track how the amount of slip on each fault changes along strike as they approach San Gorgonio Pass. Results from 40 total measurements suggest that slip along the Mission Creek strand is decreasing to the northwest but remains active until its intersection with the Pinto Mountain fault of the Eastern California Shear Zone (rather than dying out within Morongo Wash as previously thought). The Banning strand, on the other hand, increases in right-lateral slip to the northwest as it approaches San Gorgonio Pass, consistent with previous interpretations..

The second part of this project attempts to resolve the structure of the two strands in the Indio Hills, a large push-up structure in the area between the faults. Field mapping and fracture measurement will be undertaken in December, 2013. It is hypothesized that the Banning and Mission Creek faults form a positive flower structure but seismic data and previous reports are conflicting for the Mission Creek, especially in the Indio Hills.

Keywords: neotectonics, California, San Andreas fault, Coachella Valley, Indio Hills

SETP-29

Tectonostratigraphy of the Cycladic Blueschist Unit: coherent underplating of high-pressure low-temperature metamorphic rocks on a regional scale

Seman, S.[1], Stockli, DF[1], Soukis, K.[2], Shin T.[1]
spencer.seman@utexas.edu
1. Jackson School of Geosciences, The University of Texas at Austin, Austin, TX
2. Department of Geology, National and Kapodistrian University of Athens

Discerning stratigraphic and structural relationships between packages of high-pressure low-temperature (HP-LT) metamorphic rocks is a historically difficult issue. Complex poly-metamorphic and multi-stage deformation histories obscure primary stratigraphic relationships and make regional scale correlation of units problematic. Detrital zircon U-Pb geochronology has been employed to great success in these environments as a tool to determine maximum depositional age of units, and therefore the tectonostratigraphy. The Cycladic Blueschist Unit (CBU) of Greece is a HP-LT metamorphic terrane in which the blueschist and eclogite facies history has largely been obscured by greenschist and amphibolite facies retrograde metamorphism and deformation. Under the P-T conditions experienced by the CBU, detrital zircons act not only as passive markers of maximum depositional age, but also as records of the metamorphic history. As a result, teasing out which age data represent the metamorphic history and which records the maximum depositional age requires trace element analysis of zircons. Depth profiling of zircons combined with laser ablation split stream (LASS) ICP-MS analysis allows for simultaneous determination of U-Pb age data and trace element compositions. We present detrital zircon data from metasediments and metavolcanics on the regional scale of the Cyclades and suggest correlations between packages of CBU exposed on mainland Greece in Attica and in the Western Cyclades based on maximum depositional ages. These data suggests the CBU retains a remarkable amount of stratigraphic coherency and that age inversions are a rarity. Therefore during subduction, underplating, and subsequent exhumation, large packages of the CBU maintained primary stratigraphic relationships.

Keywords: high-pressure low-temperature metamorphism, underplating, detrital zircon geochronology, (U-Th)/He, LASS-ICP-MS

SETP-30

Thermal Evolution of Continential Rifting in Corsica (France)

Seymour, N.M.[1], Stockli, D.F.[1], Beltrando, M.[2]
nikki.m.seymour@utexas.edu
1. Jackson School of Geosciences, The University of Texas at Austin, Austin, TX
2. Dipartimento di Scienze della Terra, Università di Torino, Torino, Italy

The occurrence and effects of reheating in magma-poor margins has been little studied, and has implications for basin evolution and thermal structure of the thinned lithosphere across rift basins. Magma-poor rifted margins make up about 50% of the world's rifted margins, and most occur in deep-water that are difficult to image geophysically. Corsica represents the European margin of the fossil Tethys Ocean, an exposed Mesozoic analogue for these modern margins. The structure of the Tethys is described by the Wernicke extension model, which suggests that continental lithosphere accommodates extension via a lithospheric-scale detachment fault that promotes substantial thinning and exhumation of lower crust and lithospheric mantle. This model predicts upwelling of the asthenosphere below the distal margin to fill the void created by exhumation of mantle lithosphere, which could have a significant post-crystallization reheating effect on crustal rocks. Reheating could also be caused by the juxtaposition of hot mantle lithosphere past colder upper plate crustal rocks during detachment faulting.

The Tethys opened between Gondawa and Laurasia from ~170-145 Ma to form an asymmetric rift characterized by relatively little mafic magmatism. Karstification of Triassic dolostones and subsequent infill with Jurassic sediments provides constraints on the timing of subaerial exposure and subsequent drowning. This timing, combined with dating of radiolarian cherts, supports a mid- to late-Jurassic age of mantle exhumation. Rift-related faults and shear zones were reactivated during the Cenozoic Alpine orogeny, in which the African plate moved northward and collided with the Eurasian plate. This compressional event reached greenschist facies, overprinting original rift fabrics throughout the orogen. The Belli Piani subunit in the Santa Lucia nappe of Alpine Corsica preserves a suite of lower crustal rocks and continental basement slivers with a low Alpine overprint, and will serve as the focus area of this study.

This project seeks to establish the thermal evolution of the European margin on Corsica – specifically, whether reheating occurred and the onset, duration, and geometry of reheating if it was present. Apatite (U-Th)/He cooling ages throughout the stratigraphic section will be used in conjunction with the timing constraints provided by paleokarsts in order to a) establish thermal gradients for the lower crust during Mesozoic rifting and b) determine if drowning is contemporaneous with cooling from reheating. Zircon from the Mafic Complex and Diorite Granite Complex will be depth-profiled for both U-Pb and trace element concentrations via LA-ICP-MS split streaming. Depth profiles will allow the comparison of trace element diffusion both out of and, more significantly, into the zircon to simultaneously obtained U-Pb ages. A signal showing rare earth element diffusion into the zircon is a strong signal of reheating. If the predicted reheating is seen, the study will further seek to develop a cross-basin perspective on the geometry and intensity of reheating via comparison with lower crustal granulites exposed on the Adriatic margin.

Keywords: thermonochology, tectonics, rifting, Ligurian Tethys Ocean, Corsica

SETP-31

A naturally-constrained orthopyroxene piezometer

Speciale, P.[1], Behr, W.[1]
Pamela.Speciale@utexas.edu
1. Jackson School of Geosciences, The University of Texas at Austin, Austin, TX

The magnitude of stress in the continental lithosphere, particularly the lithospheric mantle, is highly uncertain and frequently debated, but is critical to understanding continental mechanics. Differential stress can be estimated using paleopiezometry, which is a relationship between the recrystallized grain size formed during dislocation creep and the flow stress. This relationship has been quantified experimentally for a wide range of earth materials, including olivine, quartz, plagioclase, calcite, and numerous metals. The empirical piezometer for olivine (van der Wal et al., 1993) is one of the best constrained and has been used to estimate stress magnitudes for mantle rocks from several regions worldwide. In contrast, piezometers for other minerals that are commonly dynamically recrystallized in mantle and lower crustal rocks, including orthopyroxene and clinopyroxene, are poorly constrained. A single attempt to quantify the piezometer for orthopyroxene experimentally was conducted by Ross & Nielsen (1978). This piezometer yields a stress (σ)–grain size (*d*) relationship of $\sigma = 9219d^{(-1.1765)}$ and predicts that orthopyroxene grain sizes will be larger than olivine at high stresses. Observations from natural rocks, however, show the opposite relationship: orthopyroxene recrystallized grain sizes are smaller than olivine at high stresses. Interpretation of experimental results is complicated by chemical gradients in natural orthopyroxene that are not associated with synthetic compositions. Additionally, the Ross & Nielsen (1978) experiments were conducted using talc as a confining medium, which induces significant friction along the margins of the sample and significantly affects the accuracy of the stress measurements.

This study explores the stress–grain size relationship between dynamically recrystallized orthopyroxene and olivine in *naturally-deformed* peridotites derived from a wide range of pressure–temperature conditions. We identify and measure orthopyroxene and olivine grains within each sample that appear to have recrystallized under identical stress conditions, but that are well segregated and not mixed. Differential stress is estimated using the existing, well constrained olivine piezometer. This allows us to establish a stress–grain size relationship for orthopyroxene. Our naturally-constrained orthopyroxene piezometer ($\sigma = 406.75d^{(-.5211)}$) predicts that recrystallized grains in orthopyroxene are smaller than olivine at stresses above ~25 MPa (~200 μm), and larger than olivine for stresses below this value. This piezometer can be used to estimate stress magnitudes in rocks in which orthopyroxene is one of the primary recrystallized phases, including granulites, pyroxenites and other mantle/lower crustal rocks in which olivine or plagioclase are unsuitable.

Keywords: orthopyroxene, olivine, dynamic recrystallization, paleopiezometer, lithospheric mantle

SETP-32

Elasticity of Single-Crystal Ferropericlase across the Spin Transition of Iron Investigated by Brillouin and Impulsive Spectroscopies

Tong, X.[1], Yang, J.[1], Lin, J.[1]
dennistong1987@gmail.com
1. Jackson School of Geosciences, The University of Texas at Austin, Austin, TX

Understanding the effect of the electronic spin transition of the iron on the elasticity of the lower-mantle ferropericlase (Mg,Fe)O is critical in our understanding of the seismic velocity structures of the Earth's lower mantle. Previous studies have reported inconsistent results about the elastic behavior of ferropericlase across the spin transition--- ISLS results showed that the spin transition is associated with softening of all elastic moduli by as much as 25% between 40 and 50 GPa (Crowhurst et al., 2008), whereas Brillouin spectroscopic studies revealed an increase in shear wave anisotropy across the transition. Inelastic X-ray scattering results, on the other hand, did not show any visible effects of the spin transition. To decipher the elasticity of the lower-mantle ferropericlase within the spin transition and in the low-spin state, we have used both Brillouin Light Scattering (BLS; sensitive to Vs) and Impulsive Stimulated Light Scattering (ISLS; sensitive to Vp) techniques to simultaneously measure the shear wave (BLS) and compressional wave (ISLS) velocities of a single-crystal ferropericlase in a high-pressure diamond anvil cell. Together with X-ray diffraction analyses, our results reveal various magnitudes of the effects of the spin transition on elastic moduli as well as Vp/Vs anisotropies of ferropericlase. These experimental results are used in thermal elastic modeling to address potential geophysical consequences of the spin transition in the lower mantle.

Keywords: Mineral physics, High-pressure behavior, Elasticity and anelasticity, Instruments and techniques, Earth mantle, Spin transition, Geophysics

SETP-33

Extensional collapse of orogens

Wu, G.[1], Lavier L.L.[1], Choi, E.[2]
glwu@utexas.edu
1. Jackson School of Geosciences, The University of Texas at Austin, Austin, TX, 78712
2. Center for Earthquake and Information, University of Memphis, Memphis, TN 38152

Lithospheric extension commonly initiates in orogens either trailing or many eons after the end of orogeny. Using thermo-mechanical models constrained by geological and geophysical observations, we studied extensional collapse of orogens. Assuming a weak mid-crustal shear zone strengthens over time due to cooling and annealing, we showed that variable intensities of decoupling induced by the shear zone between upper and middle crust of variable strength can generate a wide range of extensional structures. Simulations of young orogens with weak to strong ductile middle crust predict three modes of extension dominated by middle crustal extrusion, detachment faults and metamorphic core complexes formation, and upper crustal thinning, respectively. Simulations of old orogens instead predict core complex, diffusive and localized rift mode.

We found that core complexes and detachment faults are natural products of gravity driven middle crustal extrusion and exhumation and strong crustal decoupling along the preexisting shear zones in a favorable state of stress in collapsing orogens. Based on our numerical simulations and previous geological and geophysical observations, we categorized core complexes into four groups: i) massifs, ii) single large asymmetric core complex (classic core complex), iii) multiple less evolved core complexes, and iv) subsurface 'core complex'. We also recognized three types of detachment systems, each of which corresponds to unique styles of hanging wall normal faults as well as geological and geophysical conditions.

Depth-dependent stretching, middle crustal flow and regional stress rotation are critical for the unique styles of extension in collapsing orogens and evolution of core complexes and detachment faults. Our models consistently predict diverse geological and geophysical observations in young Cenozoic/Mesozoic orogens such as US Cordillera, the Aegean, and Papua New Guinea as well as old Caledonian to Variscan orogens along the North Atlantic margins.

Keywords: extensional collapse, core complexes, detachment faults, state of stress, crustal flow, mantle flow, lithospheric compensation

SETP-34

Single-Crystal Elasticity of the Deep-Mantle Magnesite at High Pressure and Temperature

Jing Yang[1], Zhu Mao[1, 2], Jung-Fu Lin[1], Vitali B. Prakapenka[3]
1. Jackson School of Geosciences, The University of Texas at Austin, Austin, TX
2. Laboratory of Seismology and Physics of Earth's Interior, School of Earth and Planetary Sciences, University of Science and Technology of China, Hefei, Anhui, China
3. GeoSoilEnviroCARS, The University of Chicago, Chicago, IL 60637, USA

Magnesite is believed to be a major candidate carbon host in the Earth's mantle. Studying thermal elastic properties of magnesite under relevant high pressure-temperature conditions of the mantle is thus important for our understanding of the deep-carbon storage. Thus far, the elasticity of magnesite has only been reported at ambient condition. Here we have conducted Brillouin light scattering measurements on the compressional wave (V_P) and shear wave (V_S) velocities of single-crystal magnesite in a high pressure-temperature diamond anvil cell (DAC) at relevant conditions of the Earth's mantle. Based on the experimentally-measured velocities, we have derived full elastic constants and have modeled the elasticity and elastic anisotropies of magnesite at expected upper-mantle *P-T* conditions. These results are important for our understanding of the potential effects of magnesite carbonate on the seismic profiles and seismic anisotropies in the carbonated eclogite and peridotite in the upper mantle and a subducting slab. Here we have applied the experimental results and modeled velocity profiles and seismic anisotropies to provide mineral physics references and constrains for seismic detections of potentially carbonated regions in the Earth's interior.

Keywords: single-crystal elasticity, magnesite, high pressure-temperature, Brillouin scattering, deep carbon

SHP-1

Helium enrichment during convective carbon dioxide dissolution

Akhbari, D.[1], Hesse, M.[1], Larson, T.[1]
daria.akhbari@gmail.com
1. Jackson School of Geosciences, The University of Texas at Austin, Austin, TX

Geological carbon dioxide (CO_2) storage is a means of reducing anthropogenic emissions. Dissolution of CO_2 into the brine, resulting in stable stratification, increases long-term storage security. The dissolution rate is determined by convection in the brine driven by the increase of brine density with CO_2 saturation. The rate of CO_2 dissolution is determined by mass transfer and hence the rate of convective overturn. Recent experimental work has constrained the magnitude of the convective flux in systems with constant density change.

This work focuses on two new aspects of convective CO_2 dissolution. First, we consider a closed system, where continued dissolution leads to a decline of the pressure in the CO_2 gas-cap that in turn reduces the density difference that drives the convection. The convective dissolution rate in closed systems is therefore not constant. We present experiments with both convective and purely diffusive mass transfer. Second, we study the evolution of the gas composition due to preferential partitioning of different gas components. The aim of these studies is to develop a framework to infer the amount of gas dissolved from compositional changes, in particular in noble gases.

Batch experiments were carried on in two cells with different volumes, 1239 mL and 4.25 mL. Each cell was initially filled with water, and the headspace was pressurized with CO_2 gas. Two different cells allowed us to observe the effects of convection on the CO_2 dissolution into the water. The results of these experiments verify the significant effect of convection on the CO_2 dissolution. Furthermore, comparison of the laboratory experiments and model simulation suggests a further investigation to determine the diffusion constant of CO_2 in water. Moreover, a new parameter, η, was defined to express the effect of top boundary condition on the CO_2 dissolution. The experimental results verified that the equilibrium pressure could be predicted based upon specific η of each experiment.

Besides, the experimental design allows for continuous measurement of headspace pressure as well as timed interval measurements of the CO_2/Helium (He) ratios and the $\delta^{13}C$ value of CO_2 in the headspace. Dissolution experiments were conducted for 2 systems. 1) Pure He system, and 2) 97% CO_2 and 3% He system. The final equilibrated experimental results were compared to theoretical results obtained using Henry's Law relationships. The evolution of the amount of dissolved CO_2 computed from gas pressure and gas compositions are in good agreement with Henry's Law relationships. Measured He/CO_2 ratios throughout the CO_2+He experiment preserve a non-linear trend of increasing He/CO_2 ratios through time that correlate very well with the measured pressure drop from CO_2 dissolution. This indicates that gas composition, in particular the He/CO_2 ratio, can be used to infer the amount of dissolved CO_2 in the field where pressure evolution is not available. The results of this study will be applied to the filed data from Bravo dome, New Mexico, to estimate the initial pressure in the reservoir.

Keywords: Convective dissolution, Henry's law, CO_2 capture and storage, Stable isotope geochemistry.

SHP-2

Revisiting the Utility of Hummocky Cross-Stratification in Paleohydraulic Study of Ancient Shelves and Sand Distribution Processes

Arora, K. [1], Wood, L.[1]
khushbooarora@utexas.edu
lesli.wood@beg.utexas.edu
1. Bureau of Economic Geology, Jackson School of Geosciences, The University of Texas at Austin, Austin, TX

Cretaceous-age shelf sands form some of the most prolific hydrocarbon reservoirs in the world. However, the processes responsible for transporting sands across ancient shelves, and concentrating and reworking them into quality reservoirs are poorly understood. Shelf sand deposits are often characterized by hummocky cross-stratification (HCS) and associated wave ripples (WR), which through the concepts of Airy-wave Theory, are shown to indicate the nature and magnitude of processes responsible for their deposition. Morphometric data on these bedforms can be used to estimate wave characteristics and the water depth at which these bedforms deposited, allowing for a reconstruction of conditions along paleo-shelves.

Two example localities illustrate the process and applicability of these analyses; Cape Sebastian Sandstone (CSS) in southwestern Oregon and Tocito Lentil of the Mancos Shale (TL) in southeastern San Juan Basin, New Mexico, both marine transgressive deposits of Late Cretaceous age. Field studies were done to quantify the detailed architecture of HCS and WR in these units. The HCS sands of CSS are thick, amalgamated and show few preserved hummocks. TL HCS are much muddier, and show mm-scale laminae of mud between thicker sands. HCS wavelengths in the CSS range from 2-3 meters and bed thicknesses vary from 30-40 cm. HCS beds in the TL vary in thickness from 15-30 cm with low-amplitude preserved hummocks exhibiting wavelengths from 2.5-3.5 m. HCS grain sizes are fL-fU in CSS but slightly coarser fU-mL in the TL. Calculation using WR show deeper waters of deposition for the TL (80±20 m) compared to CSS (65±15 m). Higher percentage of mud and low-amplitude larger wavelengths hummocks in the TL are supported by the deeper water setting compared to the CSS. These results suggest HCS are formed by long-period (25-42 sec) waves with heights of 1-3 m. Estimated wave periods for HCS deposition in both locations are higher than that of modern storms suggesting existence of universally higher intensity storms during the Late Cretaceous period leading to development of thick HCS deposits. Larger magnitude storms may indicate more regionally extensive backflow of bottom waters leading to a wider distribution of sands across the shelf and out into deeper waters. In addition, stronger storm and deepening storm wave base leads to more extensive reworking and subsequent concentration of higher quality sands further out onto the shelf.

Keywords: Hummocky cross-stratification, shelf sands, paleo-reconstruction, storm beds

SHP-3

New Models of Valanginian sand breaching reef margin in the eastern Gulf of Mexico

Bovay, C.[1], Snedden, J.[1], Steel, R.[2], Ganey-Curry, P.[1], Whiteaker, T.[1], Sanford, J.[1]
cbovay@utexas.edu
1. Institute for Geophysics, Jackson School of Geosciences, The University of Texas at Austin, Austin, TX
2. Department of Geological Sciences, Jackson School of Geosciences, The University of Texas at Austin, Austin, TX

The Gulf of Mexico (GOM) basin is one of the earth's most productive hydrocarbon basins, yet much is still to be learned about early Cretaceous siliciclastic deposits in the eastern portion of the basin. In particular, the Valanginian stage (133.9 to 139.4 ma) is critical for deep-water exploration as it encompasses the end of GOM sea-floor spreading and the subsequent tectonic reorganization and erosion of onshore structures like the Ocala and Peninsular arches, which in turn generated terrigenous material transported into the basin.

Utilizing 35,000 km of depth-converted 2-D seismic data, wireline well logs, and cores, I will map the 10-12 sequence stratigraphic surfaces in the Valanginian Hosston (Travis Peak) Formation in the eastern Gulf of Mexico and differentiate the siliciclastic deposits from the overlying carbonate Sligo (Pettet) Formation. Current mapping suggests two breaches in coeval reef margins where the Valanginian sands enter the deep-water, a hypothesis that will be tested with detailed seismic and log analysis. Challenges foreseen include demarcating the previously undefined Sligo-Hosston contact and differentiating a lowstand basal sequence set from the main Valanginian highstand/transgressive sequence set. Illuminating the deep-water reservoir architecture could lead to understanding the source of clastic input. Analysis of the deep-water Valanginian will yield a better understanding of the evolution of the GOM basin in the Mesozoic and may identify viable deep-water sandstone trends for hydrocarbon exploration.

Keywords: Valanginian, Hosston, Travis Peak, Gulf of Mexico, Mesozoic, Cretaceous, mixed-input, deep-water

SHP-4

Nutrient Cycling in the Bank Hyporheic Zone of the Regulated Lower Colorado River, Austin, Texas

Briody, A.[1], Cardenas, M.B.[1], Bennett, P.C. [1]
Alyse22@gmail.com
1. Jackson School of Geosciences, The University of Texas at Austin, Austin, TX

Periodic releases from an upstream dam cause rapid stage fluctuations in the Colorado River near Austin, Texas. These daily pulses modulate fluid exchange and residence times in the hyporheic region, where biogeochemical reactions have been found to be more pronounced. We have installed two transects of wells perpendicular to the river in order to further examine the reactions occurring in this zone of surface-water and groundwater exchange. One well transect records physical water level fluctuations and allows us to map hydraulic head gradients and fluid movement. The second transect allows for water sample collection at three discrete depths. Samples were collected from 12 wells every other hour for 24-hours and were analyzed for nutrients, carbon, major ions, and stable isotopes. The results provide a detailed picture of biogeochemical processes in the bank environment during low flow/drought conditions in a regulated river.

Keywords: hyporheic exchange, groundwater/surface-water interactions, regulated rivers

SHP, SETP-5

Andean Exhumation and Growth of the Subandean-Chaco Foreland Basin, Southern Bolivia: Improved Age Control and Provenance Record

Calle, A.Z. [1,], Horton, B.K.[1]
azcallep@utexas.edu
1. Department of Geological Sciences and Institute for Geophysics, Jackson School of Geosciences, The University of Texas at Austin, Austin, TX

Evolution of the Neogene Subandean fold-thrust belt since its inception along the eastern margin of the Central Andes of Bolivia has dictated petroleum systems in the Subandes and adjacent Chaco foreland basin. Few studies have assessed the linkages among surface processes and threshold responses to climate change, tectonics, and/or drainage-catchment modification in this thin-skinned fold-thrust belt and coupled foreland basin. Analyses of stratigraphic variations in the <3 km-thick Cenozoic nonmarine succession of the westernmost Subandean zone (Bartolo and Emborozú sections) indicate a major provenance shift and progressive transition from distal fluvial to proximal megafan deposition (Petaca, Tariquia, Guandacay and Emborozú formations). Sediment provenance results from paleocurrents, sandstone petrography, and conglomerate clast compositions indicate a dramatic shift in source areas. A pronounced early Miocene reversal from west-directed to east-directed paleoflow is accompanied by upward coarsening and a shift from quartzose sand rich in feldspar derived principally from the Brazilian shield to lithic-rich sandstones recycled from the Andean orogen. Conglomerate compositions in the upper part of the section further reveal the progressive introduction of diagnostic clasts reflecting unroofing of hinterland sources: Eastern Cordillera (Ordovician), Interandean zone (Devonian and younger), and Subandean zone (Carboniferous and younger). In turn, zircon U-Pb provenance results for Cenozoic basin fill reveal (1) Neoproterozoic (680-540 Ma) and (2) Sunsás-Grenville (1200-1000 Ma) age populations consistent with uplifted hinterland sources of widely distributed Ordovician rocks dominating the Eastern Cordillera, with upsection appearances of (3) Famatinian-Ocloyic ages (490-440 Ma) attributable to middle to late Miocene initiation of shortening involving Silurian–Cretaceous rocks of the Interandean and Subandean zones and (4) limited Cenozoic (<25 Ma) ages derived from the Andean magmatic arc.

New and published zircon U-Pb data for interbedded volcanic tuffs (20.8 ± 0.4, 7.4 ± 0.2, 3.8 ± 0.1 Ma) and magnetostratigraphic results within studied Subandean sections (Bartolo, Camiri, Emborozú, and Villamontes) provide improved constraints on depositional patterns, accumulation rates, and major provenance shifts. Regionally, the Neogene accumulation history shows a gradually subsiding basin until ~7-8 Ma followed by a pulse of rapid sedimentation which may reflect hinterland plateau uplift and/or climate change. High accumulation rates after 6 Ma are interpreted for proximal alluvial-fan facies and their distal counterparts within the Chaco basin. Evidence for the introduction of progressively younger rocks in the sediment source areas, as documented by conglomerate counts and detrital zircon age populations, lead us to interpret (1) protracted unroofing and sediment dispersal from the Eastern Cordillera–Interandean Zone commencing at ~20-15 Ma (as estimated from new tuff ages and accumulation rates) followed by (2) initial propagation of the deformation front into the Subandean Zone during the late Miocene. A temporal shift from axial to transverse fluvial drainage recorded by paleocurrent data reinforces evidence for an eastward advancing depocenter and structural partitioning of the older segments of the Subandean-Chaco foreland basin, particularly from 8 Ma to present.

Keywords: Subandean, provenance, Andean propagation

SHP (WITHDRAWN)

Experimental Meanders on Mars

Cleveland, J.[1], Kim, W.[1]
jclev24@yahoo.com
1. Jackson School of Geosciences, The University of Texas at Austin, Austin, TX

The existence of Martian sinuous channels is perplexing and far from easily explainable. Although these meander patterns are analogous to those observed on Earth, their developmental processes may differ significantly. This, of course, is stated under the assumption that, on Earth, where vegetation is existent, roots are capable of developing mesh-like networks that can successfully hold sediment within channel banks in a cohesive manner. When channel-bank cohesion is achieved to a significant extent, it is adequate to maintain a strong single-thread channel while letting the outer bank erode, allowing the channel to laterally migrate. However, what additional factor(s) can mimic the potential cohesive power of vegetation on a planet that lacks evidence of substantial, if any, organic activity? Possible explanations include, but are not necessarily limited to; clays, lava flows, microbial crusts, ice, and chemical precipitates. This particular experimental hypothesis lays faith in the potential of chemical precipitation, specifically that of carbonates. Carbonate precipitation serves as the Martian analogue to the vegetation effects on Earth, as its crystalline form is capable of sediment-cohesion.

Recent evidence from NASA, provided via the *Mars Reconnaissance Orbiter*, details near-infrared spectral characteristics that suggest the presence of magnesium carbonate in the graben-dominated Nili Fossae impact basin of the planet. The evidence of the presence of carbonates on Mars satisfies the basic requirement in respect to the speculation of carbonate precipitation as a mechanism to create meandering channels.

The carbonate precipitation mechanism is dependent upon three essential factors; (1) Increase in pH (Basic Solution), (2) Increase in Temperature, and (3) Degassing of CO2 (g). Based on the evidence of Mars' ancient history of volcanic and hydrothermal activity, including the presence of carbonate-saturated, basic solutions, these factors would have been successfully achieved. As super-heated, carbonate-saturated solutions flowed over surface sediment, CO2 (g) would have readily evaporated to the atmosphere. We present the initial flume experiments with and without carbonate precipitation processes in the experiments. The carbonate experiment controls the factors described above and allows for examining the causes of channel bank stability by varying carbonate precipitation conditions. Experiments with carbonate precipitation gradually organized flows into a strong sinuous channel while experiments utilizing clear water without carbonate precipitation processes developed a fully braided fluvial system. The current experiments suggest a possible mechanism to develop meandering channels on Mars without cohesion associated with vegetation.

Keywords: Mars, Meander, Channel, Carbonate, Cohesion, pH, Precipitation, NASA, Mars Reconnaissance Orbiter, Mars Exploration Rover

SHP-6

Characterization of Turbidites and Detrital Zircon Provenance of Sediments Deposited in the Miocene to Pliocene Gulf of California Exposed within Split Mountain Gorge, Southern California

Cloos, Michael.[1], Steel, Ronald.[1], Stockli, Daniel[1]
michael.cloos@utexas.edu
1. Jackson School of Geosciences, The University of Texas at Austin, Austin, TX

Split Mountain Gorge within the Fish Creek-Vallecito Basin of southern California exposes a record of sedimentation associated with the opening of the Gulf of California during the late Miocene to Pliocene.This study will focus on the deposition of the Wind Caves turbidites and also on detrital zircon provenance of the Miocene to Pliocene sedimentary units exposed at Split Mountain Gorge. The Wind Caves turbidites (a member of the Miocene to Pliocene Latrania formation) have previously been thought to have been sourced from local fluvial systems in the basal section with a shift in sediment source reflecting input from the Colorado River later in the section. Field study involving measurement of ~600 meters of section has shown that depositional style changes from graded, thick beds lower in the section to thin, more laterally extensive, finer grained beds toward the top of the section. It is hypothesized that this facies change upsection is a result of the burial of chaotic topography previously generated by emplacement of a mass transport deposit. Also possibly influencing depositional style is the integration of a larger fluvial system at some point during Wind Caves deposition. Detrital zircon U-Pb and (U-Th)/He data from sandstone samples (n=15) show a dramatic change in age populations occurring during Wind Caves deposition. Samples from early in the section (Miocene Red Rock formation fluvial and Lycium member of the Latrania formation turbidite deposits) have prominent U-Pb age peaks around 75 and 95 Ma, likely having been shed by the Peninsular Range batholith and transported to the early gulf by local streams. Upper Wind Caves and later deposits display a more diverse suite of zircon ages ranging from Proterozoic to Miocene and are consistant with the hypothesis that the later sedimentary input was brought in by a river with a larger drainage basin (such as the Colorado River) after having been eroded from diverse terranes across the Western US.

Keywords: Detrital zircon provenance, turbidites, Colorado River, Gulf of California

SHP-7

Warming of marine methane hydrates: when does free gas venting occur?

Darnell, K. N.[1,2], Flemings, P. B.[1,2], and Bryant, S. L.[3]
kdarnell@utexas.edu
1. Jackson School of Geosciences, The University of Texas at Austin, Austin, TX
2. Institute for Geophysics, The University of Texas at Austin, Austin, TX
3. Petroleum and Geosystems Engineering, The University of Texas at Austin, Austin, TX

Warming of marine methane hydrate bearing sediment may destabilize hydrate deposits leading to free gas venting. This is clearly the case when none of the sediment column is within the hydrate stability zone after the forcing. However, our findings suggest that free gas venting can occur under forcing less than this extreme warming. The venting occurs in transient pulses as result of the nonlinear thermodynamics. A salinity-driven three-phase front propagates upward, eventually dissipating and leading to a more, shallow hydrate deposit with some loss of mass during its dynamic adjustment. We present numerical simulations of multiphase, dynamic fluid flow that illustrate this new behavior.

Keywords: gas hydrates, numerical modeling, arctic climate change

SHP-8

The efficiency of storm water management structures, rain gardens and vegetated retention ponds, in reducing urban runoff and contaminants in downtown Austin, Texas

Eljuri, A.[1] , Moffett, K.B.[1]
ageljuri@sbcglobal.net
1. Jackson School of Geosciences, The University of Texas at Austin, Austin, TX

Rain gardens and retention ponds are intended to reduce storm water and pollutant runoff to rivers and streams, rain gardens by enhancing infiltration and retention ponds by promoting evaporation. The City of Austin, Texas is actively investing money and time into these storm water management solutions, but there are no data comparing their effectiveness. In particular, comparisons of rain gardens against control plots and new wetland-vegetated retention pond designs against traditional grassy pond designs are lacking. This study quantifies the quantity of storm runoff to and from five sites: three engineered sites, two rain gardens receiving direct runoff from the same residential roof and a planted retention pond receiving municipal parking lot runoff, and two control sites, a mulched residential lawn receiving direct roof runoff and a grassy municipal retention pond receiving parking lot runoff. A locally installed rain gauge monitors precipitation rates and soil moisture sensors at 10 cm, 22 cm, and 44 cm depth are used to monitor changes in soil moisture profiles over time. Evapotranspiration rates were determined using local meteorological data and stomatal conductance measurements at the sites. Infiltrometer tests, soil characterizations, and vegetation surveys were also conducted at each site. The soil at the rain gardens are highly mixed with pebbles at the top and become a more uniform soil towards the bottom of the root zone. This differs from the control site where the soil is uniform except for the thin layer of wood chips at the surface. Austin summers experience fewer rainy days than the spring, fall, and winter, but summer storms are usually high-intensity and short-duration, increasing the potential for flooding. Seasonally, rainfall is somewhat more concentrated around May and October. The rain garden sites shows a faster drying rate at shallow depths compared to deeper depths while the control rain garden dries at a slower rate evenly throughout the soil column. The vegetated retention pond also exhibits a drying curve after a rain event, but the control retention pond remains close to the max volumetric water content during the same drying period. These field data are compiled into a GIS study comparing different possible distributions of future rain gardens and vegetated retention ponds across the city to reduce storm runoff to local creeks, which provide much needed data and analysis to support decision making regarding these green storm water management solutions in central Texas.

Keywords: Hydrology, Urban Storm Water Management

SHP-9

The Response of a Mountain Channel to Bed Disruption

Ferre, M.[1], Johnson, J.[1]
megan.ferre@utexas.edu
1. Jackson School of Geosciences, The University of Texas at Austin, Austin, TX

This study attempts to quantify the response of a mountain channel to bed disruption using a flume 4m long by 0.1m wide. A stable bed condition is reached by running water at a controlled discharge rate through the flume until the amount of sediment output stabilizes at a low background quantity. Next, the surface of the bed is disrupted at 2cm grid spacing over a central portion of the flume. Finally, stable bed conditions are attempted once again by running water through the flume until the amount of sediment output restabilizes. Data is collected while water is running using a high speed video camera to visually track sediment output. Also measured are topographic profiles, flow depth, weight of sediment output, and surficial grain size distribution. A terrestrial laser scanner is used to track the changes between successive beds: initially stable, disrupted, and the final stable result. Current analysis shows that sediment output during bed steadying events occurs steadily with intermittent "bursts" that result from a weakness and subsequent release of sediment somewhere along the channel bed.

Keywords: flume, mountain channel, disruption, terrestrial laser scanner

SHP-10

Soil moisture dynamics of grasslands in response to CO_2 and biodiversity manipulations at BioCON

Raquel H. Flinker[1], M. Bayani Cardenas[1], Todd G. Caldwell[2], Roy L. Rich[3], Peter B. Reich[3], Gerald Flerchinger[4]
raquelflinker@gmail.com
1. Geological Sciences, The University of Texas at Austin
2. Bureau of Economic Geology, The University of Texas at Austin
3. Department of Forest Resources, University of Minnesota
4. Agricultural Research Service, United States Department of Agriculture

Our ability to model soil moisture variation with changes in plant cover and increasing atmospheric CO_2 concentrations can enhance our knowledge and decision making in the field of agriculture and water resources. Free-air CO_2 Enrichment (FACE) experiments have been conducted for a number of years in different countries with the focus of understanding how plant communities, soil respiration and microbes respond to increases in atmospheric CO_2 concentrations. Minimal work has been done on the hydrologic aspects of these experiments which can be valuable for investigating global warming effects on local and plot-scale ecohydrology.

The BioCON (Biodiversity, CO_2 and N) experiment is a Free-Air CO_2 Enrichment (FACE) experiment that investigates plant community response to three key environmental variables: nitrogen, atmospheric CO_2 and biodiversity. It is operated by the University of Minnesota and is located within the Cedar Creek Ecosystem Science Reserve in Minnesota, USA. The objective of this work was to characterize and model unsaturated flow for different CO_2 and biodiversity manipulations at BioCON in order to see how they affect soil moisture dynamics and groundwater recharge.

We simulated soil moisture over time for the site using the Simultaneous Heat and Water (SHAW) model. SHAW is a finite-difference 1-D heat transport and water flow model for the soil-plant-atmosphere continuum. It solves the Richards equation for water flow in the unsaturated zone. Soil properties (texture, unsaturated hydraulic conductivity and moisture retention) were measured and used as inputs to the model.

Our results show that the soil at BioCON is a homogeneous sand. This was helpful for conducting the simulations. SHAW worked very well for this site and allowed for scrutiny of soil moisture dynamics. Soil moisture at locations containing grasses seemed to be higher when atmospheric CO_2 was elevated. This could be a result of higher plant water use efficiency at higher atmospheric CO_2 concentrations.

Keywords: Free-air CO_2 Enrichment (FACE), soil moisture, SHAW model, biodiversity

SHP-11

Peculiar deepwater slope morphology in the semi-enclosed Mio-Pliocene Dacian Basin, Romania

Fongngern, R.[1], Steel, R.[1], Olariu C.[1], Krezsek C.[2]
RattanapornF@utexas.edu
1. Jackson School of Geosciences, The University of Texas at Austin, Austin, TX
2. OMV Petrom S.A., Exploration and Production, Bucharest, Romania

Shelf margin clinoforms (400-500 m high) are the prominent building blocks of the Mio-Pliocene (8.5-4.1 Ma) Western Dacian Basin, a foreland of the Southern Carpathians of Romania. The Dacian Basin was a semi-enclosed elongate, para-Tethyan seaway that underwent several brackish to freshwater transitions while being connected to the Black Sea. Well and 3-D seismic data show that the basin infill was dominated by coeval multidirectional clinoform progradation, dominantly from NE to SW and from SSE to NNW. The deepwater clinoform slopes were spectacularly irregular, with closely spaced canyons and channel-levee systems giving a 'sawtooth' appearance in both strike sections and horizontal slices. The canyons are approximately 1-2.5 km wide, 50-200 m deep and normally host slope channels. Slope channels range in width from 100-900 m and depth from 25 to 50 m. Most slope channels connected to an indented (valleyed or upper- slope scarred) shelf edge. The irregularity of the slope morphology differs from most open marine slopes which can be irregular downdip of the main shelf-edge fairway but become smoother laterally from the transport axis. It is likely that line-sourced hyperpycnal flows from multiple steep, Carpathian shelf-edge rivers were responsible for building and maintaining the unusual slope stratigraphy. The high frequency of river-flood underflows that would have been generated in the reduced salinity Dacian Basin also caused large volumes of river-derived sediments to be transported to the aggradational basin floor. Additional processes that might have contributed to the unusual slope stratigraphy is slope failure due to instability that could remove substantial amount of sediment from the clinoform foresets and deposit on the bottomsets as well.

Keywords: Clinoforms, slope channels/canyons, hyperpycnal flows, lake

SHP-12

Improved Geothermal Heat Flux Estimates for East Antarctic Subglacial Basins from Groundwater Modeling and Geophysical Observations

Gooch, B.[1, 2], Frederick, B.[1, 2], Richter, T.[2], Young, D.[2], Blankenship, D.[2]
bgooch@utexas.edu
1. Jackson School of Geosciences, The University of Texas at Austin, Austin, TX
2. University of Texas Institute for Geophysics, Austin, TX

Few studies have documented the capability of groundwater (GW) flux to affect the geothermal heat (GH) flow at the base of ice sheets. We investigate such an effect coupled to potentially elevated GH flow values due to anomalously higher radiogenic heat production from cratonic rocks hypothesized in a region under the East Antarctic Ice Sheet (EAIS). We show that for even small GW fluxes and elevated GH production values, ice-sediment interface GH flow values can be significantly higher than currently predicted. The 1D model results show even with low permeabilities, GW can greatly affect the basal heat flow. The 2D model results show that under the EAIS GW can alter the basal heat fluxes by ~10's (100's?) of mW/m^2 and elevated GH production values can raise the basal heat fluxes by ~10's of mW/m^2. Ice sheet models need to incorporate these effects in future simulations.

Keywords: Ice Sheets, Antarctica, Heat Flow, Groundwater, Numerical Modeling

SHP-13

Armor Development from Decapitated Flash Flood Bores in Supply-Limited Flume Experiments

Goodwin, K.[1], Rhodes, R.[2], Johnson, J.[1]
1. Jackson School of Geosciences, The University of Texas at Austin, Austin, TX
2. State University of New York, Brockport

In rivers assumed to have quasi-normal flow, three main processes have been used to explain bed surface armoring: i) selective entrainment and transport of smaller grains, ii) limited supply of smaller grain sizes, and iii) equal mobility of grains of different sizes, which develops through natural feedbacks such that larger, less inherently mobile grains are enriched on the surface relative to smaller grains. Flash flood-dominated river channels in arid environments often completely lack surface armoring, yet it is unclear whether increased sediment supply or transport of all grain sizes prevents armor development. In order to examine armor development in an end-member case of non-normal flow, we conducted a series of laboratory experiments using flash flood bores. The flume is 33.5 m long, 0.5 m wide, 0.8 m tall, and capable of creating reproducible flood bores by raising a high-speed computerized lift gate and releasing impounded water. For each experiment, the gate was quickly lowered as soon as the flood bore traveled the length of the flume, "decapitating" the bore from subsequent flow, to better isolate the effects of the bore alone on entrainment and transport. Sediment was not fed into the upstream end of the flume and only sourced from the gravel bed (2 mm to 40 mm), resulting in supply-limited experimental conditions. In response to repeated flood bores, the surface grain size distribution rapidly coarsened. We interpret that kinetic sieving was the dominant cause of surface armoring in these experiments. LiDAR scans of the bed topography from before and after each bore show increased surface roughness due to grain size changes, but small surface elevation changes due to relatively limited erosion. Digital gravelometry from photographs taken after each bore show increased armoring, while sediment transported out the downstream end of the flume tended to be as coarse or coarser than the bed surface. Travel distances of three sizes of RFID-tagged tracer clasts show that the largest particles were transported farthest, while the smallest particles were preferentially buried under the surface. In these experiments, the bores disrupt the bed surface and entrain grains of every size class so that the smallest size fraction is able to fall in between the larger grains, coarsening the surface and preventing the smallest grains from being transported. While the combination of decapitated bores and supply-limited gravel sizes do not directly mimic natural channel conditions, our experimental design uniquely isolates the effects of bores on transport and grain sorting. They also suggest that transport of all grain sizes is not the primary control on armoring in natural flash flood-dominated channels. Future experiments will investigate the role of sand supply on armoring and transport in flash flood bores.

Keywords: Sediment Transport, Armor Layer, Sorting, Flash Floods, LiDAR

SHP-14

Characterizing coarse bedload transport during floods with RFID and accelerometer tracers, in-stream RFID antennas and HEC-RAS modeling

Olinde, L.[1], Johnson, J.P.[1]
lindsayolinde@utexas.edu
1. Jackson School of Geosciences, The University of Texas at Austin, Austin, TX

By monitoring the transport timing and distances of tracer grains in a steep mountains stream, we collected data that can constrain numerical bedload transport models considered for these systems. We captured bedload activity during a weeks-spanning snowmelt period in Reynolds Creek, Idaho by deploying Radio Frequency Identification (RFID) and accelerometer embedded tracers with in-stream stationary RFID antennas. During transport events, RFID dataloggers recorded the times when tracers passed over stationary antennas. The accelerometer tracers also logged x, y, z-axis accelerations every 10 minutes to identify times of motion and rest. After snowmelt flows receded, we found tracers with mobile antennas and surveyed their positions. We know the timing and tracer locations when accelerometer tracers were initially entrained, passed stationary antennas, and were finally deposited at the surveyed locations. The fraction of moving accelerometers over time correlates well with discharge. Comparisons of the transported tracer fraction between rising and falling limbs over multiple flood peaks suggest that some degree of clockwise hysteresis persisted during the snowmelt period. Additionally, we apply accelerometer transport durations and displacement distances to calculate minimum virtual velocities over full tracer path lengths and over lengths between initial locations to stationary antennas as well as between stationary antennas to final positions. The accelerometer-based virtual velocities are significantly faster than those estimated from traditional tracer methods that estimate bedload transport durations by assuming threshold flow conditions. We also subsample the motion data to calculate how virtual velocities change over the measurement intervals. Regressions of these relations are in turn used to extrapolate virtual velocities at smaller sampling timescales. Maximum average hop lengths are also evaluated for each accelerometer tracer. Finally, flow conditions during the snowmelt hydrograph are modeled over the 11 kilometers of surveyed stream by utilizing 1m airborne LiDAR and HEC-GeoRAS. Cross-sectional HEC-RAS results are used to estimate the spatial distribution of longitudinal shear velocities over the observed discharges. At final accelerometer tracer positions, we analyze the HEC-RAS generated flow conditions for each disentrainment discharge magnitude. The techniques developed here have the potential to link individual grain characteristics during floods to a range of time and length scales.

Keywords: coarse bedload transport, stream monitoring, mountain channels, flow modeling, RFID tracers, and accelerometer tracers

SHP-15

A field examination of the impacts of hydropeaking on downstream surface water/groundwater interactions.

Kaufman, M.[1]
mhkaufman@utexas.edu
1. Jackson School of Geosciences, The University of Texas at Austin, Austin, TX

Hydropeaking is a process where hydroelectric dams are throttled to meet variable demand for electric power. This induces a typically diel fluctuation in river discharge downstream of the dams. In order to determine whether or not these dam operation regimes impact surface water/groundwater interactions, we constructed 7 monitoring wells on the bank of the Colorado River approximately 15km downstream of Austin, TX. Over a period of 44 hours, we monitored water table elevation, stream gauge height, river temperature, and groundwater temperature with 5-minute resolution. The results of this field study show periodic diel fluctuations in all of the monitored aspects of the system, indicating that hydropeaking dams can exert strong influences on the downstream interactions between surface water and groundwater.

Keywords: hydropeaking, surface water/groundwater interaction, hydrology, riparian

SHP-16

Characterizing heterogeneous coastal groundwater pathways using multi-scale onshore-to-offshore electrical resistivity surveys

Befus, K.M.[1], Cardenas, M.B.[1], Tait, D.R.[2], Erler, D.V.[2]
kevinbefus@utexas.edu
1. Department of Geological Sciences, Jackson School of Geosciences, The University of Texas at Austin, Austin, TX, USA
2. Southern Cross University Centre for Coastal Biogeochemistry Research, Lismore, NSW, Australia

Electrical resistivity (ER) imaging techniques are useful for investigating porewater salinity distributions and dynamics within coastal environments. However, complex coastal geology can obscure the hydrologic target of ER surveys. We investigated the geologic controls on groundwater pathways in Rarotonga, a high volcanic island with a carbonate fringe. We used three ER survey configurations to explore this hydrogeologic setting: 1) waterborne continuous resistivity profiling in the lagoon, 2) submerged cable surveys across the terrestrial-marine interface, and 3) traditional surveys on land. We designed overlapping portions of these surveys to reveal differences in how the deployment methods image subsurface ER structure. Using both the field data and forward modeling, we quantified the resolvability of ER features imaged by overlapping configurations, where the sensitivity changed both as a function of electrode spacing and boundary conditions (i.e. influence of seawater).

Waterborne ER results revealed large scale variations in the ER structure of the lagoon geology. These heterogeneities are products of Rarotonga's volcanic history and reef diagenesis that change both the electrical signature and hydrogeologic properties of the subsurface. Time-lapse, submersed ER surveys imaged groundwater salinity dynamics and resolved select ER features more effectively than the waterborne surveys. Terrestrial ER surveys traced the extent of the freshwater lens and the transition from the unsaturated-saturated conditions, i.e., the water table. The ER responses of the three field configurations were concordant but imaged different scales hydrogeologic variability. The unique spatial signatures of both methodology and the geologic setting must be incorporated into future coastal ER applications.

Keywords: electrical resistivity tomography, coastal groundwater, subterranean estuary, coastal geology

SHP-17

Topographic Scanning using Microsoft Kinect

Kline, G.[1], Kim, W.[2], Kopp, J.[2]
Rwing27@me.com
1. Cockrell School of Engineering, The University of Texas at Austin, Austin, TX
2. Jackson School of Geosciences, The University of Texas at Austin, Austin, TX

Modern topographic scanners provide amazing results. They capture time and spatial evolution in sub-millimeter accuracy and near perfect location repeatability in sub seconds. However, they are rather expensive, heavy, and hard to deal with. "Project Kinect" was created to provide an alternative solution for groups who cannot overcome the downsides of large scanners. The system is portable, easy to use, and offers reasonable accuracy. Resolution is in the millimeter range for depth, while dx/dy varies with distance from the surface, but revolves around 1.5 mm. Two software solutions were created for geomorphic applications. One, with maximum capability, is for licensed users of LabVIEW and available through email contact. The other is free to use and available for download on any Windows PC from Sedexp.net and Sourceforge.net. Although the freeware version is less capable software, it is equally as accurate in results and offers automated scanning at a near "instant" rate. Continuous upgrades will become available, including Kriging options, surface projections, and other analysis tools. This new tool will enhance educational and research projects associated with flume experiments of evolving topography.

Keywords: Topographic Scanning, Experimental Procedures

SHP-18

Evolution of Turbidite Deposits on Basin Floor and link to Shelf Margin Processes: Washakie Basin, Wyoming

Koo, W.[1], Steel, R.[1], Olariu, C.[1], Kim, W. [1]
woongmo.koo@utexas.edu
1. Jackson School of Geosciences, The University of Texas at Austin, Austin, TX

The characteristics of turbidite successions have been studied actively as the amount of oil and gas discoveries from deep marine reservoirs has increased. However, the linkage between the architecture of turbidite deposits and their coeval shelf margin processes has not been analyzed in depth. I hypothesize that significant volumes of reservoir turbidites are deposited as amalgamated channel-levee systems and as lobes when river-dominated deltas reach their shelf edge. Poorly developed mixed sandy-muddy turbidites or no reservoir turbidites are deposited when deltas fail to reach the shelf edge or when wave- and tide-dominated deltas attain a shelf edge position.

To test the hypothesis, the architectures and morphologies of Maastrichitian turbidite deposits of Washakie Basin, Wyoming will be documented by using a combination of outcrop, core, and wireline log data. Over two thousands wells have been collected in Washakie Basin for hydrocarbon exploration and production. About thirty cores are present in the basin and will be described with the scope to link textures and sedimentary structures with wireline log patterns. Second, cores will be located within the clinoformally correlated wireline logs of the basin. Based on preliminary well log correlation, several (up to three) relatively sharp-based blocky low gamma bodies, vertically separated by high gamma thins, are observed from ancient deep environments in each clinothem of the basin. The log motif of each separated interval changes horizontally from blocky to upward decreasing gamma or vice versa. The correlation between various log motifs and core in clinothems will allow the characterization of the three dimensional (3-D) architecture of deep water depositional elements within channels, levees, lobes, and sheet-like sandstone bodies as well as their linkage to shelf margin processes. Third, changes of turbidite architecture will be documented in time and correlated with changes in shelf margin processes (river, wave, and tide or estuaries in each clinothem). One particular clinothem of the basin was chosen initially to observe depositional patterns of deep water deposits. Lobe shape was identified from the upper and lower flooding surfaces within the clinothem by interim isopach maps. The different locations of thickest part from lobes within the clinothem indicates lobe switching through time. Fourth, based on the relationship between changes in shelf margin processes and architecture of correlative turbidites, a 3-D depositional facies model of deep water deposits will be built. The proposed model will also consider the link between deep water deposits, shelf margin processes, and relative sea-level changes. In addition to the field and subsurface data, I propose to conduct flume experiments in the Sediment Transport and Earth-surface Processes Basin of the University of Texas at Austin. The flume experiments will be aimed at explaining autogenic responses in the depositional patterns of turbidites related with shelf edge processes. The depositional patterns of turbidites built by river-dominated shelf edge deltas, predictably the most efficient delivery system of sands to deep water, will be tested.

The construction of a 3-D depositional facies model of turbidite evolution through time, and linkage to shelf margin processes will enhance our capability of predicting favorable oil and gas reservoirs in ancient deep marine environments.

Keywords: shelf edge deltas, turbidites, clinothems, maximum flood surfaces, channel levee, lobe sheet, 3D depositional facies model, flume experiments

SHP-19

Stream/alluvium interaction in karst aquifer recharge: Edwards Aquifer - Nueces River system

Kromann, J. [1] and Sharp, J. [1]
jennakromann@utexas.edu
1. Jackson School of Geosciences, The University of Texas at Austin, Austin, TX

The karstic Edwards Aquifer is the primary source of drinking water in south-central Texas. The greatest recharge into the aquifer occurs in the Nueces River Basin system. Aquifer recharge is a key input parameter in management decision models. Current models for resource allocation calculate recharge based on sparse gauging station data and may underestimate recharge in the basin. There are a limited number of gauges in the recharge zone of the Edwards Aquifer. Synoptic gain/loss studies conducted in 2012-2013 in the Nueces River show that: 1) that recharge is difficult to estimate without multiple gauges; 2) recharge is not always occurring over the designated recharge zone of the Edwards Aquifer; and 3) some reaches can be either gaining or losing over time. We focus on a 64-km reach of the Nueces west of Uvalde, TX, that includes the recharge and contributing zones of the Edwards Aquifer. It is estimated that 40% of aquifer recharge occurs in this segment of the river which has intermittent reaches with significant gains and losses, but aquifer recharge does not account for all losses. A significant amount of this variation is controlled by bank storage and underflow (including hyporheic flows) in the channel deposits and adjoining fill terraces. Recharge is controlled by water table elevation and alluvium permeability, not discrete karst features (e.g., dolines). Surficial transport and deposition of alluvial sediments in this system may change aquifer recharge rates. Currently research is being conducted using hydrochemical, geophysical, stream discharge, tracer test, and weather data to evaluate the sources of stream discharge, alluvial flow paths, and rates of recharge in specific areas.

Keywords: Nueces River, Edwards Aquifer, karst, alluvium, recharge

SHP-20

Optical Remote Sensing Characterization of Glaciers in the N. Himachal Pradesh

Le, D. N.[1], Catania, G.[1], Andrews, L.[1]
ledanieln@gmail.com
1. Jackson School of Geosciences, The University of Texas at Austin, Austin, TX

Glaciers in the Himalaya and high mountain Asia consist of the largest store of ice outside the polar regions. The immense quantity and variability of glaciers in the Himalayas limits the capability of conducting detailed and efficient remote sensing observations. This study aims to automate the process of detailed glacier analyses in mountainous and debris covered regions using remote sensing techniques. Basic glacier attributes such as elevation statistics, mean aspect, centroid longitude, centroid latitude, glacier area, and accumulation area are delineated from the ASTER digital elevation model, the Randolph Glacier Inventory (GLIMS Glacier Database), and reflectance thresholds from Landsat 7 Enhanced Thematic Mapper Plus (ETM+) satellite imagery. The accumulation area is estimated by defining the snow area on each glacier during the late season where the snow area is estimated to be equal to the accumulation area. Using a basic relationship between glacier mass balance and the area-accumulation ratio (AAR), we can estimate the mass balance of glaciers in this region. Glacier attributes are established for 3690 glaciers in this region and correlated with the AAR of each glacier. Preliminary results show high scatter and rough relationships between glacier attributes and the AAR. In the future, these rough trends will be used to determine benchmark glaciers and track glacier change over time. This study hopes to contribute to and improve on current glacier databases and to advance glacier analyses from remote sensing data.

Keywords: Glaciology, Himalayas, Remote Sensing

SHP -21

Experimental Analysis of Autostratigraphic Controls in Foreland Basins

Leva-Lopez, J.[1], Kim, W.[1], Steel, R.[1]
julioleva@utexas.edu
1. Jackson School of Geosciences, The University of Texas at Austin, Austin, TX

Understanding the relation between sedimentation and tectonic pulses in foreland basins is the key for adequate analysis of the evolution of morphodynamics and basin stratigraphic architecture, which is also a requirement for adequate exploration and production of fossil fuels.

Several models have been proposed to explain this relationship and help revealing basin development in natural systems. However all these models developed under the assumption that a steady allogenic forcing produces a steady stratigraphic signature. These models mostly do not account for the autostratigraphic behavior of these systems, that is, the inherent behavior due to unique geometry of the basin subsidence.

We present a mathematical model and flume experiments that aim to explore the autostratigraphic controls asserted over foreland basin type subsidence. With these experiments and the accompanying mathematical model we have identified three different modes in the fill of a foreland basin. Our analysis indicated that the three modes are dependent on the ratio between the back-tilting subsidence (typical of these basins) rate and the sediment supply to the basin.

The first autostratigraphic behavior is the already known “autoretreat”, during which the shoreline goes from progradation to an eventual retrogradation. The second presents an initial progradation followed by a constant aggradation. Finally the model shown a new behavior named “autoaccelerated progradation” in which the progradation is maintained during the whole evolution, but is accelerated after a certain point.

The simple mathematical relationship developed in this study allows for defining a threshold between these behaviors and application to natural systems. We show an application of our study in terms of the threshold sediment supply condition to a foreland basin in the North Slope of Alaska.

Keywords: Autostratigraphy, Basin analysis, Foreland basin, Shoreline trajectory, Flume experiments, Mathematical model

SHP-22

Evaluating the simulation of leaf area index in the Community Land Model 4.0

Ling, X. [1, 2], Yang, Z.[1], Guo, W.[2]
lingxl08@126.com
1. Jackson School of Geosciences, The University of Texas at Austin, Austin, TX
2. Institute for Climate and Global Change Research, School of Atmospheric Sciences, Nanjing University, Nanjing 210093, People's Republic of China

The leaf area index (LAI) influences the exchanges of momentum, carbon, energy, and water between the terrestrial biosphere and the atmosphere. As such, it is a key variable in regulating the global carbon, energy, and water cycles. This study aims to evaluate how LAI is simulated by the state-of-the-science climate models. The Community Land Model version 4.0 (CLM4.0) within the Community Earth System Model version 1.0 (CESM1.0) is utilized to assess the performance of the simulated LAI with satellite observations such as Moderate Resolution Imaging Spectroradiometer (MODIS) data and Advanced Very High Resolution Radiometer (AVHRR) data. The focus is on spatial, seasonal, and interannual variations of LAI, with particular attention to regions and timescales where largest differences between the modeled and observed occur.

Keywords: community land model, leaf area index (LAI)

SHP-23

Fluid injection and induced seismicity: A numerical modeling approach

McCormack, K. A.[1], Hesse, M. A.[1]
kimberly.mccormack@utexas.edu
1. Jackson School of Geosciences, The University of Texas at Austin, Austin, TX

On May 27, 2000 a brine injection well in Paradox Valley, Colorado that had been in operation since 1996 triggered a 4.3 magnitude earthquake. In December of 2006 a geothermal well in Basel, Switzerland induced slip on a major fault soon after injection began, producing a 3.6 magnitude earthquake and damaging homes in the area. These are just a few of the recent occurrences of injected fluid inducing moderate, and in some cases damaging, earthquakes. However, despite the rising number of injection wells worldwide - from enhanced geothermal, wastewater disposal and brine injection – the mechanisms that trigger earthquakes are still poorly understood. Why do some sites produce moderate earthquakes soon after injection begins, some years or decades after the start of injection while many sites (at least to date) have produced no significant seismicity despite long-term fluid injection?

A numerical model can help us better understand the mechanisms that cause induced seismicity from fluid injection. However, predicting the evolution of a pressure perturbation due to fluid injection is difficult largely because the permeability of the rock is highly variable and generally poorly constrained. We will use micro seismic data that has been collected at a number of injection well sites. This can help us understand how the injected fluid is moving through the subsurface, how it is changing the local stress field and considerably reduce the uncertainty of our permeability values. The model will estimate the frequency of micro seismic events both spatially and temporally as a function of the geology of the injection site and the rate of injection. With a verified forward model for micro seismic frequency, an inverse model can be created that uses 4D micro seismic data to constrain the permeability of the rock layer that the fluid is being injected into. This will improve the prediction of pressure perturbations that have the ability to trigger larger earthquakes.

Keywords: Induced seismicity, fluid injection, numerical model

SHP-24

Surface complexation models and hyperbolic theory to solve multicomponent advection-reaction problems

McNeece, C.J.[1], Hesse, M.A.[1]
cmcneece@utexas.edu
1. Jackson School of Geosciences, The University of Texas at Austin, Austin, TX

In soil science we can use surface complexation models such as the triple layer model to understand the interactions between aqueous species and dynamic, pH-dependent, mineral surfaces. The charging behavior of a diverse range of porous media can be well understood from empirical measurements of the mineral surface such as specific surface area, reaction site density, and intrinsic surface charge and potential. However, incorporating these models in numerical simulations of the transport of multicomponent system is computationally expensive. Here we use surface complexation models and laws of mass action in conjunction with hyperbolic theory to determine unique, multiscale, analytical solutions to the coupled advection-reaction problem of multicomponent systems. We plan to conduct column flow experiments through various engineered and natural media to provide a metric by which to evaluate our model. These experiments will use an ion chromatograph and inline pH sensors to measure the timing and magnitude of reaction fronts of multiple anions. Furthermore, we plan to use our model to understand how radionuclides released at the Fukushima Dai-Ichi Nuclear Power Plant will travel within the groundwater system given the unique freshwater-seawater interface present at the site.

Keywords: triple layer model, hyperbolic theory, method of characteristics, surface complexation, ion exchange reactions, advection-reaction, Fukushima

SHP-25

Controls on groundwater dynamics of a coastal fluvial delta island, Wax Lake, LA

O'Connor, M.[1], Moffett, K.[1]
moconnor12@utexas.edu
1. Jackson School of Geosciences, The University of Texas at Austin, Austin, TX

Louisiana coastal wetlands are thought to function as buffers, filtering nutrient-rich terrestrial runoff as it travels to the Gulf of Mexico. While surface water filtration by these wetlands is a large and active area of research, flow through subsurface portions of the wetlands and possible nutrient cycling in the root zone has been largely overlooked. Specifically for Louisiana's coastal deltas, the physics and chemistry of island groundwater systems is unknown. To characterize these subsurface hydraulic dynamics at Pintail Island in the Wax Lake Delta, Louisiana, we collected sediment core samples and penetrometer measurements, monitored surface water and groundwater levels and chemistry, and analyzed meteorological, tidal, and river discharge data. As a first step, we focused on identifying wetland sediment properties and the relative influence of the major hydrologic controls, tides, delta outlet discharge, rainfall, and evapotranspiration, on water table dynamics. Pintail Island is a two-layer system with fine sediments and organic matter overlying sandy deltaic deposits. The sediment layer interface occurs approximately 60 cm below ground surface, around the mean surface water level. The vegetation root zone is concentrated in the surficial layer, although willow roots can extend into the deeper, higher-permeability sandy layer. Groundwater data from the upper portion of this sandy layer (~1m deep) is most strongly influenced by tides but also responds to long-term changes in discharge. Inland groundwater data yields no tidal influence during calm weather conditions; however, during storms, the inland groundwater signal is strongly influenced by surface water tides. Although the tidally oscillating water table causes significant temporal variation in root zone fluid potentials, evapotranspiration dynamics do not appear to strongly influence groundwater dynamics at depth, consistent with the shallow concentration of roots. These findings are first steps toward a comprehensive delta island water budget and subsurface reactive-transport model, which will identify and quantify the roles of the subterranean wetland flow system within the larger Louisiana coastal buffering system.

Keywords: deltas, wetlands, evapotranspiration, surface water/groundwater interaction

SHP-26

Process variability in a sand-rich tide-influenced delta system: the Lajas Formation, Argentina

Rossi, V. M.[1], Steel, R.[1], Leva-Lopez, J[1]
Valentina.marzia.rossi@utexas.edu
1. Jackson School of Geosciences, The University of Texas at Austin, Austin, TX

Tides are an important agent of erosion, sand transport and sand sorting in many shallow marine environments. There are both commercial and scientific reasons to improve our knowledge of tide-influenced processes, environments and depositional successions. Tide-influenced and tide-dominated depositional environments (mainly within estuaries, deltas, straits and shelves) deposit sandstones and mudstones within architecturally complex stratal packages. As sedimentologists and stratigraphers we are interested in disentangling the tidal signals from the storm wave and the river signals within the stratigraphic record in general, and within these selected stratal packages.

Few models have been proposed for tide-influenced deltas and most modern examples of strongly tide-influenced deltas are fine-grained and mud-rich, as they occur in the Indo-Pacific zone, draining large, low gradient areas with a humid-tropical climate. As a result, we are programmed to think that MUD is the diagnostic criteria either as mud drapes, double mud drapes or fluid muds. In comparison little attention has been paid to clear-water, clean-sand, tidal systems.

This study focuses on the mud-poor tidal sandbodies in the coastal to shelf portion of the Bajocian Lajas Formation, Neuquén Basin, Argentina. The outcrop dataset consists of 30 stratigraphic sections linked to high resolution (Gigapan) photo-mosaics. In addition to measured sections hundreds of paleocurrent indicators have been collected to determine the paleocurrent direction (ebb vs flood tide dominance) and accretion style of these bodies (forward versus lateral accretion) in order to discriminate between compound tidal dunes and tidal bars.

The 300 m thick study succession, exposed along a 7 km outcrop belt at Lohan Mahuida in southeastern Neuquèn Basin, is interpreted as stacked deltas and estuaries dominated by cross-stratified tidal sandbodies that alternate with fine-grained lithosomes. The tidal sandbodies have a thickness range between 3.5 and 15 m and width of at least 3 km. The succession is very sand-rich (80% Net to Gross) with relatively thin (dm to a few meters) intervening mudstones.
The Lower Lajas Formation contains signals of wave, tide and river currents as follows: The wave signals consistently occur preferentially in the prodelta and offshore-transition deposits. The tidal signals are strongest on the delta fronts and transgressive estuaries where both ebb- and flood-tidal currents were strong enough to produce and preserve tidal bars hundreds of meters long and up to 4 m thick. Both river and tidal signals are strong within the lower delta plain as distributary channels and inter-distributary embayments. The trace fossil assemblages throughout the deposits are dominated by *Dactyloidites*, *Thalassinoides*, *Planolites*, *Paleophycus*, *Skolithos*, *Macaronichnus* and minor *Ophiomorpha* and *Cruziana*.

Keywords: tidal, compound dunes, tidal bars, tide-influenced delta, estuary, Jurassic, Neuquèn Basin

SHP-27

Correlations between vegetation and island geomorphology in the Wax Lake Delta, Louisiana

Smith, B.[1], Moffett, K.[1], Mohrig, D.[1]
xyzsmith@gmail.com
1. Jackson School of Geosciences, The University of Texas at Austin, Austin, TX

Understanding how deltas build and maintain themselves is critical to predicting how they will respond to perturbations such as sea level rise. This is especially an issue of interest in coastal Louisiana, where land loss is prevalent due to subsidence and decreased sediment supply. Feedbacks between ecology and geomorphology have been well documented in many different environments, but the role of vegetation in delta morphodynamics is not well understood. This study investigates spatial and temporal correlations between vegetation succession and sediment accumulation at the Wax Lake Delta in Louisiana. This low gradient, rapidly prograding, tidally influenced delta has been forming since 1973 at the mouth of the man-made Wax Lake Outlet discharging into Atchafalaya Bay. We established a 2500 m long transect along the western levee of Pintail Island, capturing the full range of island elevations and the transition from bare sediment to herbaceous plants and trees. Shallow (50-150 cm deep) sediment cores from this transect were analyzed for particle size, organic matter content, and bulk density, and dated using Pb-210. The resulting sedimentation rates and composition trends over time were compared to remote sensing-based analyses of temporal changes in vegetation extent, island shape, and flooding frequency derived from historical aerial photos and Landsat images. We find that significantly more silty and organic sediments overly fine sandy deposits, with a greater depth to sand at higher elevations. Although the depth of the textural transition might logically be related to the local mean water level along the island elevation transect, trends in flooding frequency extracted from the historical series of Landsat images show that island elevations relative to mean water level have changed over time. These results provide an empirical foundation for future mechanistic models linking mineral sedimentation, organic sedimentation, vegetation succession, elevation change, and flood frequency in the delta.

Keywords: delta, morphodynamics, vegetation, Landsat, remote sensing

SHP-28

Stone Decay and Floods: Dissolution of Limestone Tiles in the Short Term

Sturrock, C.[1], Catlos, E.[1]
colinsturrock@utexas.edu
1. Jackson School of Geosciences, The University of Texas at Austin, Austin, TX

This study focuses on the damaging effects of water on indoor tiles in the short term, which could occur in a flooded home or building. Limestone and marble tiles have been widely used as building stones since ancient times. Carbonates are especially susceptible to dissolution in water due to the reactivity of their primary mineral, calcite, with dissolved CO_2. Previous studies mostly focus on the long term durability of limestone and marble tiles, mainly in outdoor use and as indicators of climate change. The short term picture on limestone dissolution is missing from the literature and is sought after here. Five limestone and marble tile samples were obtained from a building stone supplier and imaged using a stereomicroscope and scanning electron microscope. A series of photos was taken of cracks, large grains, vugs, and regions for potential recrystallization. The tiles were then soaked in rainwater for five days—the median flood duration from 1985-2002. The same areas were then photographed again after the submergence period to look for evidence of dissolution. The mass of each sample and the pH of the rainwater were also measured before and after the submergence period to look for further evidence of dissolution. Results suggest that decay is evident, but not extensive in this time period.

Keywords: limestone, SEM, surface features, stone decay

SHP-29

Facies variability in channel-to-lobe transition zone: Jurassic Los Molles, Nequen Basin, Argentina

Tudor, E.[1], Olariu, C. [1], Steel, R. [1]
eugen.tudor@utexas.edu
1. Jackson School of Geosciences, The University of Texas at Austin, Austin, TX

The Los Molles Formation is a 1000 m thick deep water sedimentary succession deposited during the Early-Mid Jurassic in the Neuquen basin, Argentina, in a back-arc setting. The Los Molles deposits represent the slope and basin floor of basin margin clinoforms with the coeval shallow water and fluvial deposits named Las Lajas and Challaco formations respectively. This study focuses on the facies changes from the lower slope to toe-of-slope to basin floor over outcrop belts 10 km in length, in down-dip and oblique-strike directions to the basin margins. Aerial satellite images, high resolution panorama pictures and detailed geo-referenced measured sections were used to correlate and interpret the spatial variability and overall geometry of the base of slope to basin floor units. Significant changes in the geometry and depositional facies of channel-to-lobe deposits are observed from proximal to distal over about 8 km distance. Based on the overall thickness and regional geometry of the units, it is argued that the deposits described span the toe-of-slope zone. A specific characteristic of the channel-to-lobe transition zones consists of a regional change of incision rates from proximal to distal, a change in bed boundaries from dominantly erosive base to non-erosional to depositional and with a range of distinct facies changes. In the channel-to-lobe transition zone the sand to shale ratio is high, with gutter casts and deep scours, with very high degree of amalgamation, gravel lags, mud-clast layers, abrupt pinchout and lateral migrating beds. Within the same depositional unit, at the base of the slope the sandstone dominant units change from more structureless and normal graded sandstone bed in the lobe axis to more parallel laminated beds and heterolithic beds to the lobe off-axis. The lateral change of the dominant structures of the beds indicates changes in the flow regime and dominant depositional style. The sand rich fan deposits of this study are associated with a muddy slope incised by erosional channels and canyons. The paleocurrents in the area show paleo-flow towards the NE, with local sediment distribution towards the N-NW and E. The observations of this study refine the model for the channel-to-lobe transition zone with increase recognition of facies variability in systems where limited data (facies observations) are available. The results also can be used for deep water reservoir heterogeneity modeling.

Keywords: deep-water, channel, lobes, Neuquen, transition zone

SHP (WITHDRAWN)

What Creates Banded Sandstone in Deepwater Environments? An Experimental Perspective.

Ustipak, K.R.[1]
ustipak@utexas.edu
1. Jackson School of Geosciences, The University of Texas at Austin, Austin, TX

Comparison of two laboratory experiments provide a causal mechanism of sand-mud banding in deepwater argillaceous sandstones deposited by transitional flows. Hydrocarbon exploration in deepwater reservoirs is expanding, yet details of depositional processes constructing these reservoirs remain poorly understood. It is generally agreed that sand delivery to deepwater environments is dominated by sediment-laden gravity flows that include turbidity currents, debris flows, and transitional flows. Transitional flows are intermittently laminar and turbulent, thus interpreted to be capable of depositing alternating muddy and sandy layers. Numerous process-based explanations and classification schemes have been published on transitional flows (also known as hybrid flows and slurry flows) based on interpretations of their enigmatic sedimentary facies as observed in core and outcrop. Experimental results from two gravity flows released into a laboratory flume reveal that sediment supply can also control the presence of banded sand-mud layers in the resultant deposit. The experiment with a single release results in a discrete sand layer overlain by a discrete mud layer. The experiment with pulsed releases of sediment results in multiple couplets of layered sand and mud, or banding. Constraints developed from experimental study of transitional flows are needed to refine understanding of mechanisms for siliciclastic sediment delivery in deepwater environments.

Keywords: Banded Sandstone, Transitional Flow Deposit, Deepwater, Sediment Gravity Flow

SHP-30

Generalized Local Cubic Law for inertial fluid flow and solute transport through tortuous and rough fractures

Wang, L.[1], Cardenas, M. B.[1], Slottke, T. D.[1], Ketcham, A. R.[1], and Sharp, M. J.[1]
wanglichun@utexas.edu
1. Jackson School of Geosciences, The University of Texas at Austin, Austin, TX

Fundamental understanding of flow and transport processes through single rough-walled fractures remains a challenge to gain insight for interpreting hydrological phenomena at continuum scale. The Generalized Local Cubic Law (GLCL) developed here is based on (1) modifying the aperture field by orienting it with the flow direction accounting for tortuosity, and (2) correcting for roughness changes associated with flow expansion/contraction and inertial effects. We compared its performance in estimating flow rate to results of direct numerical simulations with the Navier-Stokes equations (NSE) and physical flow experiments for real and synthetic three-dimensional rough-walled fractures. We also evaluated the performance of the Local Cubic Law (LCL). The LCL consistently overestimates flow rate with relative error δ ranging from 20% to 100% with arithmetic mean of $|\delta|$ ($<|\delta|>$) equal to 45.4% depending on the degree of tortuosity and roughness. However, the GLCL performs well and improves the performance of the LCL, where δ in flow rate range from -3.1% to 11.4% with $<|\delta|>$=4.7%.

Furthermore, we generated breakthrough curves (BTCs) through direct numerical simulations based on the advection-diffusion equation with flow field resulting from solving the NSE (which are considered to the true or experimental BTCs). We revisited the applicability of random walk particle tracking (RWPT) to simulate solute transport dynamics through real fractures, where flow fields resulted from the GLCL and LCL, respectively. We found persistent early arrival and heavy tailing in the BTCs from both direct numerical simulations and RWPT, which are the salient characteristics of non-Fickian behavior. The LCL consistently overestimates mean flow velocity; whereas the GLCL improves estimating flow field, and markedly improves fits to the BTCs relative to those fitted with LCL solutions. Therefore, PWPT with flow field resulting from the GLCL is robust in predicting solute transport through tortuous and rough fractures.

Keywords: Fracture, Local Cubic Law, Navier-Stokes, Particle tracking, Breakthrough curves

SHP-31

Geochemical reactivity in the mixing zone of a coastal salt lake and its effect on microbialite formation, Lake Clifton, Western Australia

Warden, J.G.[1], Breecker, D.O.[1], Zamora, P.[1], Bennett, P.C.[1]
johnwarden@utexas.edu
1. Jackson School of Geosciences, The University of Texas at Austin, Austin, TX

The hydrochemistry of Lake Clifton, Western Australia was investigated to evaluate the effects of mixing on geochemical reactions occurring at or near the groundwater-surface water interface. Lake Clifton is a coastal salt lake known for containing modern thrombolite structures. Thrombolites are stromatolite-like carbonate mounds formed by upward growth of microbial mats, sedimentation, and mineral precipitation. The Lake Clifton thrombolites are composed of aragonite and occur in zones of groundwater input along the eastern and northeastern lakeshore. Lake Clifton has been subjected to an approximately 3-fold increase in salinity from hyposaline in the early 1990s to hypersaline at present. Recent measurements of total dissolved solids at the Lake Clifton boardwalk varied between 56132 ppm in August, 2012 and 73707 ppm in June, 2011. The mixing of carbonate saturated waters can cause nonlinear effects that might result in either mineral dissolution or precipitation. PHREEQC was used to model geochemical reactivity in the Lake Clifton mixing zone to understand the current geochemical impact of the salinity increase. The mixing model suggests that if mixing is the only process influencing water chemistry, mixtures of supersaturated, hypersaline lake water and saturated, fresh groundwater will be supersaturated above (and undersaturated below) ~16% lake water, with respect to aragonite. Data from seepage meters, pore-waters (7-50 mm depth), and piezometers (41.6-80.5 cm depth) were compared to the mixing model and represent the range of chemistry in the mixing zone. Shallow groundwater samples collected from piezometers showed the greatest range of mixing, with mixing ratios between 32-60% lake water and aragonite saturation indices ranging from 0.24 to 0.76. Pore-water and seepage meter samples were mixtures of at least 80% lake water and had saturation indices from 0.12 to 0.57. Pore-waters were less supersaturated than predicted by the mixing model, which is consistent with the occurrence of carbonate precipitation. The geochemical results shown here indicate microbialites submerged in the lake or buried shallowly within the mixing zone will be preserved under present conditions, and possibly even undergo additional secondary lithification, provided that the microbialites are not buried at a depth such that the percentage of lake water decreases below the 16% transition to aragonite undersaturation. This result contrasts with geochemical models and observations of carbonate dissolution during the mixing of seawater and dilute groundwater. A variable density model was constructed using Comsol to understand how local groundwater flow near the thombolites may influence mixing. Modeling suggested that fresh groundwater is focused through the thrombolites due to variations in density, topography, and saturated hydraulic conductivity. Preferential flow of groundwater through the thombolites may provide a source of solutes and nutrients for thrombolite formation.

Keywords: groundwater-surface water interaction, limnology, geochemical modeling, microbialite, Australia

SHP-32

Groundwater-seawater mixing in sediments overlying zones of groundwater seeps

Zamora, P.[1, 2, 3], Cardenas, M.[2], Lloren, R.[1], Siringan, F.[1]
pbzamora@utexas.edu
1. Marine Science Institute, University of the Philippines, Diliman, Quezon City, Philippines
2. Department of Geological Sciences, University of Texas at Austin, Austin, Texas, USA

The relative importance of subsurface groundwater-seawater interaction on the nutrient chemistry of coastal waters influenced by submarine groundwater discharge has long been recognized. However, mixing dynamics in permeable sediment associated with focused seepage from geologic structures such as fractures, paleo-river channels or other preferred pathways through otherwise low permeability materials have received less attention. We studied groundwater-seawater mixing dynamics in permeable coastal sediments overlying zones of focused groundwater discharge along a fractured coastal limestone at the Bolinao Peninsula, Philippines. Point measurements using seepage meters and measurements of the environmental tracer ^{222}Rn were complemented by numerical flow and transport simulations partly tuned to the field site. Our study shows high seepage rates both from the point measurements as well as the integrated estimates from ^{222}Rn. Average groundwater fluxes from the seepage meters and Rn monitoring are 28 and 73 cm/d, respectively. Spatial distribution of point seepage and salinity measurements show fluxes in seepage meters away from the shoreline in the subtidal region as high and as fresh as intertidal point measurements suggesting focused fresh groundwater input further offshore. Numerical simulations coupling flow and salt transport on a beach-ocean transect with a leaky base shows mixing patterns analogous to classical coastal freshwater-seawater mixing dynamics. A balance of ambient upward groundwater flow from the leaky underlying platform and tidal forcing sets up a series of seawater circulation cells and freshwater discharge tubes in the subtidal region. Although the magnitude and salinity of groundwater fluxes were not exactly matched in the model, processes that could give rise to such values were inferred in the simulation results. Our study showed that groundwater-seawater mixing near shorelines is not only more extensive in cases where there are focused discharge zones but are more complex compared to classic coastal unconfined aquifers.

Keywords: seawater-freshwater interaction, submarine groundwater discharge, groundwater seeps

SHP-33

The effects of diurnal temperature variations on nitrogen dynamics in bedform induced hyporheic zones

Lizhi Zheng[1], M. Bayani Cardenas[1]
lizhizheng@utexas.edu
1. Jackson School of Geosciences, The University of Texas at Austin, Austin, TX, United States.

Hyporheic flow transports solutes and energy thereby controlling the distribution and patterns of nutrients and contaminants, dissolved oxygen, and water temperature in streambeds. Heat transport across the sediment-water interface affects bacterially-mediated biogeochemical reactions in streambeds, and consequently nutrient cycling in the fluvial corridor. This study aims to investigate the effects of diurnal temperature variations of stream water on biogeochemical reactions and nitrogen dynamics in bedform induced hyporheic zones. We conducted numerical simulations of coupled turbulent open-channel fluid flow, porous fluid flow, porous heat transport and reactive solute transport to study feedbacks and coupling between these processes. The simulation results show that the depth of the denitrification zone (DZ) and the bulk reaction rate are affected by diurnal temperature variations. DZ moves up (becomes shallower) with increasing temperature and deepens with decreasing temperature. This is due to a fact that denitrification occurs only when oxygen is below the limiting concentration, whereas the consumption of oxygen, through aerobic respiration and nitrification, is dependent on the temperature in the shallow sediments. Increasing temperature accelerates oxygen depletion. Furthermore, the net flux of nitrate coming from stream follows the diurnal temperature pattern, but the phase moves ahead of the temperature pattern. This is because nitrate has a double role in the nitrification and denitrification; those two reactions are not only dependent on temperature, but also rely on the availability of DOC, oxygen and ammonium. Over-all, the models illustrate that temperature affects the ability of hyporheic zones to remove nitrate.

Keywords: Temperature effect, Nitrogen dynamics, Hyporheic zones